NOTE TO USERS

This reproduction is the best copy available.

UMI®

UNIVERSITY OF CINCINNATI

May 26, 1994

I, Pornthep Nisamaneephong,
hereby submit this as part of the requirements for the degree of:

Doctor of Philosophy

in Physics

It is entitled A Study of Ground State and Excitations of Disordered Bosons Systems.

Approved by:

A STUDY OF GROUND STATES AND EXCITIED STATES OF DISORDERED BOSON SYSTEMS

A Dissertation submitted to the

Division of Research and Advanced Studies
of the University of Cincinnati

in partial fulfillment of the
requirements for the degree of

DOCTOR OF PHILOSOPHY

in the Department of Physics
of the College of Arts and Sciences

1994

by

Pornthep Nisamaneephong

B.Sc, Mahidol University , Thailand, 1981
M.Sc, Louisiana State University, Baton Rouge, 1987

Committee Chair: Professor Michael Ma

ABSTRACT

In this dissertation, I study the ground state and excited states of the dirty boson system. I investigate the effect of quantum fluctuations on the lattice hard-core dirty boson model using the gaussian approximation. This model can be mapped onto a quantum XY model with transverse random field. The classical spin ground state corresponds to a Gutzwiller projection of the non-uniform condensate, and the gaussian fluctuation can be included by Holfstein-Primakoff spin wave approximation. I show that gaussian fluctuations, even infinitesimal, are sufficient to destroy superfluidity in 1D and 2D at finite disorder. For charged boson systems, I investigate the effect of long-ranged interaction to the dirty boson model in the localized phase. I generalize the Efros model for localized charged fermions, so that there is an on-site Hubbard repulsion U between bosons on the same site as well as the long-ranged $1/R$ Coulomb interaction between bosons on different sites. I find that similar to charged fermions, but with modifications, the interplay between disorder and the Coulomb interaction causes a depletion of the density of states at the chemical potential and open a gap in the density of states, known as *Coulomb gap*.

In the memory of my father...

ACKNOWLEDGEMENTS

First, I would like to express my deep and sincere gradtitude to Professor Michael Ma, my thesis advisor, for his patient guidance and support over the past years. I also would like to thank Visiting Professor A. Yu Zyuzin and Dr. Lizeng Zhang for many valuable discussions.

I wish to thank Professor Fu-Chun Zhang, Young Kim and Frank Pinski for serving as members of my thesis committee. I also would like to thank Professor Paul Esposito for his time reading my thesis and giving me many valuable suggestions. I appreciate Attanagoda Santha and Professor Mike Sokoloff for providing me a computer terminal. I am also indebted to Ohio State Supercomputer.

Finally and most importantly, I wish to dedicate this thesis to my late father and express my deepest gradtitude to my mother. I also would like to express my appreciation to my wife for her constant encouragement, support and understanding during the most difficult period of my life.

Contents

List of Figures

Chapter 1

INTRODUCTION

1.1 INTRODUCTION

In a perfect crystal, electrons propagate as Bloch waves. In the presence of disorder, these waves are scattered. If such disorder is strong enough, the electrons are localized due to interference effects between scattered waves. This phenomena, known as Anderson localization, was first pointed out by Anderson[1] in 1958 in his classic paper titled "Absence of Diffusion in Certain Random Lattice". In that paper, Anderson showed that disorder can produce a continuum of localized states. Subsequently, Mott[4] pointed out there should be a mobility edge, a critical energy separating localized eigenstates from extended ones. If the disorder is weak, localized states will only occur in the band tails, but with increasing disorder, the mobility edges will move into the center of the band until they merge and the whole band consists of localized states. The DC conductivity, σ, of a Fermi liquid is determined completely by the states at the Fermi energy E_F. If these states are extended, transport will be diffusive, and σ is nonzero. For localized states, $\sigma = 0$. If E_F is changed with respect to the mobility edge energy, by changing electron density or by modifying the disorder, a metal-insulator transition occurs and is called the *Anderson transition.* Unlike other insulators, including the Mott insulator, the Anderson insulator is gapless.

For boson systems, it is natural to ask the corresponding question of how disorder may cause bosons to become localized. The study of boson localization due to disorder is known as 'the *dirty boson* problem'. Without disorder, the system undergoes Bose condensation at low temperature and the ground state is a superfluid. Thus, with sufficiently strong disorder introduced to the system, we expect to have the possibility of a superfluid-insulator or superconductor-insulator transition (for charged bosons), where the insulating phase is characterized by localized bosons. Theoretical interest on this problem is further stimulated by two systems. The first is ^4He absorbed on vycor or other porus media [3], where the superfluidity is not observed (for the first few monolayers) until the coverage is increased past some critical value. The second is the disordered superconducting film, where a superconductor-insulator transition

is observed with decreasing thickness [5] or increasing magnetic field [6].

The elementary excitation of a superfluid is characterized by a linear excitation spectrum (phonon mode) for interacting bosons systems. Without disorder, the superfluidity of the interacting boson system is related to the Bose condensation of free bosons, and the non-interacting system is an acceptable starting point, with the quadratic spectrum corrected through the Bogoliubov theory. However, this is no longer true for disordered systems. Without interactions, at zero temperature all the bosons will condense into the lowest energy single-particle state. Because this is a band-tail state, it will be localized by any amount of disorder[7]. One criteria for superfluidity is its sensitivity to the boundary conditions[9]. Since localized states are insensitive to boundary conditions[8, 9], this Bose condensed state is certainly not a superfluid. However, the localized condensate is unstable with respect to repulsive interactions. While for an extended condensate, the repulsion energy per particle is of order 1, for a localized condensate, it is of order N and dominates the condensation energy. For disordered systems, the non-interacting model is not a good starting point. In order to prevent this unphysical situation (bosons collapsing into a single localized state), a *minimal* model for disordered boson systems must include the repulsive interaction between bosons, such as

$$\mathcal{H} = \sum_i \frac{-\nabla_i^2}{2m} + V(\mathbf{r}_i) + \frac{1}{2}\sum_{ij} u(\mathbf{r}_i - \mathbf{r}_j) \ . \tag{1.1}$$

In eq.(1.1), the first term is the usual kinetic energy. The second and third term, describe the disorder potential and the repulsive interaction between bosons, respectively. The repulsive interaction will prevent bosons from getting too close to each other. For the interacting system without disorder, much understanding can be achieved by first applying the Hartree approximation and then the Bogoliubov theory. Consider the Hartree approximation in the disordered case, i.e., one looks for ground state wavefunction of the form $\Psi(\mathbf{r}_1, ..., \mathbf{r}_N) = \prod_i \phi(\mathbf{r}_i)$. This wave function implies all bosons are condensed into the same one particle state. The minimization of energy

results in the Hartree equation which is a non-linear Schroedinger-like equation,

$$-\frac{\nabla^2}{2m}\phi(\mathbf{r}) + V(\mathbf{r})\phi(\mathbf{r}) + N\int u(\mathbf{r}-\mathbf{r}')|\phi^2(\mathbf{r}')|d\mathbf{r}'\phi(\mathbf{r}) = \epsilon\phi(\mathbf{r}) \ . \qquad (1.2)$$

The normalization here is $\int |\phi^2(\mathbf{r})|d\mathbf{r} = 1$. One can see that because of the non-linear term, ϕ cannot be localized no matter how strong the disorder is (since this term would be of order N while the other terms are of order of 1). The ground state solution of this equation is nodeless and is composed of multiple peaks (solid lines in fig.1) which are connected (dotted lines) due to the kinetic energy term. Thus, the Hartree approximation always yields a condensate which is finite everywhere and extends throughout space. Note that this is true even in the limit $U \rightarrow 0$, provided the product of Un, where n is the average density, remains finite[10]. This extended condensate is sensitive to the boundary conditions (kinetic energy considerations) and hence the superfluid density is finite [8].

It is not surprising that the ground state in the Hartree approximation is always a superfluid. To destroy the superfluid, phase coherence must be destroyed. However, the random potential couples directly only to the density, and any effect on the phase must be mediated by the latter. This happens because the local density and phase are conjugate variables, obeying the commutation relationship $[\rho, \theta] = i$. But, it is precisely this non-commutativity that is ignored in the Hartree approximation.

Previous analytical and numerical studies on the dirty boson problem show that the correct solution to this problem has a non-superfluid ground state if the disorder is strong enough [10-18]. Indeed, I will show in chap.3 that the quantum fluctuations in the Bogoliubov theory of dirty bosons can cause the superfluid to be unstable to disorder.

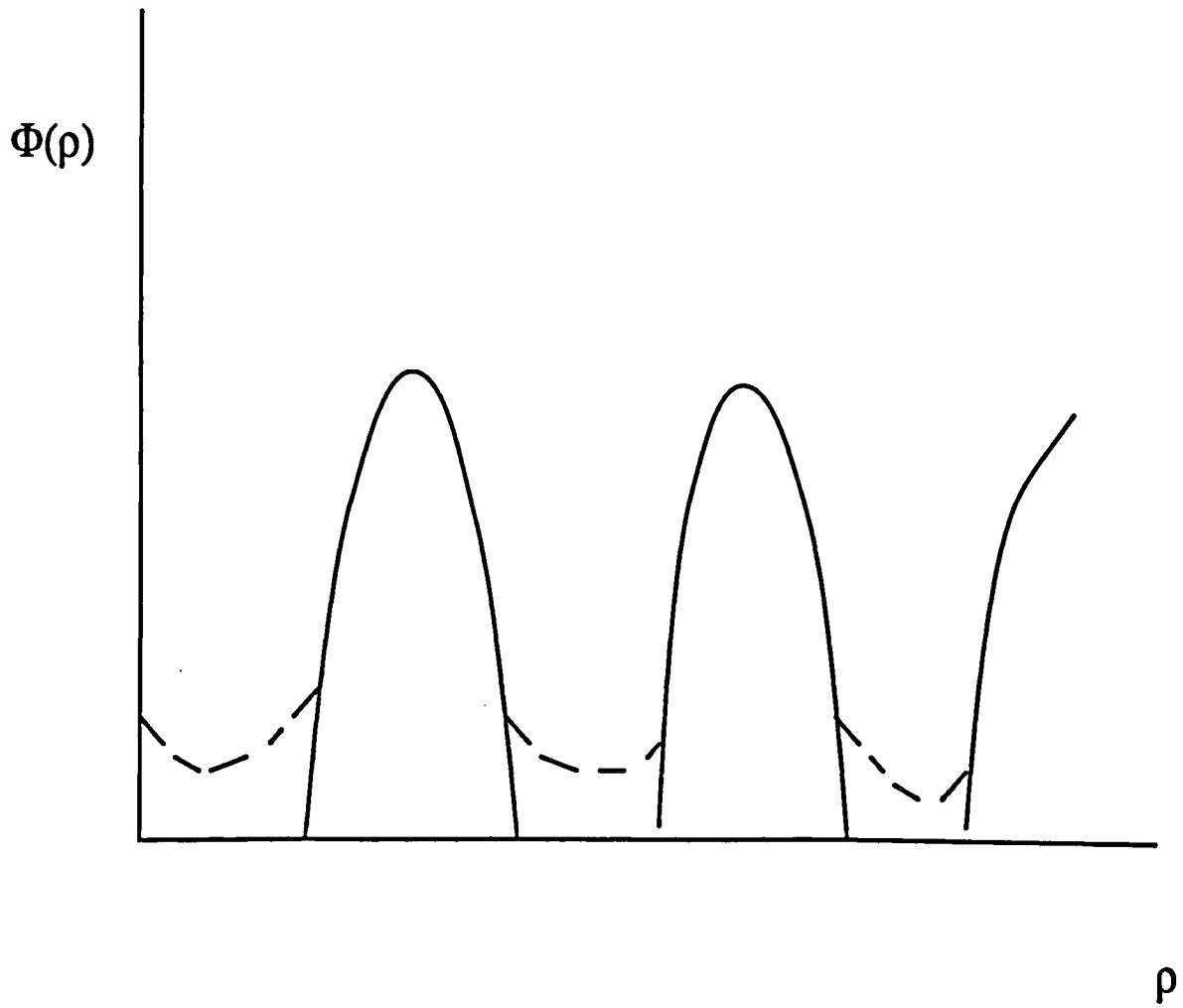

Figure 1.1: The Hartree wavefunction along an arbitrary direction.

1.2 SUPERFLUID-BOSE-GLASS PHASE TRANSITION

The interplay between the disorder (W) and the interaction (U) is a key aspect of the dirty bosons problem. With sufficient strong disorder, one expects bosons to become localized and results in a transition into the insulating phase. Thus, it is natural to ask a question about the $T = 0$ phase diagram of the dirty bosons as a plot of U v.s. W. Physically, the critical curve is a function of the density n or the chemical potential μ. Experimentally, the transition can be probed by varying these latter parameters. As far as the transition as a function of temperature, the critical temperature for the superfluid transition will decrease to zero at the $T = 0$ critical point.

Having established that generic dirty boson problem has a phase transition, we notice the following issues of interest:

1). What are the two phases? What are the ground states and their elementary excitations?

2). What are the critical phenomena of the $T = 0$ transition?

3). What can the Bogoliubov theory, so important as a microscopic theory in the pure case, tell us here?

The issue of critical phenomena has received much attention. Surprisingly, the interest on the issue (1) has been sparse by comparision. In the bulk of this thesis, I will concentrate on what (3) can tell us about (1). To foreshadow that, let us make a few general statements about the two phases.

In general, the two phases (superfluid and Bose-glass phase) are characterized by the presence or absence of off-diagonal long range order. First, the ground state properties of the ordered phase of dirty bosons are fundamentally equivalent to those without disorder, although the condensate is non-uniform and the superfluid density can be significantly less than the total density. The elementary excitations are

not well understood, although it is believed that the low-lying excitations are still phonons. The spectrum is linear at low momentum, or equivalently at low frequency, for pure systems. Since momentum is not a good quantum number in the presence of disorder, one looks at the density of states at low frequency $N(\omega) \sim \omega^{\theta}$ and asks if it deviates from the $\theta = d-1$ behavior present without disorder. Correspondingly, the low temperature specific heat obeys $C_v \sim T^{\theta+1}$. Yet another question concerns the Anderson localization of the phonons. The zero-frequency (Goldstone) mode is always extended, since it corresponds to a uniform phase rotation (but unlike the pure case, not a uniform density oscillation also). However, with sufficient disorder, the mobility edge energy can approach 0_+, in which case there will be no propagating zero sound mode. It is interesting to ask if this localization transition is correlated with the localization transition of the ground state.

In the Bose-glass phase, both LRO and superfluid density are destroyed. The low-lying excitations in this phase are single-particle like, and involve the transition of a boson from one localized state to another. Because of the disordered potential, such excitations are gapless, and their density of states is finite at vanishing energy. Consider the extreme or "site-localized" limit, so that any overlap between localized states can be ignored. In this case, the kinetic energy term in eq.(1.1) can be neglected and each localized state may be labelled by a "site" index denoting the position of its center. Therefore, the effective Hamiltonian for this case may be written as

$$\mathcal{H} = \sum_i (\phi_i - \mu) n_i + \frac{U}{2} \sum_i n_i (n_i - 1) \ , \tag{1.3}$$

where U is the on-site repulsion energy of bosons in the same localized state, n_i is the number of bosons on site i, μ is the chemical potential, and ϕ_i is the random potential. We assume each random potential ϕ_i obeys an independent probability

distribution $P(\phi_i)$, characterized by width W. Eq.(1.3) can be rewritten as

$$\mathcal{H} = \sum_i \epsilon_i n_i + constant \ , \tag{1.4}$$

where $\epsilon_i = \phi_i + Un_i$. The ground state is simply given by filling each site with the minimum n_i necessary to have all $\epsilon_i > 0$. ϵ_i here is the energy to add a boson to the site i , and is directly related to the tunneling density of states $N_1(\epsilon)$. Provided the probability of $\phi_i = 0$ is non-zero, $N_1(0)$ will be non-zero independent of the value of U. In particular, for U large compared to W, $N_1(\epsilon) = P(\epsilon)$, while for U small, $N_1(\epsilon)$ for $\epsilon < U$ will be enhanced by the factor W/U since all sites with $\phi_i < 0$ will have $0 < \epsilon_i < U$ in the ground state. Elementary excitations correspond to the transition of a boson from an occupied site i to some other (occupied or unoccupied) site j. Such an excitation has an associated excitation energy $\Delta_{ij} = \epsilon_j - \epsilon_i + U$. Again, the density of states $N(\epsilon)$ will be finite at arbitrary low energy, and with the enhancement factor for small U. Because $N(0)$ is finite, C_v at low temperature will be linear. In the case of small U, a relatively sharp decrease in slope will occur at $T \sim U$. The gapless insulating phase is known in literature as the Bose glass phase [2].

This problem is believed to be directly relevant to the ^4He films absorbed on porus Vycor glass[3]. The porus media in this case can be viewed as a random potential. According to experiments[4], the first few monolayers of absorbed ^4He is not a superfluid, even at low temperatures, but form an inert insulating layer of bosons localized by disorder. As coverage is increased, a transition from this Bose insulating to superfluid phase is observed. In the context of dirty bosons, the superfluid-Bose glass phase transition is caused by the interplay between disorder and its interaction between bosons.

In particular, this phenomena is intrinsically quantum and no amount of disorder can destroy superfludity without invoking non-commutativity of the density and its conjugate phase variable. The Hartree solution always possesses LRO, and corresponds to a non-uniform condensate. It is of interest to investigate how the inclusion

of the quantum fluctutions causes the instability of the superfluid phase.

In this dissertation, I will investigate the effect of quantum fluctuations in a gaussian approximation in disordered bosons systems. I will introduce the Bogoliubov theory in chap.2. The ground state and excited state obtained from this theory will be discussed in chap.3 and chap.4.

1.3 HARD-CORE BOSON MODEL AND QUANTUM SPIN SYSTEMS

A particularly simple model, which incorporates the necessary physics of the dirty boson problem, is the hard-core boson model with on site disorder:

$$\mathcal{H} = -t \sum_{<ij>} b_i^\dagger b_j - \sum_i \phi_i b_i^\dagger b_i \quad , \tag{1.5}$$

with the hard-core constraint, $b_i^\dagger b_i = 0,1$. It is quite useful to write eq.(1.5) in terms of quantum-spin variables. These were first used in the pure case by Matsubara and Matsuda[20] and later generalized to the disordered case by Ma, Halperin and Lee[11]. This mapping is made by taking

$$\begin{aligned} b_i \rightarrow S_i^- \quad , \quad b_i^\dagger \rightarrow S_i^+, \\ N_i \rightarrow S_i^z + \frac{1}{2} \quad , \quad t \rightarrow J \ . \end{aligned} \tag{1.6}$$

With this mapping, ones find the hard-core boson hamiltonian to be expressible as the the quantum spin-$\frac{1}{2}$ hamiltonian,

$$\mathcal{H}_{eff} = -J \sum_{ij} (S_i^x S_j^x + S_i^y S_j^y) - \sum_i h_i S_i^z \quad , \tag{1.7}$$

where $h_i \equiv \mu - \phi_i$, μ and ϕ_i are chemical potential and random on-site potential respectively.

In this quantum spin picture, the ferromagnetic ordering in x-y plane represents the bose condensation or superfluid phase. The localization transition can be studied by tuning the ratio of the variance of random field $\{h_i\}$ to the ferromagnetic coupling J[10].

Viewed as a quantum spin Hamiltonian, eq.(1.7) can be studied not only for $S = \frac{1}{2}$, but also for arbitary S. The significance of the $S \to \infty$ in the boson langauge is seen by noting that the two spins states for $S = \frac{1}{2}$ case corresponding to zero boson or one boson on each site. For general S, the $(2S + 1)$ spin states then correspond to 0,1,...,2S bosons on each site, and $S \to \infty$ corresponds the weak interaction limit (as increasingly large number of bosons are allowed to inhibit a site). The non-trivial limit corresponds to $< S^z > /S = \alpha$, where $-1 < \alpha < 1$, and $< S^z >$ is the average of S^z over the ground state and sites. This implies that the average number of bosons on a site will diverge as $S \to \infty$ for fix α. Thus, the spin $S \to \infty$ limit corresponds to the interaction strength $U \to 0$ and the density, n, tending to infinity, so that the product of Un remains finite.

Disordered quantum spin systems have received much interest, recently due not only to their relevance to the high T_c cuprates, but also to their intrinsic value in illuminating the physics of disordered quantum systems. Particularly interesting are those cases where quantum spins behave qualitatively differently from classical spins. Eq.(1.7) is in fact an example of this. For classical spins ($S \to \infty$), LRO persists for all disorder, while for quantum spins ($S < \infty$), LRO will be destroyed by finite disorder.

1.4 SUPERCONDUCTOR-INSULATOR TRANSITION

The interplay between superconductivity and localization [11, 21] is a phenomenon of fundamental interest. While superconductivity is the most spectacular manifestation of coherence between electron (pair) states, localization is the extreme consequence of disorder leading to disjointedness (Cooper pair breaking). One expects, as disorder increases, that states become localized and superconductivity in a given material disappears. However, the complete understanding of the superconductor-insulator transition, and in particular in the recently discovered high temperature superconductors, is still unknown.

In conventional superconductors, as one cools the system below a certain critical temperature, electrons form 'Cooper pairs'. This Cooper pairing is mediated by electron-phonon interaction. Although electrons are fermions, a fermion pair behaves like a boson. These Cooper pairs then undergo Bose condensation and the system becomes superconducting. However, the Bose condensation can be inhibited by disorder[21], giving rise to the superconductor-insulator transition.

In the traditional theory, proposed by Anderson[22] and Gor'kov[23], superconductivity is relatively insensitive to disorder which conserves time-reversal-invariance (i.e. nonmagnetic impurites). However, this theory does not take into account either the localizing effect of strong disorder or the interference between interaction and disorder. Experimentally, superconductivity is observed to be destroyed by increasing disorder[25]. The theoretical studies on this problem were reinvestigated in [26]. The fundamental question related to this problem is whether superconductivity can persist as the normal state crosses the mobility edge into the localized phase, and if so, when and how does it eventually break down? To address this question, Ma and Lee[21] suggests a criteria (within BCS model, ignoring the effects of Coulomb repulsion and quantum fluctuations) which shows that superconductivity may persist into

the insulating phase, so that a coherent state with localized quasiparticle exitations may be possible.

Recent experiments have concentrated on the superconductor-insulator transition in 2D. For example, on the experiments done on Bi thin films [5], the zero temperature superconductor-insulator transition is seen by varying the thickness of thin film to some critical value. The $T = 0$ value of the resistance at the criticality was found to be finite and very close to the quantum resistance of electron pairs, $h/(2e)^2$ or 6455 Ω. The values of T_c decreased monotonically with increasing normal sheet resistance R_N. Similar results are also found in the high T_c materials. Since superconductivity is due to the Bose condensation of Cooper pairs, it is tempting on physical grounds to adopt the dirty boson model to study the superconductor-insulator transition. However, as a quantitative model, there are two reservations. First, Cooper pairs are not point objects, but have finite size, which in fact is typically very large ($\sim 10^3 A$) in clean BCS superconductors. Second, because spatial extent of Cooper pairs implies there is sizable overlaps between pairs, exchanges between electrons in different Cooper pairs occur frequently. The size of Cooper pairs is limited by the localization length, which can be rather short. Nevertheless, it is instructive to consider a model of electrons when the dirty boson model can be derived formally.

One possible way for a bound state of charged-2e boson to be formed may be described via a negative Hubbard model[24]. First, consider a system of N electrons having M sites with Coulomb interaction on different sites as well as an on-site Hubbard repulsion between electrons on the same sites.

$$\mathcal{H} = \mathcal{H}_0 + \mathcal{H}_1 + \mathcal{H}_2 \quad , \tag{1.8}$$

where

$$\mathcal{H}_0 \;=\; -U \sum_{i,\sigma} n_{i,\sigma} n_{i,-\sigma} \quad , \tag{1.9}$$

$$\mathcal{H}_1 = \sum_{i,j,\sigma} t_{ij} a^\dagger_{i\sigma} a_{i\sigma} \ , \quad and \tag{1.10}$$

$$\mathcal{H}_2 = \sum_i \phi_i n_i \ , \tag{1.11}$$

where t_{ij} represents a hopping integral due the overlapping between the eigenstates and $n_{i,\sigma} = a^\dagger_{i\sigma} a_{i\sigma}$ is a number operator and ϕ_i is a random potential on site i. In the limit, $U >> t$, we can treat $\mathcal{H}_1$ perturbatively. At $T = 0$, without hopping, all electrons are bound in pairs localized at sites. The unperturbed groundstate is comprised of $\frac{N}{2}$ sites occupied by pairs of opposite-spin electrons. When $\frac{N}{2} < M$, the groundstates are degenerate with energy $-\frac{1}{2}NU$. For $T \neq 0$, a given site will have some probability to be empty or singly or doubly occupied. The probability of a site to be occupied by a single electrons is proportional to $e^{-\frac{U}{k_B T}}$, and is negligible for $T << U$.

As the perturbation $\mathcal{H}_1$ is turned on, two types of excitations, due to single and double particle (pair) excitations, occurs. As a result of pair breaking, the energy increases by an amount U with an energy gap in the single particle excitation spectrum. Since a pair excitation costs no energy, there is no gap in its excitation spectrum.

To the second order perturbation, the effective hamiltonian can be written as,

$$\begin{aligned} \mathcal{H}_{eff} &= -U \sum_i a^\dagger_{i\sigma} a_{i\sigma} a^\dagger_{i-\sigma} a_{i-\sigma} + \sum_i \phi_i n_i \\ &\quad - \sum_{ij\sigma} \frac{|t_{ij}|^2}{U} (a^\dagger_{i\sigma} a_{j\sigma} a^\dagger_{j\sigma} a_{i\sigma} + a^\dagger_{i\sigma} a^\dagger_{i-\sigma} a_{j-\sigma} a_{j\sigma}) \ , \end{aligned} \tag{1.12}$$

where eq.(1.12) involves electron pairs only, and not individual electrons.

It is more convenient to work with the a pair creation and annihilation operators: $b_i = a_{i\sigma} a_{i-\sigma}$ and $b^\dagger_i = a^\dagger_{i\sigma} a^\dagger_{i-\sigma}$. The pair-number operator for a site is $N_i = b^\dagger_i b_i$. These operators introduced here satisfied by the commutation rules:

$$b_m b^\dagger_m - \eta_{mm'} b^\dagger_{m'} b_m = \delta_{mm'} \ , \tag{1.13}$$

where $\eta_{mm'} = 1 - 2\delta_{mm'}$. Eq.(1.13) is *fermion-like* ($\eta = -1$) on the same site, and *boson-like* ($\eta = 1$) on different sites ($m \neq m'$). The fermion-like property for $m \neq m'$ restricts the eigenvalue of N_m to be 0 or 1, ie. these are hard-core bosons. This simply comes from the fact that only one electron pair can occupy any one site. Furthermore, within the subspace of paired electrons only, $n_{i,\sigma} = n_{i,-\sigma}$, and $n_{i\uparrow} + n_{i\downarrow} = \frac{N_i}{2}$, eq.(1.12) can then be rewritten in term of b_i, $b_i^\dagger$ as

$$\mathcal{H}'_{eff} = \mathcal{H}_o + \mathcal{H}' + \mathcal{H}'' \quad , \tag{1.14}$$

where

$$\mathcal{H}_o = -U \sum_i N_i + \sum_i \phi_i b_i^\dagger b_i \ , \tag{1.15}$$

$$\mathcal{H}' = 2\frac{t^2}{U} \sum_{ij} N_i N_j \ , \quad and \tag{1.16}$$

$$\mathcal{H}'' = -2\frac{t^2}{U} \sum_{ij} b_i^\dagger b_j \ . \tag{1.17}$$

Except for the repulsive interaction between bosons on neighbouring sites, eq.(1.14) is identical to the hard-core boson hamiltonian.

In the context of dirty bosons, the universal conductivity of two-dimensional films at the superconductor-insulator transition was theoretically investigated[29, 9] by assuming charge-2e bosons moving in the random potential. Such a theory[9] assumes charge-2e bosons persist across the transition even on the insulating side of superconductor-insulator transition. However, it is unclear whether bosons persist into the insulating side or break up in to fermions instead. It is therfore interesting to study the system of charged bosons in the insulating phase.

In the case of charged bosons, the effective hamiltonian of localized charged bosonic system can be written as

$$\mathcal{H} = \sum_i \phi_i n_i + \frac{1}{2}\sum_{i\neq j} \frac{e^2}{r_{ij}} n_i n_j + \frac{U}{2}\sum_i n_i(n_i - 1) \ . \qquad (1.18)$$

Here I consider the extremely localized limit in which the kinetic energy of the system can be ignored.

The first term in eq.(1.18) describes the disordered potential energy of a boson on site i. For granular system, this site can be a localized state or a grain. The second term describes the long-ranged Coulomb interaction between charged bosons on different sites. The last term arises from the additional short- ranged interaction between bosons on the same site. In granular systems, this Hubbard U term can be interpreted as a charging energy of a grain which is inversely proportional to the size of a grain. The inclusion of the long-ranged Coulomb interaction is crucial, as it cannot be screened by localized electron pairs.

For a disordered fermionic insulator with strongly localized electronic states, the spatial distribution of the electrons is strongly influenced by the long-ranged Coulomb interaction. This leads to a depletion of single-particle density of states at the chemical potential, known as the Coulomb gap[10]. This gap has an entirely different origin from the band gap, for example, in the semiconductor. Furthermore, the effect of this long-ranged Coulomb interaction also causes the deviations at low temperatures from Mott 's $T^{\frac{1}{d+1}}$ to $T^{\frac{1}{2}}$ law for the electrical conduction by variable-range hopping[10].

In the last chapter, I will present a study of the effect of long-ranged interaction in the system of localized charged bosons described by eq.(1.18). I will investigate the existence of the Coulomb gap for this system. I will then contrast the properties of the charged Bose glass to the charged Fermi glass as a possible way of distinguishing the two systems.

Bibliography

[1] P. W. Anderson, Phys. Rev. **109**, 1492 (1958).

[2] N. F. Mott and E. A. Davis, Electronic Processes in Non- Crystalline Processes. Oxford:Clarendon Press (1971).

[3] See J. D. Reppy, J Low Temp. Phys, **87**, 205 (1992). and references therein.

[4] B.C. Cooker, E. Hebard, E.N. Smith, Y. Takano and J.D. Reppy, *Phys. Rev. Lett.*, **51**, 666 (1983); M.H.W. Chan, K.I. Blum, S.Q. Murphy, G.K.S. Wong and J.D. Reppy, *Phys. Rev. Lett.* , **61**, 1950 (1988); D. Finotello, K.A. Gillis, A. Wong and M.H.W. Chan, *Phys. Rev. Lett.* , **61**, 1954 (1988); G.K.S. Wong, P.A. Crowell, H.A. Cho and J.D. Reppy, *Phys. Rev. Lett.* , **65**, 2410 (1990); M. Larson, N. Mulders and G. Ahlers, *Phys. Rev. Lett.*, **68**, 3896 (1992).

[5] D. B. Haviland, Y. Liu and A. M. Goldman, Phys. Rev. Lett, **62**, 2180 (1989).

[6] A. F. Hebard and M. A. Paalanen, Phys. Rev. Lett., **65**, 927 (1990); Phys. Rev. Lett., **69**, 1604 (1992).

[7] D.J. Thouless, Phys. Rep., **13C**, 93 (1974).

[8] M. E. Fisher, M. N. Barber and D. Jasnow, Phys. Rev. B **8**, 1111 (1973).

[9] For a recent discussion of the various criteria of superfluidity, see D. J. Scalapino, S. R. White and S. C. Zhang, Phys. Rev. Lett., **68**, 2830 (1992).

[10] D.K.K. Lee and J.M.F. Gunn, J. Phys. **C2**, 7753 (1990).

[11] M. Ma, B.I. Halperin and P.A. Lee, Phys. Rev. B, **34**, 3136 (1986).

[12] M.P.A. Fisher, P.B. Weichman, G. Grinstein and D.S. Fisher, Phys. Rev. B , **40**, 546 (1989).

[13] T.Giamarchi and H.J. Schulz, Phys. Rev. B, **37**, 325 (1988).

[14] L. Zhang and M. Ma, Phys. Rev. A, **37**, 960 (1988).

[15] L. Zhang and M. Ma, Phys. Rev. B, **45**, 4855 (1992); L. Zhang, X.Q. Wang, Phys. Rev. B, **47**, 11518 (1993).

[16] L. Zhang, Phys. Rev. B, **47**, 14364 (1993).

[17] K.G. Singh and D.S. Rokhsar, Phys. Rev. B, **46**, 3002 (1992).

[18] K. Runge, Phys. Rev. B, **45**, 13136 (1992).

[19] W. Krauth and N. Trivedi, Europhys. Lett. **14**, 627 (1991); N. Trivedi, D.M. Ceperley, and W. Krauth and N. Trivedi, Phys. Rev. Lett., **67**, 2307 (1991); R.T. Scalettar, G.G. Batrouni, and G.T. Zimanyi, Phys. Rev. Lett., **66**, 3144 (1991); E.S. Sorensen, M. Wallin, S.M. Girvin and A.P. Young, Phys. Rev. Lett., **69**, 828 (1992); M. Makivic, N. Trivedi and S. Ullah, unpublished.

[20] T. Matsubara and Matsuda, Prog. Theor. Phys., **16**, 569 (1956).

[21] M. Ma and P.A. Lee, Phys. Rev. **B32**, 5658 (1985)

[22] P.W. Anderson, J. Phys. Chem. Solids **11**, 26 (1959).

[23] A.A. Abrikosov, L.P. Gorkov, JETP **35**, 1158 (1958); **36**, 319 (1959).

[24] V.J. Emery, Phys. Rev. **B14**, 2989 (1976).

[25] Y. Shapiro and G. Deutscher, Phys. Rev. **B27**, 4463 (1983). A.F. Hebard and M.A. Palanaan, Phys. Rev. **B30**, 4063 (1984).

[26] S. Maekawa and Fukuyama, Physica **107B**, 123 (1981); J. Phys. Soc. Jpn., **51**, 1380 (1982); H. Fukuyama, Physics **126B**, 306 (1984). P.W. Anderson, K.A. Muttalib, and T.V. Ramakrishnan, Phys. Rev. **B21**, 117 (1983). M. Ma and P.A. Lee, Phys. Rev. **B32**, 5658 (1985). A. Kapitulnik, G. Kotliar, Phys. REv. Lett., **54**, 473 (1985). L.N. Bullaevskii, M.V. Sadovskii, JETP Lett., **43**, 76 (1986). M. Ma and E. Fradkin, Phys. Rev. Lett., **56**, 1416 (1986).

[27] Y. Liu, D.B. Haviland, B. Nease, and A.M. Goldman, Preprint to be published in Phys. Rev B.

[28] P.A. Lee and T.V. Ramakrishnan, Rev. Mod. Phys., **57**, 287 (1985).

[29] M.C. Cha, M.P.A. Fisher, S.M. Girvin, M. Wallin, and A.P. Young, Phys. Rev. B, **44**, 6883 (1991)

[30] M.P.A. Fisher, G. Grinstein and S.M. Girvin, Phys. Rev. Lett., **64**, 587 (1990)

[31] E.L. Efros, J. Phys. **C:9**, 2021 (1976).

Chapter 2

GAUSSIAN THEORY FOR DIRTY BOSONS

2.1 INTRODUCTION

Without interactions, the bosons will all condense into the lowest energy eigenstate, which is localized for any finite disorder. Any amount of repulsion will prevent this from happening, and cause the condensate to become spatially extended. Interaction, on the other hand, will also scatter particles out of the condensate. Thus, the interactions play a dual role. It is essential to include the interaction between bosons as a starting point for dirty boson systems. In the presence of disorder, the superfluid-Bose glass transition [1] – [9] may take place by tuning the randomness. However, this transition is intrinsically quantum in nature and cannot be explained by ordinary mean-field theory in which quantum fluctuations are ignored. It is worthied to ask what minimal effects are necessary and sufficient to cause such a transtion.

In this dissertation, I will investigate the effect of quantum fluctuations on the lattice hard-core dirty boson model by studying the fluctuations in a gaussian approximation. This model can be mapped onto a quantum XY model with transverse random field. The classical spin ground state corresponds to a Gutzwiller projection[10] of the non-uniform condensate, and the gaussian fluctuation can be included by the Holstein-Primakoff spin wave approximation[11]. Since our gaussian Hamiltonian is a quadratic operater, the Hamiltonian (in principle) can be diagonalized through a Bogoliubov transformation. I will show that gaussian quantum fluctuations, even infinitesimal, are sufficient to destroy superfluidity in 1D and 2D at finite disorder.

My starting point is the hard-core boson model with on-site disorder which can be written as

$$\mathcal{H} = -t \sum_{<i,j>} b_i^\dagger b_j + H.C. + \sum_j (\phi_j - \mu) b_j^\dagger b_j \ , \tag{2.1}$$

where $b_j^\dagger$, b_j are boson creation and anihilation operators at lattice site j, with the hard-core constraint imposed by limiting the eigenvalues of $b_j^\dagger b_j = 0, 1$. $< i, j >$ indicates nearest neighbor and ϕ_j is the random on-site potential obeying certain independent distribution. (In my calculations I use the gaussian distribution). This

model is equivalent to a spin-1/2 XY magnet with a transverse random fields [1, 3, 4] (see the discussion preceding) eq.(1.7).

The superfluid phase in this model corresponds to spin long-range order in the XY plane. The random field $\{h_j\}$ is given by independent gaussian distribution function $P(h_j)$ having width h. It will not effect the physics, provided the magnitude of the mean value of $P(h_j)$, h_o, is not too large (see later). In this calculation, I take $h_o = 0$. I pick this model because while it contains the features believed to be essential for the SF-BG transition, it has a simple classical solution and a 'built-in' parameter which can be used to systematically investigate quantum fluctuations. It is also of interest as a disordered quantum spin system [3] - [5].

For later convenience, we perform a global rotation in spin space such that

$$\mathcal{H} = -J \sum_{<i,j>} (S_i^x S_j^x + S_i^z S_j^z) - \sum_j h_j S_j^y \ . \tag{2.2}$$

The off-diagonal LRO of the boson system is now related to the magnetic LRO in the $x-z$ plane. The classical solution for this model corresponds to treating the spins as classical vectors. In terms of bosons, one is dealing with a variational wavefunction of the form $\prod_j (u_j + v_j b_j^\dagger)|0\rangle$, which when projected into states of definite N are Jastrow wavefunctions given by Gutzwiller projection of condensate wavefunction $(\sum_j \frac{v_j}{u_j} b_j^\dagger)^N |0\rangle$. In ref. [1], it was shown for the spin model that, provided there is no gap in the spectrum (a sufficient condition is $|h_o| \leq zJ$, where z is the lattice coordination number), the classical ground state is always ordered. However, it was also seen that, taking into account the quantum (specifically $S = 1/2$) nature of the spin operators with strong disorder, the ground state does not have long-range order. Following the motivation discussed in the previous paragraph, it is thus of interest to find out if the destruction of LRO can be achieved by gaussian quantal effects. In the spin formalism, these gaussian effects, are included by spin wave analysis[5]. From now on I will refer this theory as a gaussian theory.

Within such an approach, the first question is the signature of destruction of the

LRO [6]. Since the spin-wave analysis is an expansion about the ordered state, this destruction is signified by an instability. Possible scenarios are 1) a diverging fluctuation in the order parameter, 2) negative excitation energies, or 3) complex excitation energies (e.g., Bogoliubov's solution to bosons with attractive interactions). In the pure case, scenario 1) is observed in 1D. Exact solution for $S = 1/2$ [13] and general understanding of 1D spin systems indicates this diverging fluctuations destabilize the LRO and the ground state has algebraically decaying correlation functions.

In the subsequent section, some results for pure systems will be briefly reviewed. The descriptions of gaussian theory for the disordered system will be studied in detail in section 2.3.

2.2 PURE SYSTEM

Before discussing the disordered system, let me first briefly discuss the result for the pure system. In 1D, the quantum correction to the order parameter, δm, is divergent[14], reflecting the lack of true LRO in the quantum spin-$\frac{1}{2}$ XY model. While for two and higher dimensions, it has been shown rigorously that finite magnetization exists in the XY plane[15], and indeed the quantum correction to the classical magnetization in the spin wave theory becomes finite as well. The decreasing of δm with the increasing dimensionality indicates that spin wave theory becomes a better approximation in higher dimensions.

The hamiltonian for pure system, after rotation, is

$$\mathcal{H}^0 = -J \sum_{<i,j>} (S_i^x S_j^x + S_i^z S_j^z) \ , \tag{2.3}$$

where the ground state is assumed to be in the ordered (ferromagnetic) phase with broken symmetry in z direction. The usual Holstein-Primakoff transformation[11] allows ones to study the fluctuations about the classical ground state given by $< S_i^z >= S$:

$$\begin{aligned} S_j^+ &= \sqrt{2S}(1 - a_j^\dagger a_j/2S)^{1/2} a_j \ , \\ S_j^- &= \sqrt{2S} a_j (1 - a_j^\dagger a_j/2S)^{1/2} \ , \quad and \\ S_j^z &= S - a_j^\dagger a_j \ . \end{aligned} \tag{2.4}$$

Here $a_j^\dagger$ and a_j are boson creation and annihilation operators with $[a_i, a_j^\dagger] = \delta_{ij}$, $[a_i, a_j] = [a_i^\dagger, a_j^\dagger] = 0$. In terms of Fourier coefficients,

$$a_k^\dagger = \frac{1}{\sqrt{N}} \sum_j e^{-i\vec{k}\cdot\vec{r}_j} a_j^\dagger \quad and \quad a_k = \frac{1}{\sqrt{N}} \sum_j e^{i\vec{k}\cdot\vec{r}_j} a_j \ . \tag{2.5}$$

After rescaling $J \rightarrow J/S^2$, and after expanding the square root in (2.4) in powers of $\frac{1}{S}$, ones find the hamiltonian (2.3) to be can be written as,

$$\mathcal{H}^0 = -\frac{z}{2}NJ + \frac{zJ}{S}\sum_k a_k^\dagger a_k - \frac{zJ}{4S}\sum_k \gamma_k(a_k^\dagger a_k + a_k a_{-k} + H.C.) + \mathcal{O}(\frac{1}{S^{3/2}}) \ , \quad (2.6)$$

where,

$$\gamma_k = \frac{1}{z}\sum_{\vec{\delta}} e^{i\vec{k}\cdot\vec{\delta}} \ . \quad (2.7)$$

Here $\vec{\delta}$ is a lattice vector and z is the the nearest neighbour number.

The Bogoluibov transformations are,

$$a_k = u_k b_k + v_k b_{-k}^+ \quad and \quad a_k^+ = u_k b_k^+ + v_k b_{-k} \ . \quad (2.8)$$

The Hamiltonian (2.6) can be diagonalized to give

$$\mathcal{H}^0 = E^0 + \sum_k \omega_k^0 b_k^+ b_k \ , \quad (2.9)$$

with

$$E^0 = \frac{zJ}{2S}\sum_k (\sqrt{1-\gamma_k} - 1) - \frac{z}{2}NJ \quad (2.10)$$

and

$$\omega_k^0 = \frac{zJ}{S}\sqrt{1-\gamma_k} \ . \quad (2.11)$$

For small k ($k\delta << 1$), eq.(2.11) can be approximated as $\omega_k^0 \approx ck$, where δ is a lattice spacing and c is a speed of sound. Here, b_k^+ and b_k are the transformed creation and annihilation operators, such that

$$b_k = u_k ak - v_k a_k^+ \quad and \quad b_k^+ = -v_k a_k + u_k a_k^+ \ , \quad (2.12)$$

with

$$u_k^2 = \frac{1}{2}\left(\frac{1-\frac{\gamma_k}{2}}{\sqrt{1-\gamma_k}}+1\right), \quad v_k^2 = \frac{1}{2}\left(\frac{1-\frac{\gamma_k}{2}}{\sqrt{1-\gamma_k}}-1\right), \quad and \quad 2u_kv_k = \frac{\frac{\gamma_k}{2}}{\sqrt{1-\gamma_k}} \ . \tag{2.13}$$

The second term in eq.(2.10) represents the energy of the classical state and the first term corresponds to the contribution arising from the spin wave osillations. The order parameter can be defined as

$$m = < S_{iz} > = m_{classical} - \delta m \ , \tag{2.14}$$

where $m_{classical} = S$. δm is the reduction due to the quantum fluctuation:

$$\begin{aligned} \delta m &= \frac{1}{N}\sum_{k\neq 0} < a_k^\dagger a_k >, \\ &= \frac{1}{N}\sum_{k\neq 0} v_k^2, \\ &= \frac{1}{2}\int_{k\neq 0} \frac{d^dk}{(2\pi)^d}\left(\frac{1-\frac{\gamma_k}{2}}{\sqrt{1-\gamma_k}}-1\right) \ . \end{aligned} \tag{2.15}$$

For $d > 1$, the singularity is integrable, and δm is finite in the limit $N \to \infty$. In particular in 2D, $\delta m \simeq 0.06 << m_{classical}$ even for $S = \frac{1}{2}$, strongly suggesting that LRO is stable. In 1D, $\sqrt{1-\gamma_k} \sim k$ for small k, and

$$\delta m \sim \int_{\frac{1}{N}} \frac{dk}{k} \sim lnN \ . \tag{2.16}$$

Eq.(2.16) implies the fluctuation, δm, diverges logalithmically with size N. This result reflects the lack of true long-ranged order in 1D. The spin-spin correlation for pure case in 1D has an algebraic power behaviour $\frac{1}{r^\eta}$ with $\eta = \frac{1}{2}$ for $S = \frac{1}{2}$[4]. In figs. 2.1 and 2.2, I show the plot of δm v.s lnN (δm is calculated from eq.(2.15) for 1D and 2D. As we can see in fig.2.1, δm diverges as lnN in 1D while fig.2.2 shows that δm is

finite in 2D.

Next, let me consider a transverse uniform field case, $h_j = h_0$. In the boson problem, changing the uniform field corresponds to changing the chemical potential, and the transition is from a superfluid phase to the vaccuum ($n_i \equiv 0$) or fully filled ($n_i \equiv 1$) state by tuning the applied field h_0. For classical spins, the transition occurs at $h = \pm zJ$. It turns out this holds for quantum spins also. Within spin-wave theory, this can be understood as follows. From ref.[5], the quantum fluctuations in the uniform field case are given by

$$\begin{aligned} \frac{\delta m(h_0)}{S cos\theta_0} &= \frac{1}{NS}\sum_k < a_k^\dagger a_k > \\ &= \frac{1}{2S}\int \frac{d^dk}{(2\pi)^d}\left(\frac{1-\frac{\gamma_k}{2}(1+H_0^2)}{\sqrt{(1-\gamma_k)(1-\gamma_k H_0^2)}} - 1\right) , \end{aligned} \tag{2.17}$$

where in the above equation $H_0 = \frac{h}{zJ}$. It can be seen from eq.(2.17), as $h \rightarrow \pm zJ$, $m_{classical} \rightarrow 0$, $\delta m \rightarrow 0$, but in addition $\frac{\delta m}{m_{classical}} \rightarrow 0$, indicating that quantum fluctuations are negligible for this transition. This result is in contrast to the random field problem, where at a critical disorder, $m_{classical}$ is finite but $\delta m \rightarrow -\infty$.

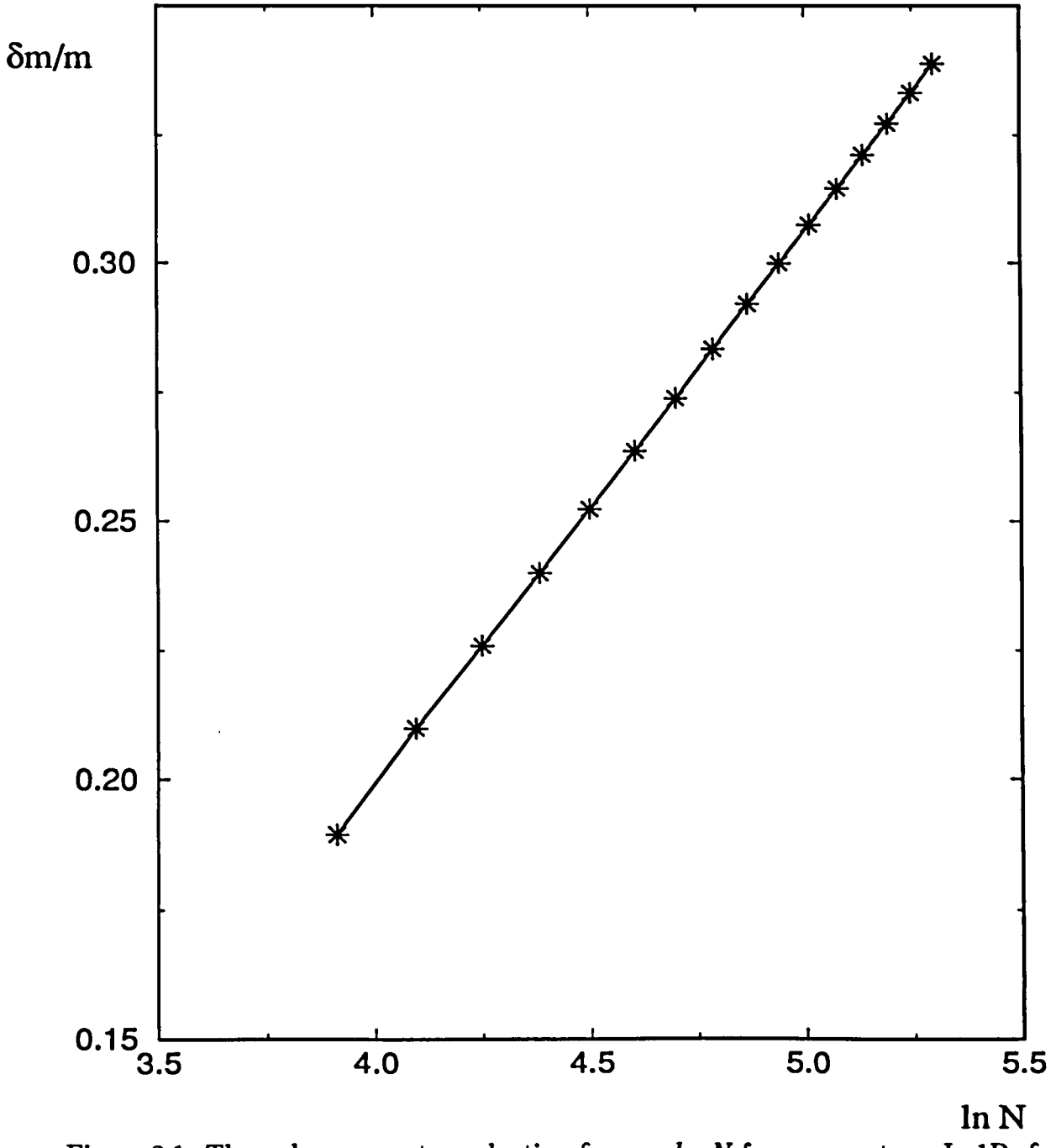

Figure 2.1: The order parameter reduction δm v.s. $logN$ for pure system. In 1D, δm diverges logarithmically with the system size N.

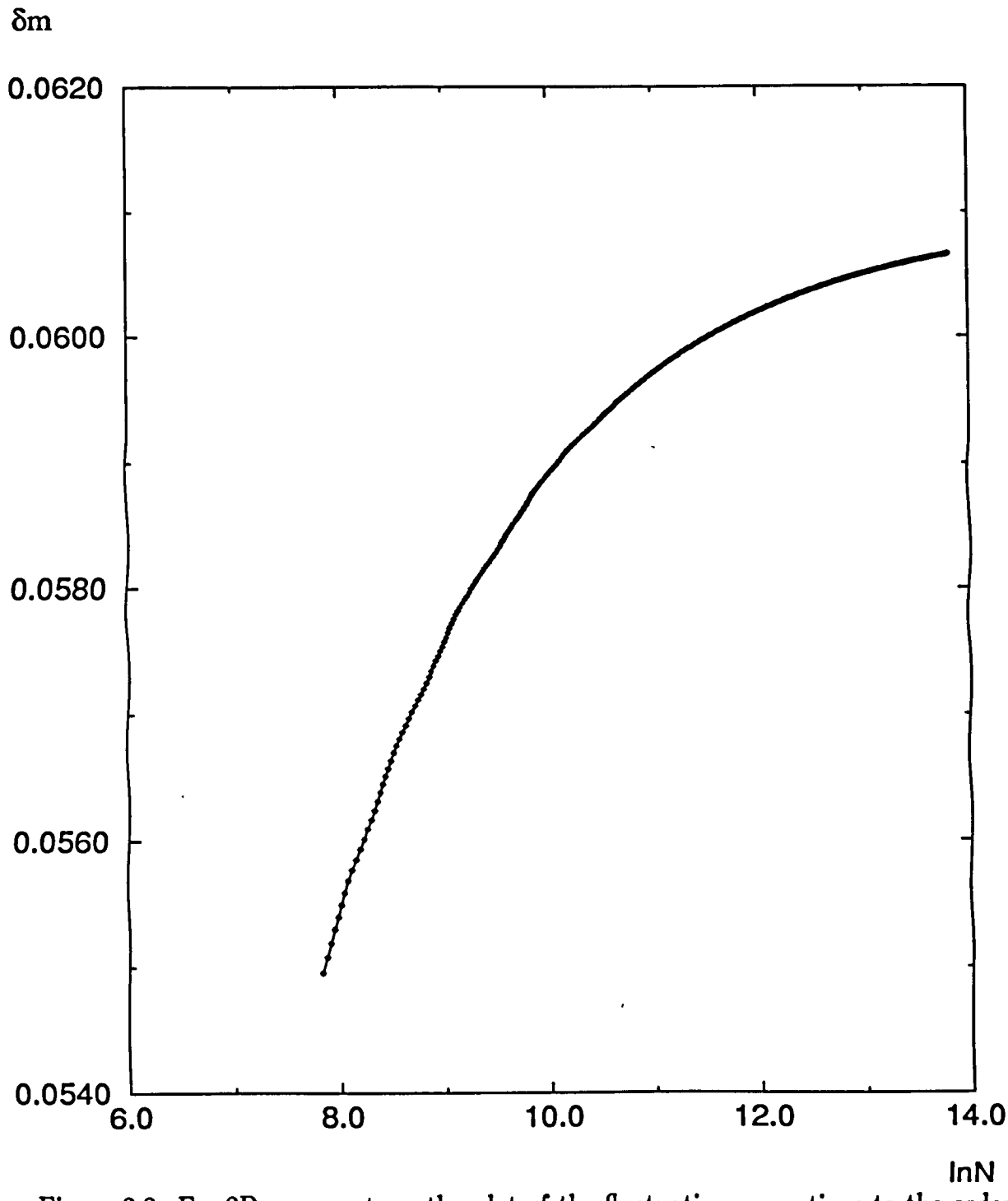

Figure 2.2: For 2D pure system, the plot of the fluctuation corrections to the order parameter, δm v.s. lnN. We can see that δm is finite.

2.3 GAUSSIAN THEORY FOR DIRTY BOSONS

As mentioned earlier, the main feature of the gaussian theory for dirty bosons is to include the gaussian or quadratic quantum fluctuations into the Hamiltonian (2.2) by spinwave approximation. This quadratic Hamiltonian can be diagonalized by a Bogoliubov transformation. In this section, I derive the effective Hamiltonian for disordered boson systems.

I first generalize Hamiltonian (2.2) to arbitrary spin S by rescaling $J \rightarrow J/S^2$ and $h_j \rightarrow h_j/S$. In the infinite S limit, the spins behave classically. Taking the z-axis as the ordering axis, ones find the spin on site j to lie on the $y-z$ plane at angle θ_j from the z-axis, with $\{\theta_j\}$ given self-consistently by

$$sin\theta_j J \sum_{<j'>} cos\theta_{j'} = h_j cos\theta_j \ , \tag{2.18}$$

where $< j' >$ indicates nearest neighbors of the site j. The self-consistent eq.(2.18), can be solved iteratively to get a set of classical angles $\{\theta_i\}$. For a pure system, the system is ordered in the z direction and eq.(2.18) reduces to $(\theta_i = \theta, h_i = h)$

$$tan\theta = \frac{h}{zJ} \ , \tag{2.19}$$

where z is the number of nearest neighbor.

In terms of hard-core boson operators, the classical spin ground state described by (2.18) corresponds to a BCS wavefunction.

$$|\Psi_{BCS}>= \prod_j (sin\varphi_j + cos\varphi_j b_j^+)|0> \ , \tag{2.20}$$

with $\varphi_j = \pi/4 - \theta_j/2$. As in the BCS wavefunction for superconductivity, ψ_{BCS} can

be projected into a state of definite particle number N_B as;

$$|\psi_G>= P_G \sum_i (cot\varphi_i b_i^\dagger)^{N_B}|0> \quad , \tag{2.21}$$

where the Gutzwiller projection operator P_G eliminates all states with $n_i > 1$. Viewed as a Jastrow wavefunction, evidently $\cot\varphi_i$ plays the role of a condensate of uniform phase but with a non-uniform amplitude.

Minimizing the energy $E =< \Psi_{BCS}|\mathcal{H}|\Psi_{BCS} >$ with respect to $\{\theta_j\}$, one recovers (2.18). In this state, the order parameter

$$b \equiv \frac{1}{N}\overline{< \Psi_{BCS}|\sum_j b_j|\Psi_{BCS} >} = \frac{1}{2N}\overline{\sum_j cos\theta_j} \quad , \tag{2.22}$$

the overline in the above equation implying the configuration average in eq.(2.22) which is equivalent to the in-plane magnetization of the classical spins (with $S = 1/2$) considered previously. The quantum fluctuations described by the spin-wave theory correspond to gaussian fluctuations about this Gutzwiller state. For the classical ground state, LRO persists for arbitary strong disorder, as revealed by the solution to eq.(2.18) having all $\cos\theta_j \neq 0$ independent of the value of h. This is true even if $h >> sJ$. In that case, the $h_i S_i^y$ term will dominate. This term would prefer every spin to be either parallel or anti-parallel to the y-axis, depending on the sign of a random field h_i. However, there will be of the order $(J/h)^2$ spins which will have sufficiently weak y-fields that they prefer to cant into the xz-plane and form nucleation centers for ferromagnetic ordering in this plane.

As one can see from the above construction, the ground state of the classical spin is always ordered. The result of $cos\theta_i$ v.s. i for 1D with $N = 200$ (where i is a site idex) is shown in fig. 2.3 for both weak disorder (solid line) and strong disorder (dotted line). As one can see in this figure, for weak field case all the $cos\theta_i \approx 1$. While for the strong field, due to the nature of the random field distribution, even though most sites have strong fields, some sites have very small (or zero) fields. On

these sites, $cos\theta_i$ will be closed to 1, while between them, $cos\theta_i$ will be small but nevertheless non-zero.

To form a spin wave theory, local rotation about the x-axis is performed so that each classical spin points along the new z-axis. After rotation eq.(2.2) becomes

$$\mathcal{H} = -\frac{J}{s^2}\sum_{<i,j>}(S_i^x S_j^x + cos\theta_i cos\theta_j S_i^z S_j^z + sin\theta_i sin\theta_j S_i^y S_j^y$$
$$-sin\theta_i sin\theta_j S_i^y S_j^z - cos\theta_i sin\theta_j S_i^z S_j^y - \sum_j \frac{h_j}{S}(sin\theta_j S_j^z + cos\theta_j S_j^y) \ . \qquad (2.23)$$

The usual Holstein-Primakoff transformation [11] of the spins into boson operators given by eq.(2.4) now can be defined in the rotated frame. To order $1/S$, one arrives at a quadratic Hamiltonian for the bosons [5]:

$$\begin{aligned}\mathcal{H} &= \mathcal{H}_{classical} + \frac{1}{S}\mathcal{H}_{SW} \\ &= -J\sum_{<i,j>} cos\theta_i cos\theta_j - \sum_j h_j sin\theta_j - \frac{1}{2S}\sum_{<i,j>}(J_{ij}a_i^\dagger a_j + K_{ij}a_i a_j) \\ &\quad + H.C.) + \mathcal{O}(\frac{1}{S^{3/2}}) \ , \end{aligned} \qquad (2.24)$$

where $J_{ij} = J(1 + sin\theta_i sin\theta_j) + \frac{h_j}{sin\theta_j}\delta_{ij}$ and $K_{ij} = J(1 - sin\theta_i sin\theta_j)$. Eq.(2.24) describes gaussian fluctuations of strength $1/S$ about the classical ground state. In ref. [5], eq.(2.24) is studied perturbatively for weak disorder. In this dissertation, I have diagonalized eq.(2.24) numerically on several finite-sized lattices, and have not limited myself to weak disorder. This enables me to study the destruction of LRO. Eq.(2.24) is formally diagonalized by a Bogoliubov transformation [12], such that

$$[\mathcal{H}, \gamma_\alpha] = \omega_\alpha \gamma_\alpha \ , \qquad (2.25)$$

where ω_α is the excitation energy. This transformation is accomplished by taking

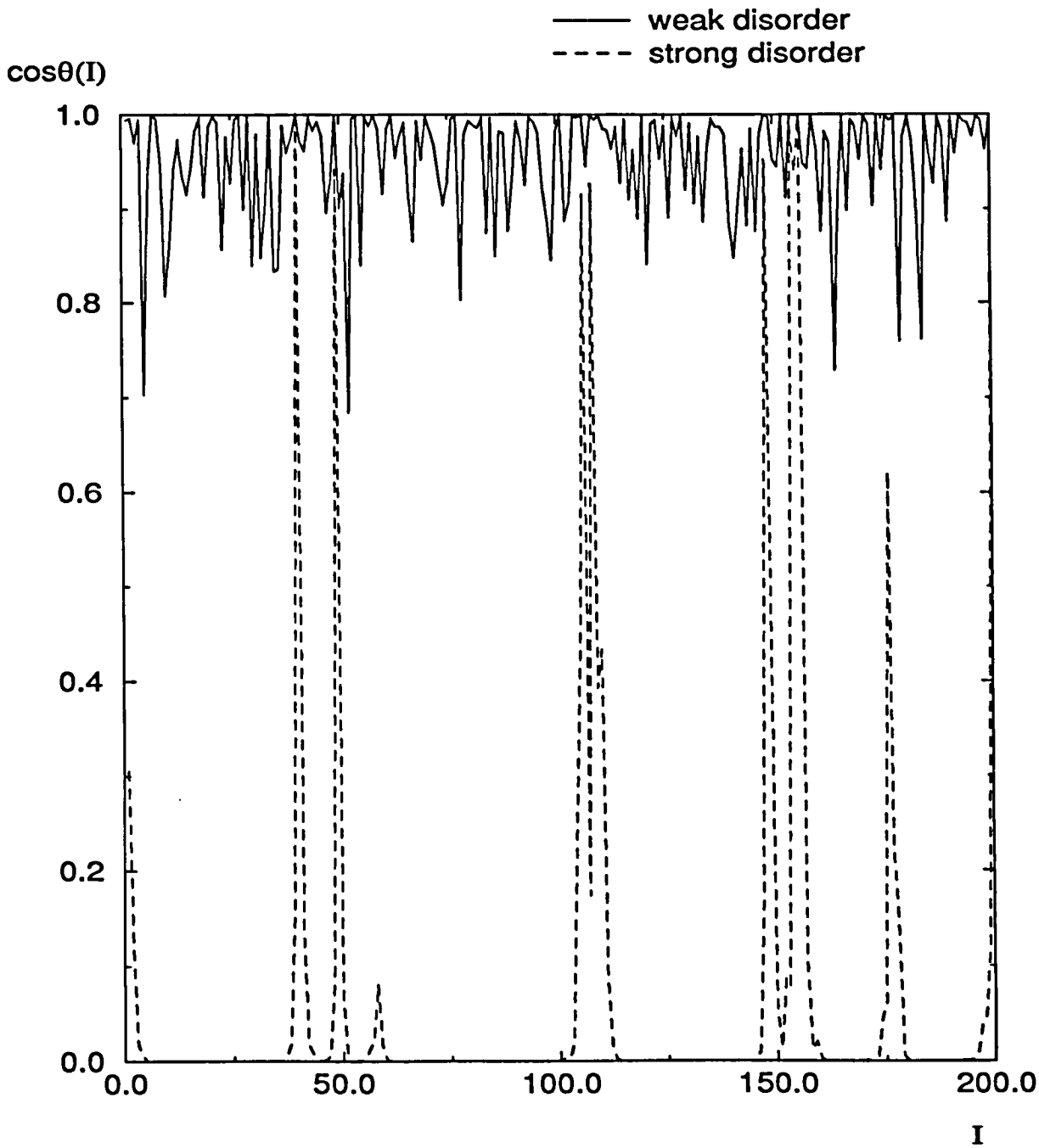

Figure 2.3: The plot of $cos\theta_i$ v.s. site i for both weak disorder and strong disorder are plotted in the same graph. The dotted line is for strong disorder and solid line is for weak disorder. For both cases, all $cos\theta_i \neq 0$. For weak disorder, all $cos\theta_i \approx 1$. For strong disorder, $cos\theta_i$ is very small except at the sites where $|h_i|$ are small.

linear combinations of creation and annihilation operators:

$$\gamma_\alpha = \sum_\alpha (u_{j\alpha} a_j + v_{j\alpha} a_j^\dagger) \ . \tag{2.26}$$

And for the ground state, $\gamma_\alpha |0> = 0, \forall \alpha$. To satisfy (2.25), the coefficients $u_{j\alpha}$, $v_{j\alpha}$ must obey the generalized eigenvalue equation

$$\begin{pmatrix} -\mathrm{J}_{jj'} & -\mathrm{K}_{jj'} \\ \mathrm{J}_{jj'} & \mathrm{K}_{jj'} \end{pmatrix} \begin{pmatrix} u_{j'\alpha} \\ v_{j'\alpha} \end{pmatrix} = \omega_\alpha \begin{pmatrix} \delta_{jj'} & 0 \\ 0 & -\delta_{jj'} \end{pmatrix} \begin{pmatrix} u_{j'\alpha} \\ v_{j'\alpha} \end{pmatrix} \ . \tag{2.27}$$

For N sites, this is a $2N \times 2N$ matrix with $2N$ eigenstates. The $\gamma's$ are bosons operators if

$$\begin{pmatrix} u_{j\alpha} & v_{j\alpha} \end{pmatrix} \begin{pmatrix} \delta_{\alpha\alpha'} & 0 \\ 0 & -\delta_{\alpha\alpha'} \end{pmatrix} \begin{pmatrix} u_{j'\alpha'} \\ v_{j'\alpha'} \end{pmatrix} = \delta_{\alpha\alpha'} \ . \tag{2.28}$$

Since I want the solution to be in the form

$$\mathcal{H}_{SW} = E^0 + \sum_\alpha \omega_\alpha \gamma_\alpha^\dagger \gamma_\alpha \ , \tag{2.29}$$

the non-hermitian matrix (2.27) has to be normalized by the conditions (2.28). The quasiparticle operators $\gamma_\mu^\dagger$ obey Bose commutation relations: $[\gamma_\mu, \gamma_{\mu'}^\dagger] = \delta_{\mu\mu'}$ and $[\gamma_\mu, \gamma_{\mu'}] = 0$.

Note that if $\binom{u}{v}$ is a solution with excitation energy ω, then $\binom{v}{u}$ is a solution with $-\omega$. However, only one of these can be consistent with eq.(2.28), and the other is unphysical, leaving me with N physical solutions. The Goldstone mode, corresponding to uniform spin rotation about y-axis in(1.18),is given by $u_i = v_i \propto cos\theta_i$.

From eq.(2.26), I can write down the quantum fluctuation, $\langle a_i^\dagger a_i \rangle$ in term of canon-

ical varibles,

$$\begin{aligned} \langle a_i^\dagger a_i \rangle &= \langle (u_{i,\alpha}\gamma_\alpha^\dagger + v_{i\alpha}\gamma_\alpha)(u_{i\alpha}\gamma_\alpha + v_{i\alpha}\gamma_\alpha^\dagger) \rangle \\ &= \sum_\alpha v_{i\alpha}^2 \ , \end{aligned} \tag{2.30}$$

where the above result in eq.(2.26) is satisfied by

$\langle [\gamma_i^\dagger, \gamma_j] \rangle = \langle [\gamma_i, \gamma_j] \rangle = 0$, $\langle [\gamma_i, \gamma_j^\dagger] \rangle = \delta_{ij}$.

The order parameter, $\sum_i < S_{iz} >$ in the original spin coordinate systems, is given by

$$m = \frac{1}{N}\overline{\sum_i cos\theta_i (S - < a_i^\dagger a_i >)} = m_{classical} - \delta m \ , \tag{2.31}$$

where the overline here implies the configuration average. The first term, $m_{classical}$, is the classical ($S = \infty$) condensate. δm, is the reduction of order parameter due to quantum fluctuations. From (2.30), δm can be written as

$$\delta m = \frac{1}{N}\sum_i cos\theta_i v_{i\alpha}^2 \ . \tag{2.32}$$

2.4 NUMERICAL APPROACH

Within the gaussian model, I first solve the classical Hartree equation of motion eq.(2.18), for a given configuration to get a set of classical angle $\{\theta_i\}$. This can be accomplished by numerical iteration. This solution will give the parameters in the gaussian Hamiltonian. Then a numerical diagonalization via Bogoliubov transformation is performed on finite lattices with periodic boundary condition to get both eigenenergies and eigenstates. For N sites, the matrix size will be $2N \times 2N$ real non-symmetric matrices with N *physical eigenstates* (as remarked earlier, only half of the eigenstates is consistent with the condition in eq.(2.28), the other half are unphysical). Since the calculation is done on finite size system, I perform a finite size scaling and extrapolate $N \rightarrow \infty$ to get the results for large system. For disordered

systems of finite size N, the physical quantities are not self-averaged and the results are averaged over many disordered configurations. Calculations in 1D are done on lattices of size 50 - 120, averaging over 500 configurations for each value of $\Delta \equiv J/h$ (small Δ implies strong disorder) and 2D on 6x6 to 15x15 lattices averaging over 400 configurations. Extrapolating the solution to infinite size ($N \rightarrow \infty$), ones find an approximate theory of the ground state and excitations of the systems.

Bibliography

[1] M. Ma, B.I. Halperin and P.A. Lee, *Phys. Rev. B*, **34**, 3136 (1986).

[2] M.P.A. Fisher, P.B. Weichman, G. Grinstein and D.S. Fisher, *Phys. Rev. B* , **40**, 546 (1989).

[3] L. Zhang and M. Ma, *Phys. Rev. A*, **37**, 960 (1988).

[4] L. Zhang and M. Ma, *Phys. Rev. B*, **45**, 4855 (1992); L. Zhang, X.Q. Wang, *Phys. Rev. B*, **47**, 11518 (1993).

[5] L. Zhang, *Phys. Rev. B*, **47**, 14364 (1993).

[6] Our philosophy here deviates from the recent study by Huang and Meng (Phys. Rev. Lett., **69**, 644 (1992)), who look for the transition by considering $\delta\rho_s = -\rho_s$.

[7] K.G. Singh and D.S. Rokhsar, *Phys. Rev. B*, **46**, 3002 (1992).

[8] K. Runge, *Phys. Rev. B*, **45**, 13136 (1992).

[9] W. Krauth and N. Trivedi, *Europhys. Lett.* **14**, 627 (1991); N. Trivedi, D.M. Ceperley, and W. Krauth and N. Trivedi, *Phys. Rev. Lett.*, **67**, 2307 (1991); R.T. Scalettar, G.G. Batrouni, and G.T. Zimanyi, *Phys. Rev. Lett.*, **66**, 3144 (1991); E.S. Sorensen, M. Wallin, S.M. Girvin and A.P. Young, *Phys. Rev. Lett.*, **69**, 828 (1992).

[10] M. Gutzwiller, Phys. Rev. **A137**, 1726 (1964).

[11] T. Holstein and H. Primakoff, *Phys. Rev.*, **58**, 1908 (1940).

[12] E.M. Lifshitz and L.P. Pitaevskii, *Statistical Physics (Part 2)*, Pergamon Press (1980).

[13] E. Lieb, T. Schultz and D. Mattis, *Ann. Phys. (N.Y.)*, **16**, 407 (1961).

[14] G. Gomez-Santos and J.D. Joannoloulos, *Phys. Rev. B*, **36**, 8707 (1987).

[15] T. Kennedy, E.H. Lieb and B.S. Shastry, *Phys. Rev. Lett.*, **61**, 2582 (1988).

[16] T. Kennedy, E.H. Lieb and B.S. Shastry, *Phys. Rev. Lett.* , **61**, 2582 (1988).

[17] M. Makivic, N. Trivedi and S. Ullah, *unpublished*

Chapter 3

GROUND STATE OF DISORDERED BOSON SYSTEMS

As discussed in the introduction chapter, the two phases (superfluid and Bose-glass phases) are characterized by the presence or absence of the LRO. In the presence of weak disorder, the ground state of the system is still a superfluid with a finite superfluid density. The condensate density of the disordered bosons is non-uniform and is reduced with increasing disorder. The low-lying excitations of a uniform Bose condensate are phonons with a linear dispersion, $\omega = ck$. The corresponding low-temperature specific heat in the ordered phase is characterized by $C_v \sim T^d$ which is quadratic in T for 2D. It has been shown [1] that for $S = 1/2$ any amount of disorder will change the power law behavior of the spin-spin correlation function to an exponential one in 1D, signifying the instability of superfluidity of the hard-core boson system. For general boson sytems, a renormalization group study [2] shows that superfluidity may persist in the presence of (weak) disorder, if the value of the exponent η of the correlation function in the corresponding pure system is less than a critical value $\eta_c = 1/3$.

In this chapter, I will concentrate on the ground state properties of disordered bosons systems, namely, the question of LRO and the superfluid density in the gaussian theory. Concerning the LRO, the first question one might ask is, 'What would be the instability criteria of LRO in the gaussian theory?' Since the Hartree solution fails to give an insulating phase, I wish to investigate whether the zero-point quantum fluctuations can cause the instability of the superfluid phase. The possible scenarios for the destruction of LRO are:

1). Diverging fluctuations in the order parameter.

2). Negative excitation energies.

3). Complex excitation energies.

My results show that criteria 1) signifies the instability of LRO in the gaussian theory and a transition occurs with finite disorder.

First, let me discuss the result in 1D. As remarked in chap.2, the reduction in the order parameter due to gaussian fluctuations, δm, diverges logarithmically with

N_{sample}	$SIZE$	$\frac{\delta m}{m}$	σ	$\frac{\sigma}{\sqrt{N_{sample}}}$
500	50	2.7903E-01	5.043E-02	2.25E-03
500	60	3.1431E-01	4.604E-02	2.06E-03
500	70	3.4140E-01	4.265E-02	1.91E-03
500	80	3.6859E-01	3.987E-02	1.18E-03
500	90	3.9239E-01	3.759E-02	1.68E-03
500	100	4.1691E-01	3.566E-02	1.60E-03
500	110	4.3847E-01	3.400E-02	1.52E-03
500	120	4.6183E-01	3.255E-02	1.46E-03
100	300	7.3334E-01	4.297E-02	4.30E-03

Table 3.1: Data table of $\frac{\delta m}{m}$ for 1D, $\Delta = 0.5$

system size even in the pure case (see fig.2.1). As argued in chap.2, and later in this chapter, I take the log N behaviour to indicate that the ground state lacks true LRO, but has algebraically decaying correlation functions. As disorder is introduced, δm continues to diverge as lnN, with the slope increasing with disorder, and the system is still a superfluid. However, at a critical disorder, the lnN behaviour is replaced by a stronger divergence. Thus, I argue that the transition is signified by δm diverging faster than lnN. This result is shown in fig.3.1, with the critical value of $\Delta = \Delta_c \approx 0.6$ independent of S (recall $\Delta = \frac{J}{h}$ and lesser value of Δ implies stronger disorder). To ensure that $\Delta = 0.5$ diverges faster than lnN, I perform the calculation for the system size up to N=300. This result is shown in fig. 3.2.

Thus, the transition occurs at finite disorder. Since in the gaussian theory, the Hamiltonian is comprised of a classical part and spin waves, $\mathcal{H} = \mathcal{H}_{classical} + \frac{1}{S}\mathcal{H}_{SW}$, the theory becomes exact in the large S limit. Since there is no transition for $S = \infty$, there will be a discontinuity between $S \rightarrow \infty$ and $S = \infty$, i.e. quantum spins do not extrapolate smoothly to classical spins.

The behaviour of the fluctuation, δm, as a function of disorder Δ is shown in fig.3.3 for size N =120. We can see δm increases with the decreasing Δ (or increasing disorder). The behaviour of δm as a function of size can be summarized as follows.

In the ordered phase, $\Delta > \Delta_c$, δm is linearly proportional to lnN with the slope $\beta(\Delta)$ increasing with increasing disorder, i.e. decreasing Δ. This is shown in fig.3.1 where

$$\delta m = \beta(\Delta) lnN \ . \tag{3.1}$$

In the Bose glass phase, $\Delta < \Delta_c$, δm is characterized by

$$\delta m \simeq N^{\theta} \ . \tag{3.2}$$

The results show the value of $\theta = 0.576 \pm 0.043$ for $\Delta = 0.5$ and $\beta(1.5) = 0.106 \pm 0.002$, $\beta(0.6) = 0.145 \pm 0.001$

Unlike the case of 1D, for 2D δm is finite for the pure case (shown in Fig.2.2) as $N \rightarrow \infty$, which implies the LRO is stable against quantum fluctuations. This is consistent with the exact result for $S = 1/2$ [10]. Disorder enhances the fluctuations but δm remains finite up to a critical point. Fig. 3.4 shows $\delta m/m$ v.s. ln N for different values of Δ. As $N \rightarrow \infty$, δm is finite up to a critical value of $\Delta = \Delta_c$, with $0.08 < \Delta_c < 0.1$. For $\Delta < \Delta_c$, $\delta m \rightarrow \infty$ as $N \rightarrow \infty$, signifying the instability. This result should be contrasted to the uniform-field case discussed in chap.2, where, $m_{classical} \rightarrow 0$, while $\frac{\delta m}{m_{classical}} \rightarrow 0$ at the transition, suggesting that the transition is a classical one and quantum mechanics plays no role. Here, $m_{classical}$ remains finite while δm diverges strongly indicating a quantum transition. In fig.3.5, δm v.s. Δ, for a system size 15×15 shows the fluctuations increasing with increasing disorder (decreasing Δ). The transition is signified by the rapid rise in δm near the critical point ($\Delta < 0.1$). Similarly, in fig.3.3 for 1D (system size N=120), I also see the fluctuations increasing with increasing disorder and δm rising rapidly near the critical point ($\Delta \leq 0.6$).

Thus, in contrast to the classical case which always has a long-ranged order in the ground states, there is a transition from a superfluid phase with algebraic spin-spin correlation function in 1D and with true LRO in 2D superfluid phase to a disordered

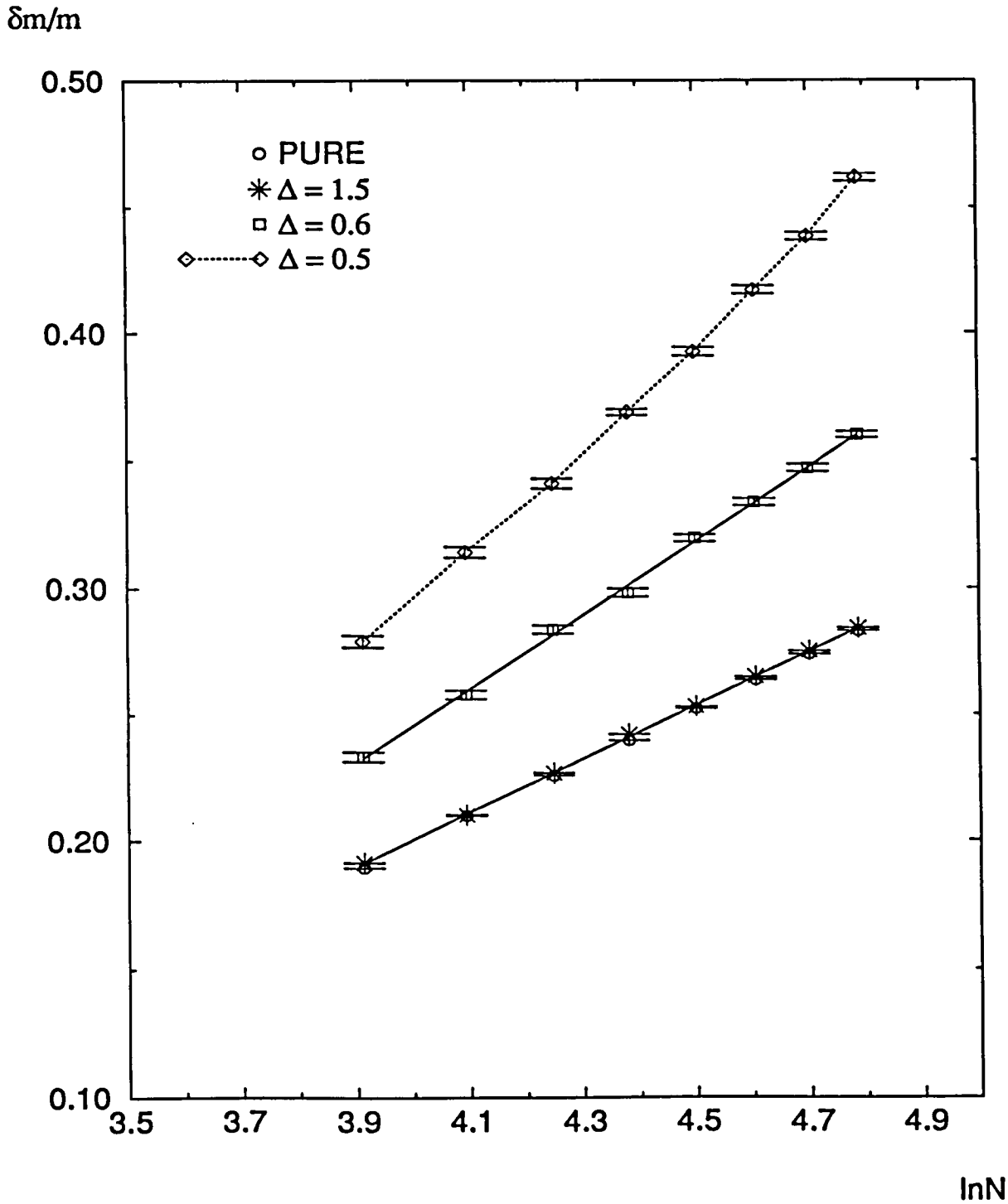

Figure 3.1: Fluctuation corrections to the order parameter $\frac{\delta m}{m}$ is plotted against logN. The divergence becomes faster than logN as Δ exceeds a critical value $\Delta_c \approx 0.6$. The solid lines are obtained through a linear fit and the dashed line is a guide to the eyes.

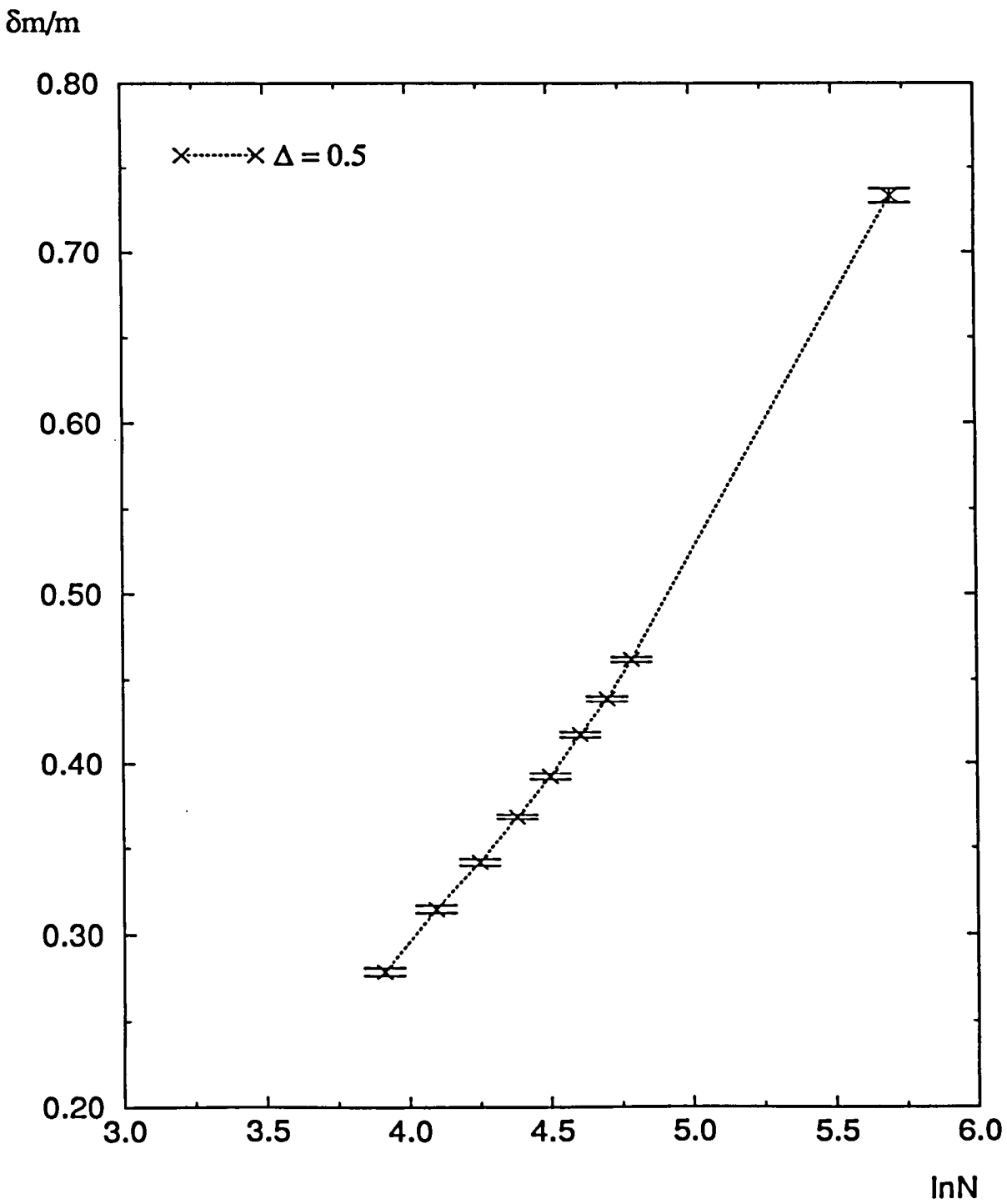

Figure 3.2: $\frac{\delta m}{m}$ v.s. lnN in 1D for $\Delta = 0.5$. The largest size shown in this figure is N=300.

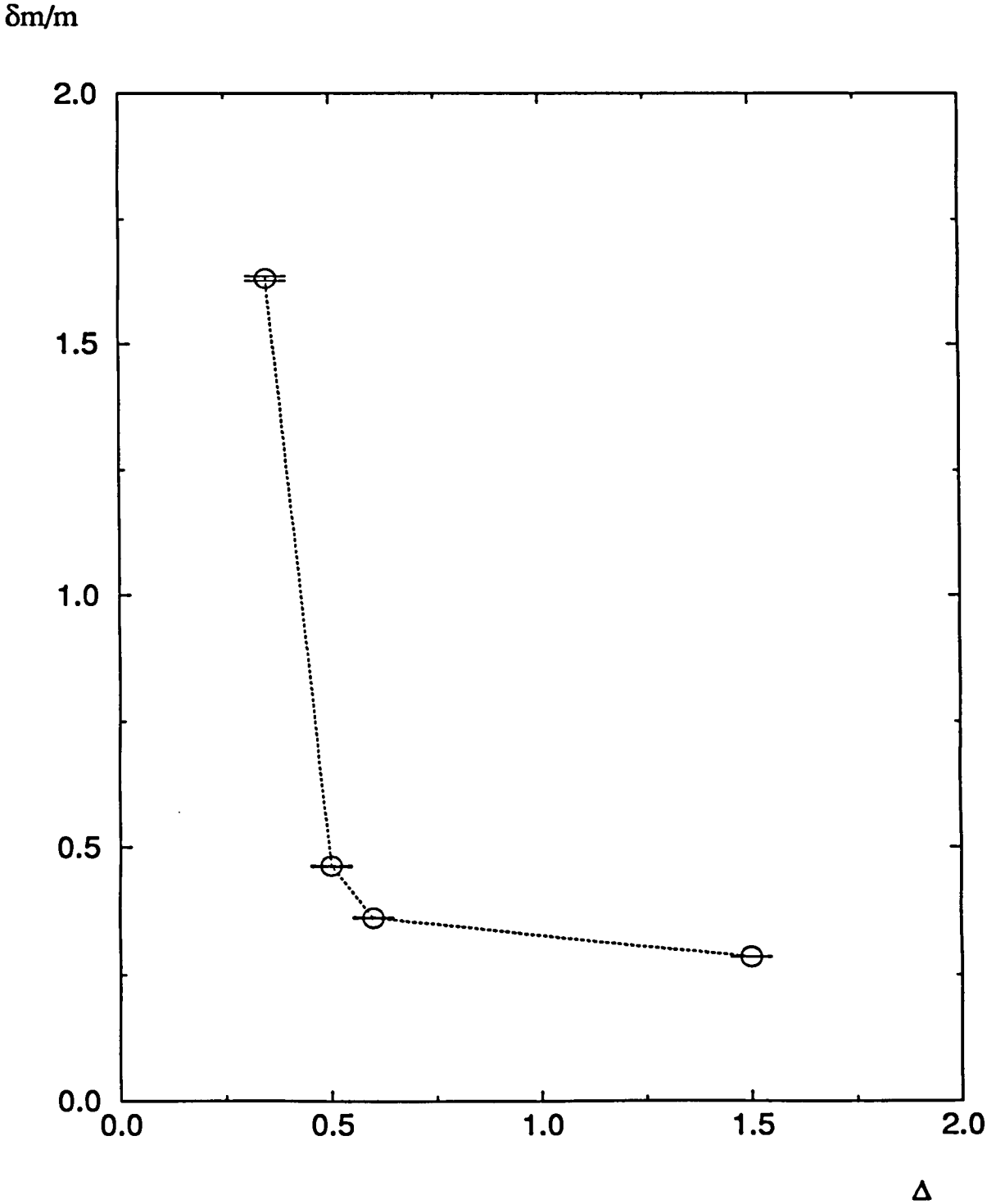

Figure 3.3: Show $\frac{\delta m}{m}$ v.s. Δ in 1D for size N=120. As one can see in this figure, δm decreases with the decreasing Δ (the increasing disorder).

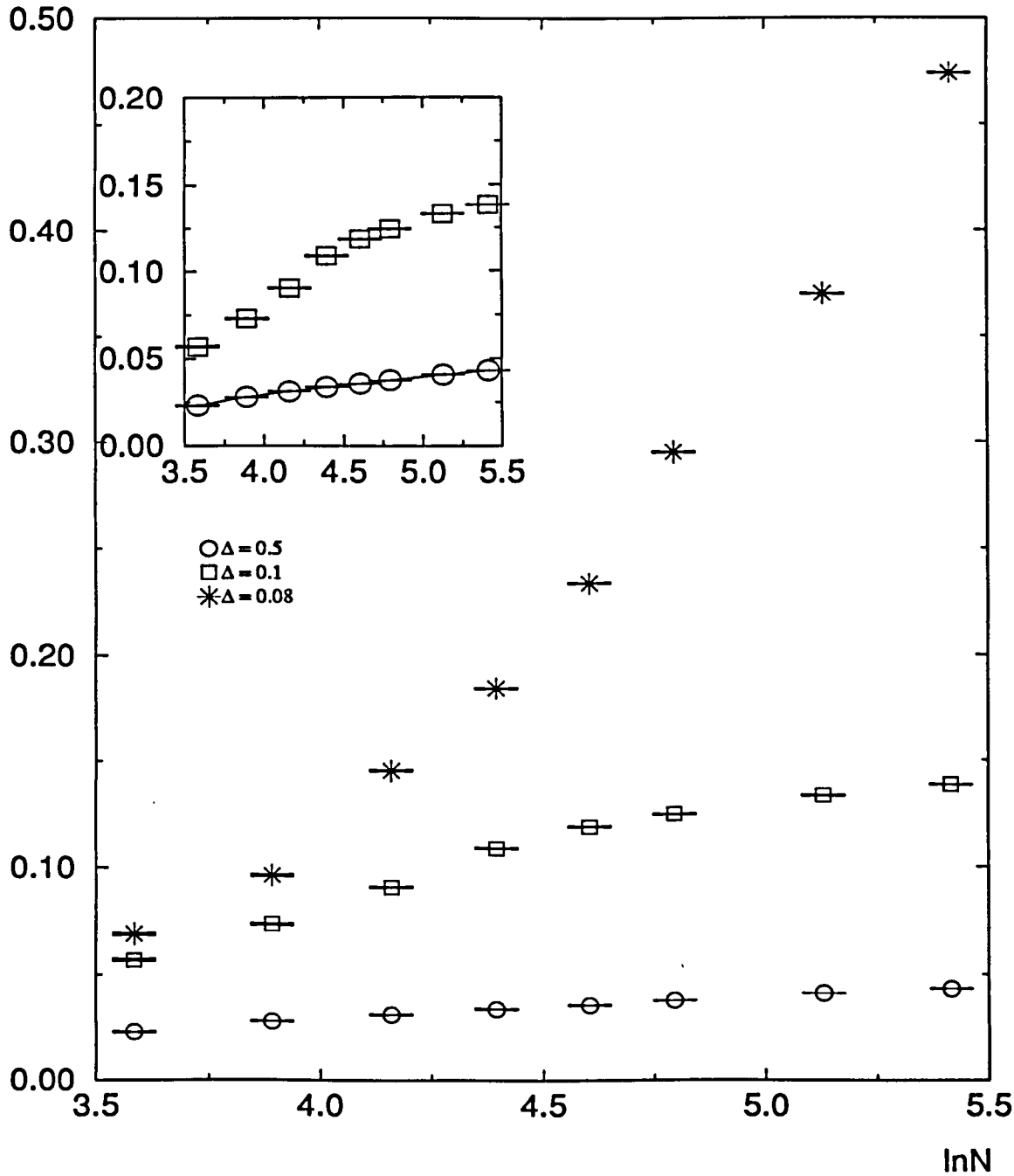

Figure 3.4: The same as Fig.3.1, plotted for 2D systems. For 2D, δm is finite for weak disorder and diverges for $\Delta < \Delta_c$, where the critical value is between 0.1 and 0.08. δm for $\Delta = 0.5$ and 0.1 are replotted (in the small frame on the top left of this figure) on the different scale to show clearly the δm is finite as $N \to \infty$.

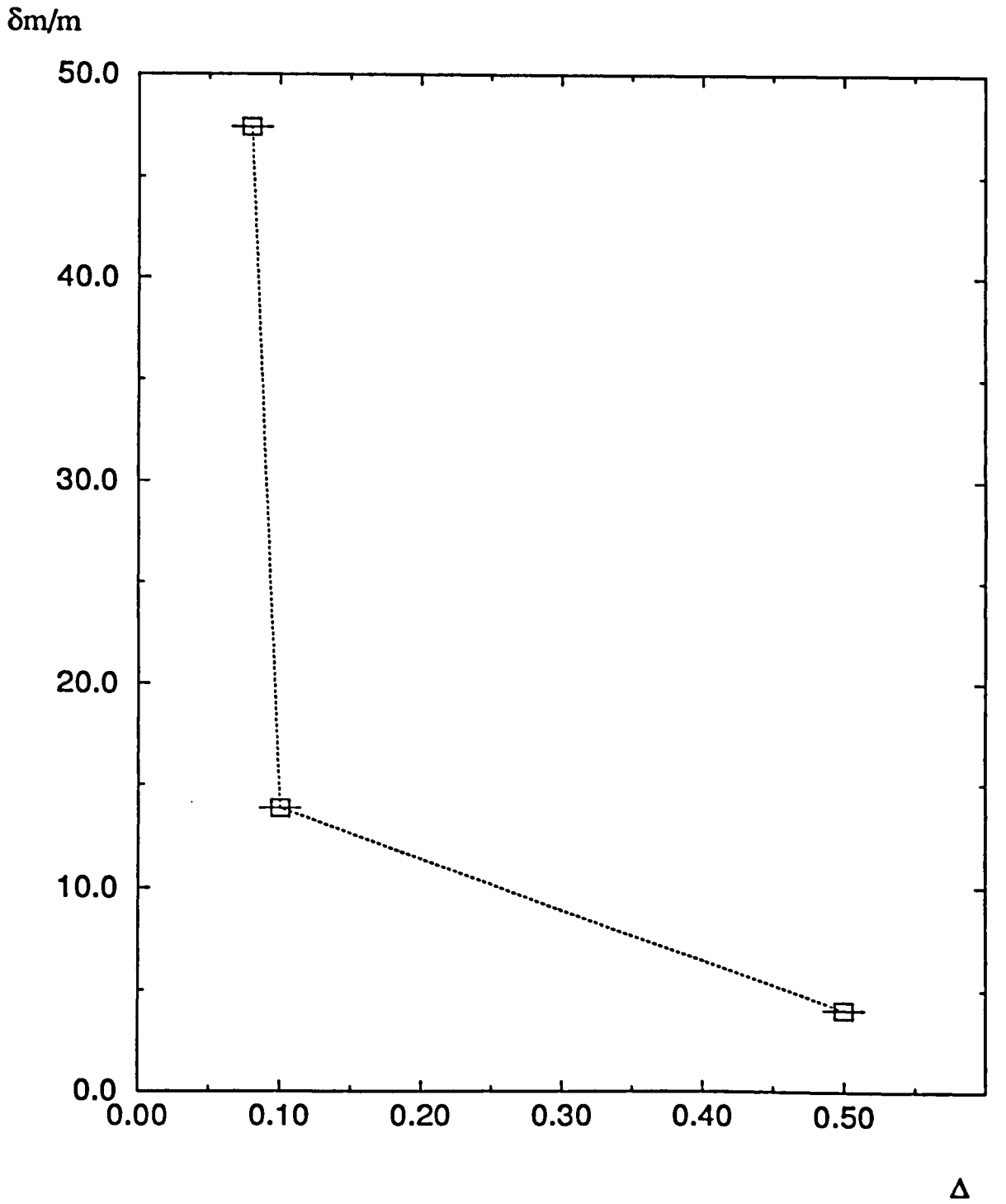

Figure 3.5: δm v.s Δ in 2D for system size 15×15. The δm decreases with the increasing disorder (or decreasing Δ).

phase in the gaussian theory. Since in this model, the classical ground state is the Gutzwiller state, $1/S$ in this case serves as an expansion parameter for quantum fluctuations. I find quantum fluctuations are sufficient to destroy LRO with a finite critical disorder. What is the phase diagram of disorder v.s. $\frac{1}{S}$ in the gaussian theory? In the gaussian theory, the critical disorder is independent of S, including $S \to \infty$. There is a discontinuity between $S \to \infty$ and $S = \infty$. However, to higher order in $\frac{1}{S}$, one expects to have the critical disorder depend on $\frac{1}{S}$. Since we know $\Delta_c = 0$ for $S = \frac{1}{2}$ [1], we expect Δ_c to decrease with decreasing S, $\Delta_c \to 0$ at some $S_c \geq \frac{1}{2}$. A schematic plot of Δ_c v.s. $\frac{1}{S}$ in 1D is shown in fig. 3.6, where the dashed line represents the result of the gaussian theory with the wiggle line represents the discontinuity between $S \to \infty$ and $S = \infty$. The solid line in fig.3.6 shows the expected behaviour beyond the gaussian theory. The schematic phase diagram for 2D is similar, except the ordered phase now has a true LRO, and Δ_c should be finite for $S = \frac{1}{2}$. What about a phase diagram of disorder v.s. U? Since the physics is sufficient general, this result should hold true for more general Hubbard-U type models. The differences between hard-core and soft-core are just the parameters involved in the S_{eff} (which are the compressibility, κ, and superfluid density, ρ_s) described in the appendix of this chapter. However, the general feature of main physics remains the same[14]. Since bosons will condense into the lowest energy (localized) state for $U = 0$, the critical disorder = 0. What about $U \to 0$? The problem is that increasing U both affects the classical condensate and enhances quantum fluctuations. In fact, the Hartree solution becomes extended with infinitesimal U(as remarked in chap.1) provided Un remains finite. Thus, the $U \to 0$ limit should not be qualitatively different from the limit of $1/S \to 0$, and the critical disorder is again finite. Thus fig. 3.6 can equally well be a schematic diagram of disorder $(\frac{1}{\Delta})$ v.s. U, with the wiggle line indicating the discontinuity between U=0 and $U \to 0$. The crossed line in this fig. shows the conjecture of Giamarchi and Schultz[2] which based on our results we believed to be incorrect. The result of the gaussian theory that Δ_c is finite as $U \to 0$ is in agreement

with numerical works performed on the disordered boson Hubbard model[3].

In 1D, ref.[2] predicted that the renormalized critical exponent η is universal and equal to 1/3 at the superfluid-Bose-glass phase transition based on a perturbative renormalization group calculation. One might ask what the value of η is in the gaussian theory. The spin wave theory as formulated cannot rigorously produce a power-decaying correlation function (see appendix). However, η and β, the coefficient of $\ln N$ in $\delta m/m$, are proportional in the pure case. Assuming the relation holds even with disorder, one finds

$$\frac{\eta_c}{\eta_{pure}} = \frac{\beta_c}{\beta_{pure}} \quad . \tag{3.3}$$

From the slope of the $\Delta = 0.6$ (the closest point to Δ_{c+}) curve in Fig. 3.1, I estimate $\eta_c/\eta_{pure} \approx 1.4$ (1.37$\pm$0.03). This ratio is universal, while η_c is not. $\eta_c \to 0$ as $1/S \to 0$ in gaussian model, or as $U \to 0$ in Hubbard type models.

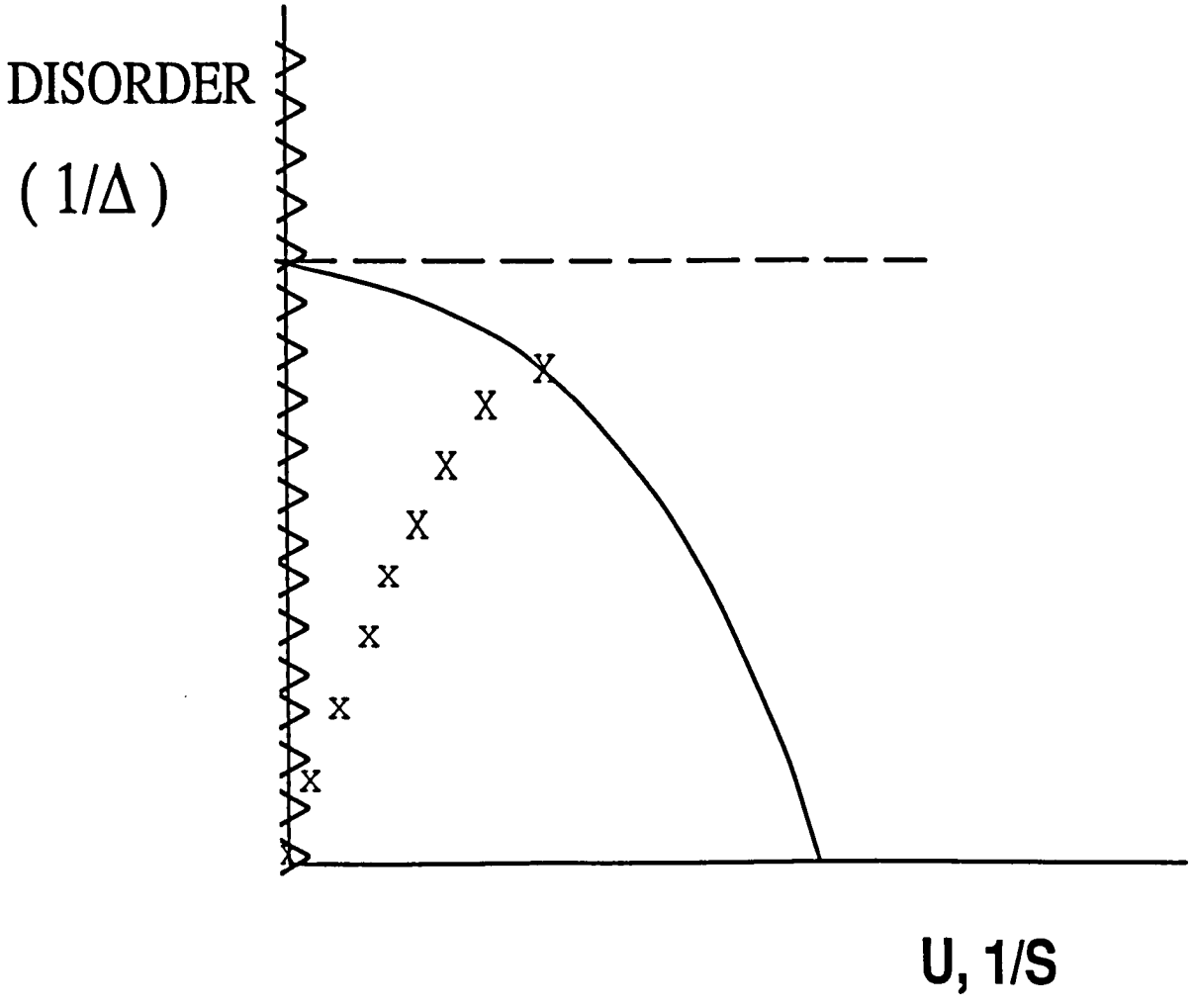

Figure 3.6: Schematic plot of phase diagram of disorder (Δ) v.s. repulsion (U). The $U \rightarrow 0$ limit is taken with Un remaining finite. Dotted lines show the result of our gaussian theory. Solid lines show expected behaviour beyond our approximation. The discontinuity between $U, \frac{1}{S} \rightarrow 0$ and $U, \frac{1}{S} = 0$ is introduced by the wiggle lines. Crosses show conjecture by Giamarchi and Schulz.

APPENDIX

In the long wave length limit, the effective action, S_{eff}, for 1D is given by[14],

$$S_{eff} = \frac{1}{2}\int dx \int d\tau \frac{\rho_s}{m}(\partial_x\varphi)^2 + \kappa(\partial_\tau\varphi)^2 \ , \tag{3.4}$$

where ρ_s and κ are superfluid density and compressibility respectively. And the speed of sound, C, is given by $\sqrt{\frac{\rho_s}{m\kappa}}$. Next I am going to show that the correlation function of the order parameter $< \psi(x,\tau)\psi(x',\tau) > \approx R^{-\eta}$ in the limit $R = |x - x'| \to \infty$. Since the effective action, S_{eff}, is quadratic,

$$\begin{aligned} \langle\psi(x,\tau)\psi(x',\tau')\rangle &= n\langle e^{i(\varphi(x,\tau)-\varphi(x',\tau'))}\rangle \\ &= ne^{-\frac{1}{2}\langle(\varphi(x,\tau)-\varphi(x',\tau'))^2\rangle} \ , \end{aligned} \tag{3.5}$$

where in the above result, I assume the density fluctuations,
$< \delta n(r)^2 >$ are small. The propagator of the above effective action is given by

$$\langle\varphi(k,\omega)\varphi(k',\omega')\rangle = \frac{m}{\rho_s k^2 + m\kappa\omega^2}\delta_{k,k'}\delta_{\omega,\omega'} \ , \quad so \tag{3.6}$$

$$\langle(\varphi(x,\tau) - \varphi(x',\tau'))^2\rangle = \sum_{\omega,k<k_o} \frac{m}{\rho_s k^2 + m\kappa\omega^2}|e^{i(kx-\omega\tau)} - e^{i(kx'-\omega\tau')}|^2 \ ; \quad then \tag{3.7}$$

$$\begin{aligned} \langle(\varphi(x,\tau) - \varphi(x',\tau'))^2\rangle|_{\tau=\tau'} &= 2m\int\frac{dk}{2\pi}\int\frac{d\omega}{2\pi}\frac{1}{\rho_s k^2 + m\kappa\omega^2} \\ &\quad (1 - cos(k(x - x')) \ , \\ &= \frac{1}{2\pi}\frac{m}{\sqrt{m\rho_s\kappa}}\int\frac{dk}{k}(1 - cosk(x - x')) \ , \\ &= \frac{1}{2\pi}\sqrt{\frac{m}{\rho_s\kappa}}\int_{\frac{1}{R}}^{K_o}\frac{dk}{k} \\ &+ \ non - divergent \ \ term, \\ &\approx -\eta \cdot lnR \ , \end{aligned} \tag{3.8}$$

where $\eta = \frac{1}{2\pi}\sqrt{\frac{m}{\rho_s \kappa}}$. Therefore,

$$\lim_{R\to\infty} \langle \psi(x,\tau)\psi(x',\tau') \rangle \approx R^{-\eta} \ . \tag{3.9}$$

Next I estimate the coefficient of the order parameter reduction, β. Since the order parameter is given by $< \psi >= \psi_o < e^{i\varphi} >$, where ψ_o is its value without fluctuations, the order parameter reduction can be written as,

$$\begin{aligned} \frac{\delta\langle\psi\rangle}{\psi_o} &= e^{-\frac{1}{2}\langle\varphi^2\rangle} - 1 \ , \\ &\approx -\frac{1}{2}\langle\varphi^2\rangle \ , \\ &= \beta \cdot lnR \ . \end{aligned} \tag{3.10}$$

From my result, the value of the slope, β_{pure} is 0.106 ± 0.002 and the slope closes to the critical point is $\beta_c = \beta(\Delta = 0.6)$. Therefore,

$$\frac{\eta_c}{\eta_{pure}} = \frac{\beta_c}{\beta_{pure}} \approx 1.4 \ \ (1.37 \pm 0.03) \ . \tag{3.11}$$

Bibliography

[1] L. Zhang and M.Ma, Phys. Rev. **37**, 960 (1988)

[2] T. Giamarchi and H.J. Schulz, Phys. Rev.**B37**, 325 (1988)

[3] W. Krauth and N. Trivedi, *Europhys. Lett.* **14**, 627 (1991); N. Trivedi, D.M. Ceperley, and W. Krauth and N. Trivedi, *Phys. Rev. Lett.*, **67**, 2307 (1991); R.T. Scalettar, G.G. Batrouni, and G.T. Zimanyi, *Phys. Rev. Lett.*, **66**, 3144 (1991); E.S. Sorensen, M. Wallin, S.M. Girvin and A.P. Young, *Phys. Rev. Lett.*, **69**, 828 (1992).

[4] B.C. Cooker, E. Hebard, E.N. Smith, Y. Takano and J.D. Reppy, *Phys. Rev. Lett.*, **51**, 666 (1983); M.H.W. Chan, K.I. Blum, S.Q. Murphy, G.K.S. Wong and J.D. Reppy, *Phys. Rev. Lett.* , **61**, 1950 (1988); D. Finotello, K.A. Gillis, A. Wong and M.H.W. Chan, *Phys. Rev. Lett.* , **61**, 1954 (1988); G.K.S. Wong, P.A. Crowell, H.A. Cho and J.D. Reppy, *Phys. Rev. Lett.* , **65**, 2410 (1990); M. Larson, N. Mulders and G. Ahlers, *Phys. Rev. Lett.*, **68**, 3896 (1992).

[5] D.K.K. Lee and J.M.F. Gunn, J. Phys. **C2**, 7753(1990).

[6] K. Huang and H.F. Meng, Phys. Rev. Lett., **69**, 664(1992).

[7] K.G. Singh and D.S. Rokshar, to be published.

[8] F. London, Superfluids (Wiley, New York, 1950), Vol. I, p. 27-95.

[9] For a recent discussion of the various criteria of superfluidity, see D. J. Scalapino, S. R. White and S. C. Zhang, Phys. Rev. Lett., **68**, 2830 (1992).

[10] T. Kennedy, E.H. Lieb and B.S. Shastry, *Phys. Rev. Lett.* , **61**, 2582 (1988).

[11] P. Nozieres and D. Pines, *The Theory of Quantum Liquids*, V.II, Addison-Welsley Publishing Company, INC.

[12] E.M. Lifshitz and L.P. Pitaevskii, *Statistical Physics (Part 2)*, Pergamon Press (1980); G.D. Mahan, *Many Particle Physics* Plenum, 2nd Edition, (1990).

[13] L. Zhang, Phys. Rev. **B47**, 14364 (1993).

[14] V. N. Popov, *Functional Integrals in Quantum Field Theory and Stat. Phys.*, Kluwer Academic Pub. (1983).

Chapter 4

SUPERFLUID DENSITY

4.1 INTRODUCTION

In the previous chapter, I calculated the dependence of the order parameter on disorder. The divergence of the reduction due to quantum fluctuations can be interpreted as signifying the destruction of LRO, hence superfluidity. However, the true measure of superfluidity is the superfluid density (as exemplified in 1D without disorder, where there is no true LRO, but ρ_s is nevertheless nonzero). Thus, one would like to calculate ρ_s directly and address the destruction of the superfluidity directly from the superfluid density, as opposed to indirectly through the order parameter. The destruction of superfluidity would then be shown by the vanishing of superfluid density. In the pure case, the paramagnetic current vanishes and only the diamagnetic part contributes to the superfluid density. While for the disordered case, the paramagnetic part is non-zero and increases with increasing disorder. The instability of superfluidity occurs when the paramagnetic part cancels out the diamagnetic part [6, 7, 9].

In this chapter, I will concentrate on the semiclassical approximation to the superfluid density in the gaussian model. Within this model as previously defined , this corresponds to the $S \rightarrow \infty$ limit. My result shows that the paramagnetic term is enhanced by disorder and the superfluid density vanishes at the same critical disorder as that for the order parameter δm for 1D ($0.5 < \Delta_c < 0.6$) and 2D ($0.08 < \Delta_c < 0.1$).

4.2 DESCRIPTION OF MY APPROACH

In 1935, London[8] pointed out that the rigidity in the electronic wave function of the superconductivity will prevent the paramagnetic current from adjusting itself to an applied weak magnetic field. This leads to a finite diamagnetic current proportional to the vector potential. This relationship is known as the *London equation.* The essential difference between the normal and superconducting phase is that the paramagnetic and diamagnetic currents do not cancel in the long wave length limit

in the latter.

The current response function to the vector potential consists of the diamagnetic ($\mathcal{K}_{xx}$) and paramagnetic (current-current correlation function, $\Pi_{xx}(\mathbf{q},\omega)$) part. If $\Pi_{xx}(\mathbf{q}=0,\omega=0)\neq 0$, the system is a perfect conductor. While $\Pi_{xx}(\omega=0,q_x=0,q_y\to 0)\neq 0$ gives rise to the Meissner effect and is related to the superfluid density in the London equation,

$$J_x(q_y) = -\rho_s A_x(q_y) \ , \tag{4.1}$$

where the superfluid density ρ_s is defined as

$$\rho_s = \mathcal{K}_{xx} - \Pi_{xx}(\omega=0,q_x=0,q_y\to 0) \ . \tag{4.2}$$

Although superconductivity is most naturally associated with perfect conductivity, the hallmark of a superconductor is actually perfect diamagnetism (ie. Meissner effect). In the pure case, $\Pi_{xx}(\mathbf{q}=0,\omega=0)$ always vanishes due to translational invariance, giving rise to a perfect conductor. However, $\Pi_{xx}(\omega=0,q_x=0,q_y\to 0)$ does not necessary vanish and whether $\Pi_{xx}=\mathcal{K}_{xx}$ (hence $\rho_s=0$), or $\Pi_{xx}<\mathcal{K}_{xx}$ ($\rho_s>0$) distinguishes a perfect metal from a superconductor. For neutral boson systems like ^4He, ρ_s can still be defined through (4.1). Here the "vector potential" is due to a transverse external probe[11]. Eqs. (4.1) and (4.2) defines superfluidity rigorously. However, with disorder, $\Pi_{xx}(\mathbf{q}=0,\omega=0)$ no longer vanishes by symmetry. In a disordered metal, $\Pi_{xx}(\mathbf{q}=0,\omega\to 0)=\Pi_{xx}(\omega=0,\mathbf{q}\to 0)=\mathcal{K}_{xx}$, while in a disordered superconductor, both $\Pi_{xx}<\mathcal{K}_{xx}$. Thus with disorder, infinite conductivity is sometimes used as a criteria for superfluidity or superconductivity. Yet a third criteria is the sensitivity to the boundary condition, which can be shown by a gauge transformation to be equivalent to infinite conductivity. See ref.[9] for a complete discussion of these criteria of superfluidity or superconductivity.

4.3 LINEAR RESPONSE THEORY FOR LATTICE MODEL

Starting with the hard-core model eq.(2.1), in the presence of a vector potential the hopping term is modified by an additional phase factor $e^{iA_{ij}}$ [9], and the hamiltonian (2.1) can be rewritten as,

$$\begin{aligned}\mathcal{H} &= -t\sum_{<ij>}(e^{iA_{ij}}b_i^\dagger b_j + H.C.) + \sum_i (W_i-\mu)b_i^\dagger b_i \ , \\ &= -t\sum_j\sum_\delta (e^{iA_{j+\delta,j}}b_{j+\delta}^\dagger b_j + e^{-iA_{j+\delta,j}}b_j^\dagger b_{j+\delta}) \\ &+ \sum_i (W_i-\mu)b_i^\dagger b_i \ , \end{aligned} \tag{4.3}$$

where δ implies the unit vector in the positive x, y, z direction.

For small A, to the order of A^2, we recast the hamiltonian (4.3) as

$$\mathcal{H} = \mathcal{H}_0 + \mathcal{H}' \ , \tag{4.4}$$

where

$$\mathcal{H}_0 = -t\sum_j\sum_\delta (b_{j+\delta}^\dagger b_j + b_j^\dagger b_{j+\delta}) + \sum_i (W_i-\mu)b_i^\dagger b_i \tag{4.5}$$

and

$$\begin{aligned}\mathcal{H}' &= -it\sum_j\sum_\delta A_{j+\delta,j}(b_{j+\delta}^\dagger b_j - b_j^\dagger b_{j+\delta}) + \frac{t}{2}\sum_j\sum_\delta A_{j+\delta,j}^2(b_{j+\delta}^\dagger b_j + b_j^\dagger b_{j+\delta}) \\ &= \mathcal{H}^p + \mathcal{H}^d \ . \end{aligned} \tag{4.6}$$

The first and second term in eq.(4.6) correspond to the paramagnetic and diamagnetic part of the hamiltonian, respectively.

The local current operator, $J_\delta(j)$, can be obtained by differentiating eq.(4.4) with

respect to $A_{j+\delta,j}$;

$$\begin{aligned} \mathcal{J}_\delta(j) &= -\frac{\delta \mathcal{H}}{\delta A_{j+\delta,l}} , \\ &= J^p_\delta(j) + J^d_\delta(j) , \end{aligned} \tag{4.7}$$

where the first term in eq.(4.7) is the paramagnetic current operator and is given by

$$\mathcal{J}^p_\delta(j) = it(b^\dagger_{j+\delta} b_j - b^\dagger_j b_{j+\delta}) , \tag{4.8}$$

and the diamagnetic part by

$$\mathcal{J}^d_\delta(j) = -t(b^\dagger_{j+\delta} b_j + b^\dagger_j b_{j+\delta}) A_{j+\delta,j} , \tag{4.9}$$

which is simply related to the kinetic energy density operator. To first order in $A_\delta(j)$, the linear response of current operator $J_\delta(j,\tau)$ is related to a nonlocal kernel, $K_{\delta,\delta'}$:

$$\mathcal{J}_\delta(j,\tau) = \int_{-\infty}^{\infty} d\tau \sum_{j'} \sum_{\delta'} K_{\delta,\delta'}(j,j',\tau,\tau') A_{\delta'}(j',\tau') , \tag{4.10}$$

where the kernel $K_{\delta,\delta'}$ is given by

$$\begin{aligned} K_{\delta,\delta'}(j,j',\tau,\tau') = &-t\langle b^\dagger_{j+\delta} b_j + b^\dagger_j b_{j+\delta}\rangle \delta_{j,j'} \delta_{\delta,\delta'}(\tau - \tau') \\ &+ i\langle [J^p_\delta(j,\tau), J^p_{\delta'}(j',\tau')]\rangle \theta(\tau - \tau') . \end{aligned} \tag{4.11}$$

After taking Fourier transform with respect to τ, I find that eq. (4.10) becomes

$$\mathcal{J}_\delta(j,\omega) = \sum_{j'} \sum_{\delta'} K_{\delta,\delta'} A_{\delta'}(j',\omega) , \tag{4.12}$$

with

$$K_{\delta,\delta'}(j,j',\omega) = -t\langle b^{\dagger}_{j+\delta}b_j + b^{\dagger}_j b_{j+\delta}\rangle \delta_{j,j'}\delta_{\delta,\delta'} + \int_{-\infty}^{\infty} d\tau e^{i\omega\tau}\{i\theta(\tau) \langle [J^p_{\delta}(j,\tau), J^p_{\delta'}(j',0)]\rangle\} \ . \qquad (4.13)$$

4.3.1 PURE SYSTEMS

First, I will discuss the results for a pure system. The diamagnetic part of Kernel (first term in eq.(4.13)) in spin langauge can be rewritten as

$$\begin{aligned} \mathcal{K}^o_{xx} &= -t\langle b^{\dagger}_{j+x}b_j + b^{\dagger}_j b_{j+x}\rangle \ , \\ &= -\frac{J}{S^2}\langle (S^z_{j+x}S^z_j + S^x_{j+x}S^x_j)\rangle \ . \end{aligned} \qquad (4.14)$$

Applying a Holstein-Primakoff transformation and keeping the leading term in 1/S, I find

$$\begin{aligned} \mathcal{K}^o_{xx} &= -\frac{J}{S^2}\langle (S^2 - Sa^{\dagger}_{j+x}a_{j+x} - Sa^{\dagger}_j a_j) + \\ &\quad \frac{S}{2}(a_{j+x} + a^{\dagger}_{j+x})(a_j + a^{\dagger}_j)\rangle \ . \end{aligned} \qquad (4.15)$$

From Bogoliubov transformation eq.(2.8) (discussed in chapter 2), $\mathcal{K}^o_{xx}$ may be written in term of canonical variables u,v as

$$\mathcal{K}^o_{xx}(j) = -J\langle (1 - \frac{1}{S}\sum_{\alpha}(v^2_{j+\delta,\alpha} + v^2_{j,\alpha}) - \frac{1}{2S}\sum_{\alpha}(u_{j+\delta,\alpha} + v_{j+\delta,\alpha})(u_{j,\alpha} + v_{j,\alpha})\rangle \ . (4.16)$$

After taking the Fourier transform, $u_{j\alpha} = u_k e^{i\vec{k}\cdot\vec{R}_j}$, $v_{j\alpha} = v_k e^{i\vec{k}\cdot\vec{R}_j}$, I find the diamagnetic term eq.(4.16) to be

$$\mathcal{K}^o_{xx}(j) = -J\{\mathcal{K}^o_{classical} + \mathcal{K}^o_{\frac{1}{S}}\} \ , \qquad (4.17)$$

where

$$\mathcal{K}^{o}_{classical} = 1 \tag{4.18}$$

and

$$\begin{aligned}
\mathcal{K}^{o}_{\frac{1}{S}} &= \frac{1}{S}\{-\frac{2}{N}\sum_k v_k^2 + \frac{1}{2N}\sum_k \gamma_k (u_k + v_k)^2\} \ , \\
&= \frac{1}{S}\{-\frac{1}{N}\sum_k (\frac{1-\frac{\gamma_k}{2}}{\sqrt{1-\gamma_k}} - 1) + \frac{1}{N}\sum_k \frac{\frac{\gamma_k}{2}}{\sqrt{1-\gamma_k}}\} \ , \\
&= \frac{1}{SN}\sum_k (1 - \sqrt{1-\gamma_k}) \ .
\end{aligned} \tag{4.19}$$

The paramagnetic current $\mathcal{J}^{p}_{\delta}(j)$ can be written in term of spin operators as

$$\mathcal{J}^{p}_{\delta}(j) = J(S^{z}_{j+\delta} S^{x}_{j} - S^{z}_{j} S^{x}_{j+\delta}) \ . \tag{4.20}$$

Apply the Holstein-Primakoff transformation and keeping only the lowest order term, I have eq.(4.20) in the form

$$\mathcal{J}^{p}_{\delta}(j) = \frac{J}{\sqrt{2S}}\{(a_j + a_j^{\dagger}) - (a_{j+\delta} + a^{\dagger}_{j+\delta})\} \ . \tag{4.21}$$

The Fourier transform of eq.(4.21) is given by

$$\mathcal{J}^{p}_{\delta}(\mathrm{q}) = \frac{J}{\sqrt{2S}}(1 - e^{-i\mathrm{q}\cdot\delta})(a_{-\mathrm{q}} + a^{\dagger}_{\mathrm{q}}) \ . \tag{4.22}$$

From eq.(4.22), the transverse current ($\mathcal{J}^{p}_{x}(q_y)$) identically vanishes (independent of q_y) while the longitudinal current ($\mathcal{J}^{p}_{x}(q_x)$) does not. This is not surprising since the quasiparticles in this case are phonons which, in a fluid, are purely longitudinal excitations with translational invariance. For pure system, both $\Pi^{o}_{xx}(\mathrm{q} = 0, \omega = 0)$ and $\Pi^{o}_{xx}(\omega = 0, q_x = 0, q_y \to 0)$ vanish due to the translational invariance. The paramagnetic current-current correlation function, $\Pi^{o}_{xx}(\omega = 0, q_x)$, in term of Bogoliubov

's varibles (u_q, v_q) is given by

$$\begin{aligned}\Pi^o_{xx}(q_x) &= \int_{-\infty}^{\infty} d\tau e^{i\omega\tau}\{i\theta(\tau)\langle[J^p_\delta(j,\tau), J^p_{\delta'}(j',0)]\rangle\} \\ &= \frac{J^2}{S}\frac{2(1-cosq_x)(u_{q_x}+v_{q_x})^2}{\omega_{q_x}} \ . \end{aligned} \tag{4.23}$$

From chap.2, $(u_q + v_q)^2 = \frac{1}{\sqrt{1-\gamma_q}}$ and $\omega_q = \frac{4J}{S}\sqrt{1-\gamma_q}$. Thus, $\Pi^o_{xx}(q_x \to 0) = J$. Note that this result is of order $(\frac{1}{S})^o$. This term exactly canceled out $\mathcal{K}_{classical}$. This cancellation is required since current conservation implies for ω=0, $q_x J_x = 0$. Thus, for any $q_x \neq 0$, $J_x \equiv 0$, a result that must hold to all orders in $\frac{1}{S}$. Formally, this is seen by the fact that for $\omega = 0$, $q_y = 0$, $q_x \neq 0$, $\vec{A}$ corresponds to a pure gauge field, and can be removed by a gauge transformation. The current conservation and gauge invariance holds even when disorder is present.

4.3.2 DISORDER SYSTEMS

The total current is defined as a sum of the diamagnetic and paramagnetic current. To the lowest order in $\frac{1}{S}$, this can be written as

$$\mathcal{J} = \sum_{j,\delta} \mathcal{K}_\delta(j) + J^p_\delta(j) \ , \tag{4.24}$$

where $\mathcal{K}_\delta(j)$ and $J^p_\delta(j)$ are diamagnetic and paramagnetic current and defined in eq.(4.25) and (4.26) respectively.

$$\mathcal{K}(j) = -Jcos\theta_{j+\delta}cos\theta_j \ , \tag{4.25}$$

$$J^p_\delta(j) = \frac{J}{\sqrt{2S}}\{cos\theta_{j+\delta}(a_j + a^\dagger_j) - cos\theta_j(a_{j+\delta} + a^\dagger_{j+\delta})\} \ . \tag{4.26}$$

By performing Bogoliubov transformation eq.(2.8), I can express the paramagnetic

current in terms of the cannonical variables u and v

$$J^p_\delta(j,\tau) = \frac{J}{\sqrt{2S}}\sum_\alpha\{cos\theta_{j+\delta}(u_{j\alpha}+v_{j\alpha}) - cos\theta_j(u_{j+\delta,\alpha}+v_{j+\delta,\alpha})\} (\gamma_\alpha e^{-i\omega_\alpha\tau} + \gamma^\dagger_\alpha e^{i\omega_\alpha\tau}) \ . \tag{4.27}$$

The current-current correlation function can be defined as

$$\Pi_{\delta,\delta'}(j,j',\omega) = \int_{-\infty}^{\infty} d\tau e^{i\omega\tau}\{i\theta(\tau)\langle[J^p_\delta(j,\tau), J^p_{\delta'}(j',0)]\rangle\} \ . \tag{4.28}$$

From eq.(4.27) and (4.28) the paramagnetic current-current correlation function can be written as

$$\Pi_{\delta\delta'}(\omega=0,q_x=0,q_y\to 0) = \frac{J^2}{S}\sum_\alpha\frac{1}{\omega_\alpha}\frac{1}{N}\sum_j\sum_{j'} e^{iq_y(v_j-v_{j'})} [cos\theta_{j+\delta}(u_{j,\alpha}+v_{j,\alpha}) - cos\theta_j(u_{j+\delta,\alpha}+v_{j+\delta,\alpha})] [cos\theta_{j'+\delta'}(u_{j',\alpha}+v_{j',\alpha}) - cos\theta_{j'}(u_{j'+\delta',\alpha}+v_{j'+\delta',\alpha})] \ . \tag{4.29}$$

Since only the real part is of interest, the triple sum in eq.(4.29) can be reduced to a double sum,

$$\Pi_{\delta\delta}(\omega=0,q_x=0,q_y\to 0) = \frac{J^2}{S}\sum_\alpha\frac{1}{\omega_\alpha}\frac{1}{N}\sum_j[cos\theta_{j+\delta}(u_{j,\alpha}+v_{j,\alpha}) - cos\theta_j(u_{j+\delta,\alpha}+v_{j+\delta,\alpha})]^2\{cos^2 q_{y_j} + sin^2 q_{y_j}\} \ . \tag{4.30}$$

To the lowest order approximation, the superfluid density can be defined as

$$\rho_S = \delta\rho_{classical} \ , \tag{4.31}$$

where

$$\delta\rho_{classical} = \frac{1}{N}\sum_j\frac{1}{d}\sum_\delta\overline{\mathcal{K}_\delta(j) - \Pi_{xx}(\omega=0,q_x=0,q_y\to 0)} \ , and \tag{4.32}$$

where the overbar in eq.(4.32) implies the configuration average. The first term is defined in eq.(4.25). The second term in eq.(4.32) is the current-current correlation function in static ($\omega = 0$) and long wave-length limit with a transverse gauge. This term is given by eq.(4.29).

As discussed before, the Meissner effect is related to $\Pi_{xx}(\omega = 0, q_x = 0, q_y \rightarrow 0)$ while the perfect conductivity is related to the limit $\Pi_{xx}(\mathbf{q} = 0, \omega = 0)$. The limit $q_y \rightarrow 0$ and $q = 0$ can produce different results[9]. However, in a disordered system, since the system does not possess a translational invariance, $\Pi_{xx}(\mathbf{q} = 0, \omega = 0)$, need not vanish, and $q_y \rightarrow 0$ and $q = 0$ may be identical. Indeed, no disordered system has been observed to exhibit the behaviour of perfect conductivity without superconductivity.

4.4 THE SUPERFLUID DENSITY: SENSITIVITY TO THE BOUNDARY CONDITION

Another method to calculate superfluid density is via changing boundary conditions. Here I consider going from periodic to antiperiodic boundary condition in the x-direction.

By gauge transformation, this is identical to applying an uniform ($\vec{q} = 0, \omega = 0$) vector potential $A_x = \frac{\pi}{L}$. The classical Hamiltonian corresponding to the antiperiodic boundary condition is described by

$$H^{AP} = -J \sum_{<i,j>}{}' cos(\phi_j - \phi_i) cos\theta_i cos\theta_j - \sum_i h_i sin\theta_i \ , \tag{4.33}$$

where the $'$ indicates that the couplings between spins with $i_x = L$ and $i_x = 1$ takes on an additional minus sign (ie. are antiferromagnetic). Unlike the case of periodic boundary condition, the energy is no longer minimized by having ϕ_i uniform on all

sites.

The superfluid density is ρ_s is then defined as

$$\delta E = \frac{1}{2}\rho_s(\frac{\pi}{L})^2 + \mathcal{O}(\frac{\pi}{L})^4 \ , \tag{4.34}$$

where δE is the increase in the ground state energy due to the change in boundary condition.

To $\mathcal{O}(\frac{\pi}{L})^2$, the classical equation of motion for the antiperiodic boundary condition is given by

$$\sum_{<j>}{}' cos\theta_j^{(0)} sin(\phi_j - \phi_i) = 0 \ , \tag{4.35}$$

where $\theta^{(0)}$ is the classical solution of θ for the periodic boundary condition (eq.(2.18) discussed in chap.2). The superfluid density , ρ_s, is then

$$\rho_s = \frac{2}{\pi^2 L^{d-2}} J \sum_{<i,j>} (1 - cos(\phi_i - \phi_j)) cos\theta_i^{(0)} cos\theta_j^{(0)} \ . \tag{4.36}$$

This *thermodynamic* ρ_s will be compared to ρ_s calculated from the linear response theory of the previous section.

4.5 THE COMPRESSIBILITY

The compressibility measures the change in density due to a change in the local chemical potential. In the spin representation of our problem, this corresponds to adding the term defined in eq.(4.37) to the Hamiltonian eq.(2.2)

$$\mathcal{H}' = -\frac{1}{S}\sum_i h_i' S_{iy} \ . \tag{4.37}$$

From linear response, the compressibility in spin language can be written as

$$\kappa_{ij}(t-t') = -i\theta(t-t')\langle[S_{iy}(t), S_{iy}(t')]\rangle \ . \tag{4.38}$$

After rotation about x-axis and applying Holstein-Primakoff transformation, to the lowest order eq.(4.38) becomes,

$$\kappa_{ij} = -i\theta(t-t')\frac{S}{2}cos\theta_i cos\theta_j\langle[a_i(t-t') - a_i^\dagger(t-t'), a_j(0) - a_j^\dagger(0)]\rangle \ . \tag{4.39}$$

From Bogoliubov transformation eq.(2.8), κ_{ij} can be written as,

$$\kappa_{ij} = -i\theta(t)\frac{S}{2}cos\theta_i cos\theta_j \sum_l [e^{-i\omega_l t}(u_{il} - v_{il})(v_{jl} - u_{jl}) - e^{i\omega_l t}(v_{il} - u_{il})(u_{jl} - v_{jl})] \tag{4.40}$$

After taking Fourier transform, I find that eq.(4.40) for ω=0 and real κ is given by

$$\kappa(q, \omega = 0) = \frac{S}{N}\sum_l |\sum_i cos\theta_i (u_{il} - v_{il}) e^{iq\cdot r_i}|^2 \frac{1}{\omega_l} \ . \tag{4.41}$$

The uniform compressibility is given by $\kappa(q \to 0, \omega = 0)$. For pure case, $cos\theta_i = 1$ and $\sum_i e^{iq\cdot r_i}(u_{il} - v_{il}) = u_q - v_q$. Eq.(4.41) is reduced to

$$\kappa^0(q) = \frac{S}{N}\sum_q (u_q - v_q)^2 \frac{1}{\omega_q} \ . \tag{4.42}$$

From eq.(2.11) and (2.13),

$$\kappa^0(q) = \frac{S^2}{zJ} \ . \tag{4.43}$$

This is the linear response compressibility to $\mathcal{O}((\frac{1}{S})^0)$. Alternatively, one can calculate the thermodynamic (uniform) compressibility to this order by finding the minimum energy solution for the classical spins to first order in $h_i' = h'$. This gives

$$sin\theta = \frac{h'}{zJ} \tag{4.44}$$

and

$$\langle S_{iy} \rangle = S sin\theta = \frac{Sh'}{zJ} \ . \tag{4.45}$$

The classical thermodynamic compressibilty is therefore given by,

$$\kappa_{classical} = \frac{\langle S_{iy} \rangle}{h'/S} = \frac{S^2}{zJ} \ . \tag{4.46}$$

Eq.(4.46) is in agreement with eq.(4.43). I will compare the thermodynamic and linear response compressibility when disorder is present.

4.6 RESULTS AND DISCUSSIONS

As discussed in the introduction of this chapter, the destruction of superfluidity should be signified by a vanishing of superfluid density. The superfluid density that I consider is a semiclassical approximation and corresponds to $S \to \infty$ in the gaussian model. From linear response theory discussed in section 4.3, the total superfluid density is defined in eq.(4.31)

$$\rho_s = \delta\rho_{classical} \quad , \tag{4.47}$$

where $\delta\rho_{classical}$ is given by eq.(4.32) as a difference between the diamagnetic and paramagnetic current-current correlation function. My results show that the paramagnetic current-current correlation function increases as disorder increases and cancels the the diamagnetic current at the same or close to the same critical disorder (Δ_c) as that for the order parameter δm for 1D and 2D. On the other hand, my result for the thermodynamic ρ_s (defined in eq.(4.36)) decreases as disorder increases but is still finite at the critical disorder (Δ_c).

4.6.1 ONE DIMENSIONAL RESULTS

First, consider the results from the linear response theory in 1D. For 1D, the current response, Π_{xx}, for finite q_x is constant and cancels the diamagnetic term. This cancelation is required by gauge transformation and true for both pure and disordered case. This fact is also seen numerically in fig. 4.1 (Π_{xx} is calculated through eq.(4.30)). In fig. 4.1, I present the plot of current-current correlation function, $\Pi_{xx}(\omega = 0, q_x)$ v.s. q_x, for various disorder. In this fig., Π_{xx} is averaged over 50 different configurations with system size $L = 50$. As one can see, Π_{xx} for finite q_x is constant and cancels out the diamagentic current. $\Pi_{xx}(\omega = 0, q_x = 0)$ also increases as disorder increases.

For finite size calculation, one needs to calculate $\Pi_{xx}(q_x = 0)$ for various sizes and extrapolate $L \to \infty$. However, the extrapolation results are not quite trustworthy since I do not know exactly how $\Pi_{xx}(L)$ behaves as a function of size (the extrapo-

lations that I make and will present later is by taking the value of Π_{xx} of the three largest sizes and extrapolating by a straight line). In fig. 4.2 - 4.5, I show the plots of finite size scaling, $\Pi_{xx}(q_x = 0)$ v.s. $\frac{1}{L}$ for L=50, 90, 130 and 170 and averaging over 50 different configurations. In fig. 4.2, I present the plot of $\Pi_{xx}(q_x = 0)$ v.s. $\frac{1}{L}$ for $\Delta = 0.9$. The extrapolation of Π_{xx} as $L \rightarrow \infty$ in this fig. gives the infinite size value for the current response function $\Pi_{xx}(q_x = 0)$. The filled symbol in this fig. represents the diamagnetic current and is plotted in the same graph for comparision. One clearly sees in fig. 4.2 that for Δ =0.9 the system is still in the superfluid phase with finite superfluid density. Similar to fig. 4.2, figs. 4.3 - 4.5 show the plots of $\Pi_{xx}(q_x = 0)$ v.s. $\frac{1}{L}$ for $\Delta = 0.7$, 0.6 and 0.5 respectively. In these figs., one can see that the extrapolation of $\Pi_{xx}(q_x = 0)$ to $L \rightarrow \infty$ for $\Delta = 0.6$ and 0.7 still give a finite superfluid density while for Δ_c= 0.5 the paramagnetic current cancels out the diamagnetic term (hence $\rho_s = 0$).

In fig. 4.6, I present the plot of the total superfluid density, ρ_s v.s. Δ, showing ρ_s decreasing as disorder increases, and $\rho_s \rightarrow 0$ as $\Delta \rightarrow 0.5$. As discussed previously, another method to calculate superfluid density is via changing boundary condition going from periodic to antiperiodic boundary condition (I refer ρ_s calculated by this method as thermodynamic ρ_s). The thermodynamic ρ_s that I consider here is calculated by eq.(4.36). Unlike linear response theory (in which ρ_s vanishes at $0.5 < \Delta_c < 0.6$), the thermodynamic ρ_s is still finite at Δ_c. Fig.4.7 illustrates the plot of total superfluid density (ρ_s) v.s. disorder (Δ) (size N=170) for both linear response and thermodynamic ρ_s. As one can see in this fig., $\rho_s(\Delta)$ calculated via the linear response theory and changing the boundary condition give different results. I do not understand the reason for this difference.

Next I will discuss the result for the compressibility (κ). First consider the thermodynamic κ. In fig. 4.8, I show the plot of $< sin\theta >$ v.s. $< h' >$ for different disorder ($\Delta = 0.5$, 0.6, 0.7 and 1.5), where $< sin\theta >$ is calculated through the classical equation of motion described in chap.2 and $< h' >$ is the mean value of a random

field ($< sin\theta >$ is averaged over 500 different configurations). The thermodynamic compressibility is given by the slope in fig. 4.8. The value of the compressibility calculated from linear response (to the lowest order approximation) gives a different result from the thermodynamic limit. The comparision of linear response and thermodynamic compressibility are shown in fig. 4.8 for each disorder (as one can see in this fig. the difference between linear response and thermodynamic compressibility is greater than the error bars). In fig. 4.9, I present the plot of linear response compressibility κ v.s. Δ (N=170). The compressibility decreases as disorder increases.

How are ρ_s and κ related to the critical exponent discussed in chap.3 ? From the appendix in chap.3, the ratio of the critical exponent can be defined (in term of superfluid density (ρ_s) and compressibility (κ) as $\frac{\eta_c}{\eta_p} = \sqrt{\frac{\rho_p \kappa_p}{\rho_c \kappa_c}}$. I find that $\frac{\eta_c}{\eta_p}$ (with ρ calculated via changing boundary condition) is in agreement with that calculated from the order parameter in chap.3 ($\frac{\eta_c}{\eta_p} = 1.56 \pm 0.00$ and $\frac{\eta_c}{\eta_p} = \frac{\beta_c}{\beta_p} = 1.37 \pm 0.03$ (see chap.3).

4.6.2 TWO DIMENSIONAL RESULTS

Using the rigorous definition of ρ_s one needs to calculate $\Pi_{xx}(\omega = 0, q_x = 0, q_y \rightarrow 0)$. This necessitates evaluating eq.(4.30) for a few q_y 's, and is a task rather computer intensive. Since q_y is quantized in a unit of $\frac{2\pi}{L}$, the extrapolation to $q_y \rightarrow 0$, means extrapolating to $L \rightarrow \infty$. However, (as discussed in section 4.3.2) for disordered systems, $\Pi_{xx}(\omega = 0, q_x = 0, q_y \rightarrow 0)$ may be the same as $\Pi_{xx}(\omega = 0, \vec{q} = 0)$. To check this, I perform finite size calculations of $\Pi_{xx}(q_y)$ v.s. q_y (extrapolate $q_y \rightarrow 0$) and $\Pi_{xx}(\vec{q} = 0)$ v.s. $\frac{1}{L}$ (extrapolate $L \rightarrow \infty$). In fig. 4.10, I show the plot of $\frac{1}{\Pi_{xx}(\omega=0,q_x=0,q_y)}$ v.s. q_y ($q_y = \frac{2\pi N}{L}$, N=1,2,3,4 and L is a linear dimension of a square lattice $L \times L$) for various system sizes (from 11$\times$ to 15$\times$15) and different disorder strength ($\Delta = 0.3, 0.1, 0.08$). Π_{xx} for finite q_y is averaged over 50 different configurations. As one can see in this figure, $\Pi_{xx}(q_y)$ for finite q_y does not have a finite size effect since all the points merge into a single curve for each disorder. Therefore, the infinite size value

of $\Pi_{xx}(q_y)$ can be obtained by extrapolating $\Pi_{xx}(q_y) \rightarrow \Pi_{xx}(q_y = 0)$. In fig. 4.11, I present a plot of $\Pi_{xx}(\omega = 0, q_y)$ v.s. q_y (size 11×11 and 15×15) with Δ=0.3, 0.1 and 0.08.

In fig.4.12, I present a finite size scaling plot of $\frac{1}{\Pi_{xx}(q_y=0)}$ v.s. $\frac{1}{L}$ for Δ=0.3. The y-intercept point in this figure is the $q_y \rightarrow 0$ value obtained in fig. 4.10. Figs. 4.13 - 4.14 show similar plots to fig. 4.12 for Δ= 0.1 and 0.08 respectively. In fig. 4.16 - 4.18, I plot $\Pi_{xx}(\omega = 0, q_y = 0)$ v.s. $\frac{1}{L}$ for disorder Δ= 0.3, 0.1 and 0.08. If there is no difference between $\Pi_{xx}(q_y \rightarrow 0)$ and $\Pi_{xx}(q_y = 0)$, the extrapolation of $\frac{1}{\Pi_{xx}(q_y)}$ v.s. q_y (fig. 4.10) should be the same as the extrapolation of $\frac{1}{\Pi_{xx}(q_y=0)}$ v.s. $\frac{1}{L}$ (fig. 4.13 - 4.15). It can be seen in fig. 4.12 and 4.13 that the agreement is quite good for Δ = 0.3 and 0.1. I thus conclude for these disorder, perfect conductivity and through Meissner effect are inchangeble criteria for superfluidity. For Δ= 0.08, however, no conclusion can be made as the $\frac{1}{\Pi}$ v.s. $\frac{1}{L}$ curve has a negative curvature at the largest size.

In fig.4.19, I present the plot of total semiclassical superfluid density (ρ_s) against disorder (Δ). The total superfluid density decreases as the disorder increases as expected. Indeed, it becomes negative at $\Delta = 0.08$. The negative value is probably due to the uncertainty associated with the extrapolation. More likely, ρ_s vanishes at this disorder. This can be interpreted as a destruction of superfluid density. In fig.4.20 shows the plot of Π_{xx} normalized by K_c, $\frac{\Pi_{xx}(\omega=0,q_y=0)}{K_c}$ v.s. Δ. As one can see in this figure, $\frac{\Pi_{xx}}{K_c}$ increases as disorder increases. A rapid change of slope at $0.08 \leq \Delta < 0.1$ indicates $\frac{\Pi_{xx}}{K_c}$ is enormously enhanced near the critical point. In fig. 4.21, I give the plot of total superfluid density as a function of disorder via linear response theory and changing boundary condition method. Similar to 1D, linear response theory gives a different result from the changing boundary method (discussed in section 4.4).

In conclusion, in this chapter I have presented the result of semiclassical superfluid density for 1D and 2D. The total superfluid density, ρ_s decreases with increasing disorder but is still positive for $\Delta > \Delta_c$ ($\Delta_c \sim 0.5$ for 1D, and ~ 0.08 for 2D). The

linear response ρ_S seems to vanish at the same critical disorder as that of the order parameter, while the thermodynamic ρ_S is still finite at the critical disorder. While appealing, I do not know whether ρ_s and m having the same critical disorder is a coincidence or reflects some deeper physics. Similar studies on other models will be thus of interest.

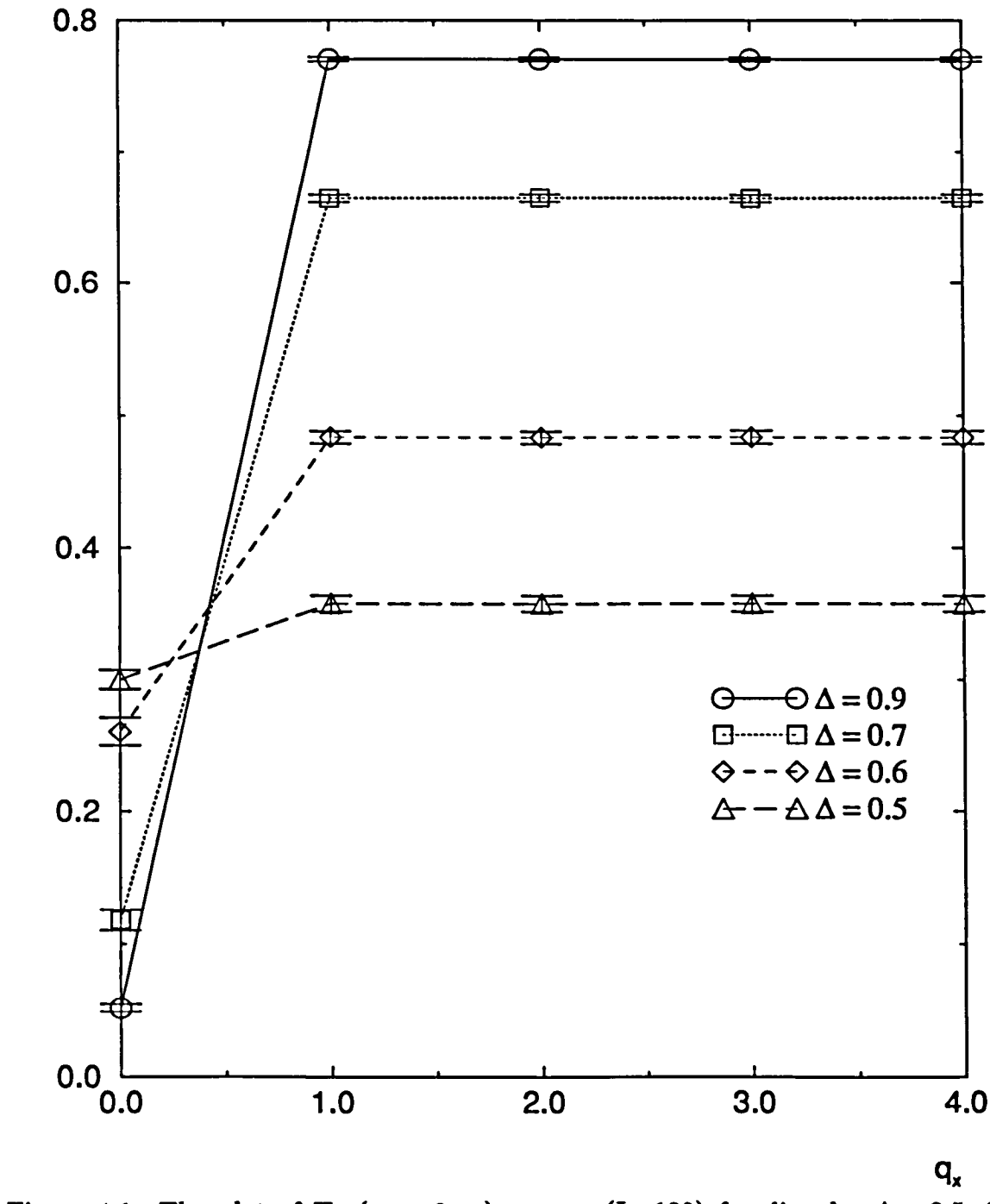

Figure 4.1: The plot of $\Pi_{xx}(\omega = 0, q_x)$ v.s. q_x (L=130) for disorder Δ= 0.5, 0.6, 0.7 and 0.9. Π_{xx} for finite q_x is constant and equals the diamagnetic term while $\Pi_{xx}(\omega = 0, q_x = 0)$ increases as disorder increases.

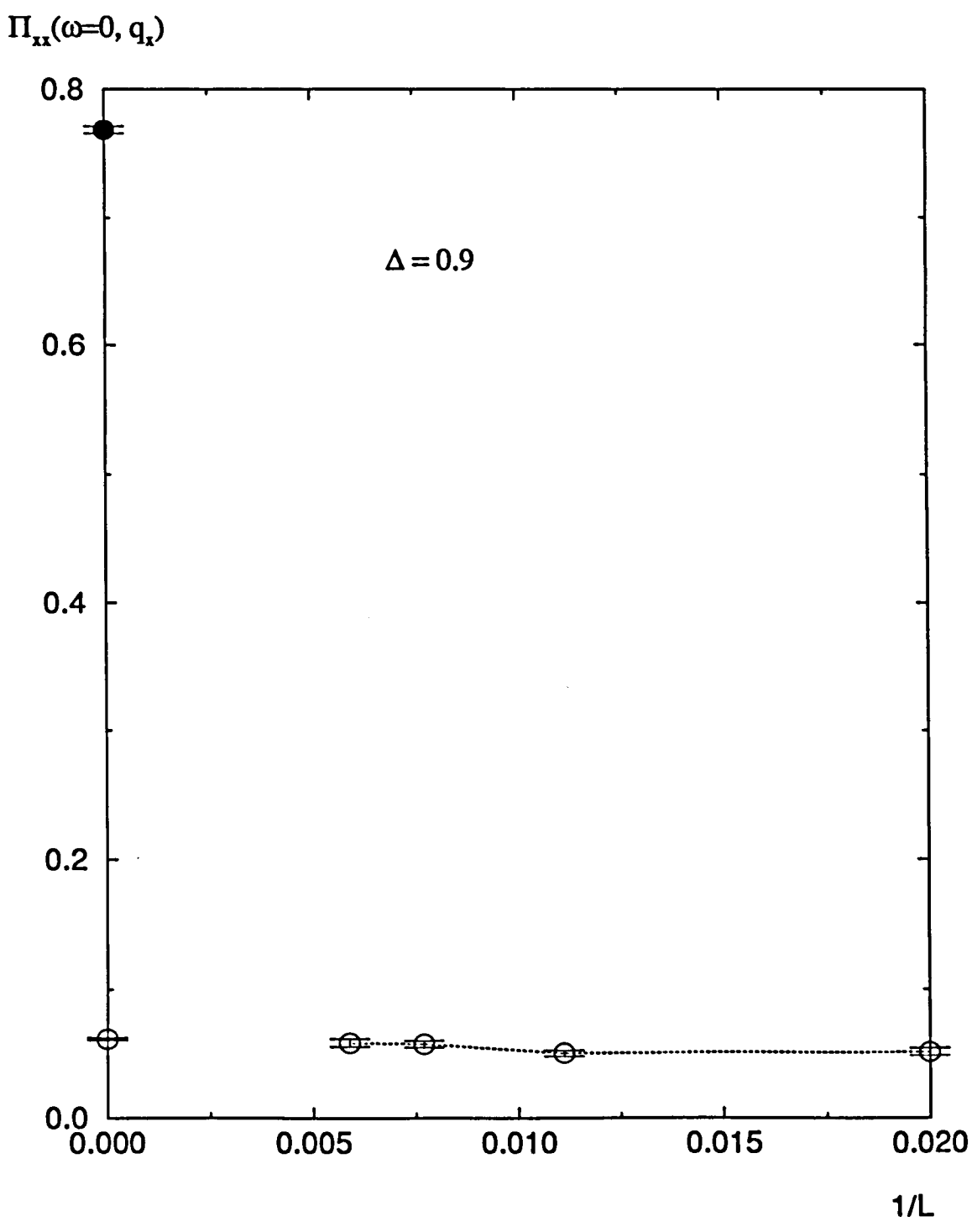

Figure 4.2: $\Pi_{xx}(q_x = 0)$ v.s. $\frac{1}{L}$ is plotted for Δ=0.9. The filled symbol in here represents the diamagnetic current response. The y-intercept of unfilled symbol in this fig. is the extrapolation of $\Pi_{xx}(q_x = 0)$ as $L \to \infty$. It can be seen clearly in this fig. that, at Δ=0.9, the superfluid density is still finite (ρ_s=0.717$\pm$0.004).

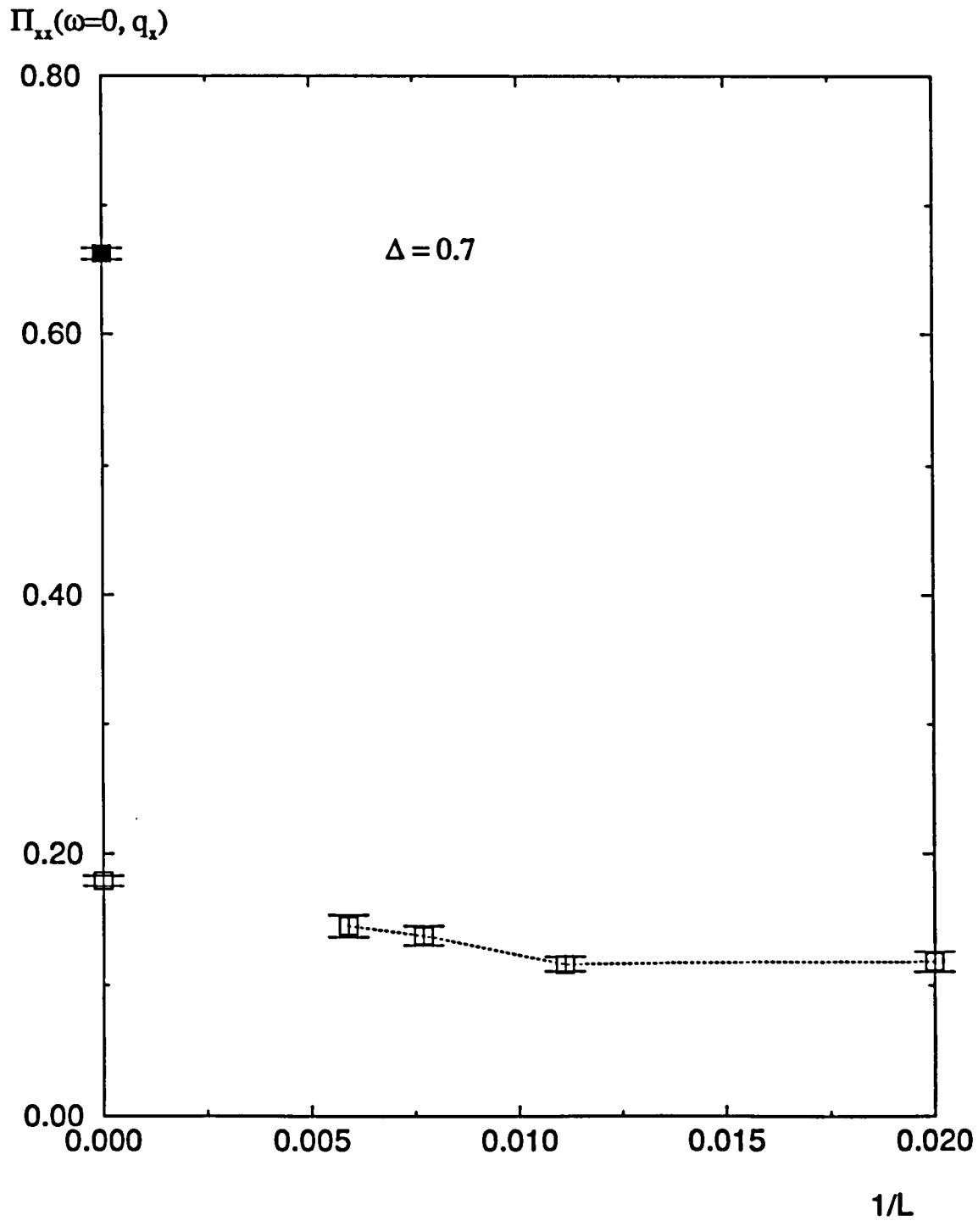

Figure 4.3: Similar to fig. 4.2, here is the plot of $\Pi_{xx}(q_x = 0)$ v.s. $\frac{1}{L}$ for Δ=0.7. In this fig., the total superfluid density decreases but is still finite, with ρ_s=0.484±0.006.

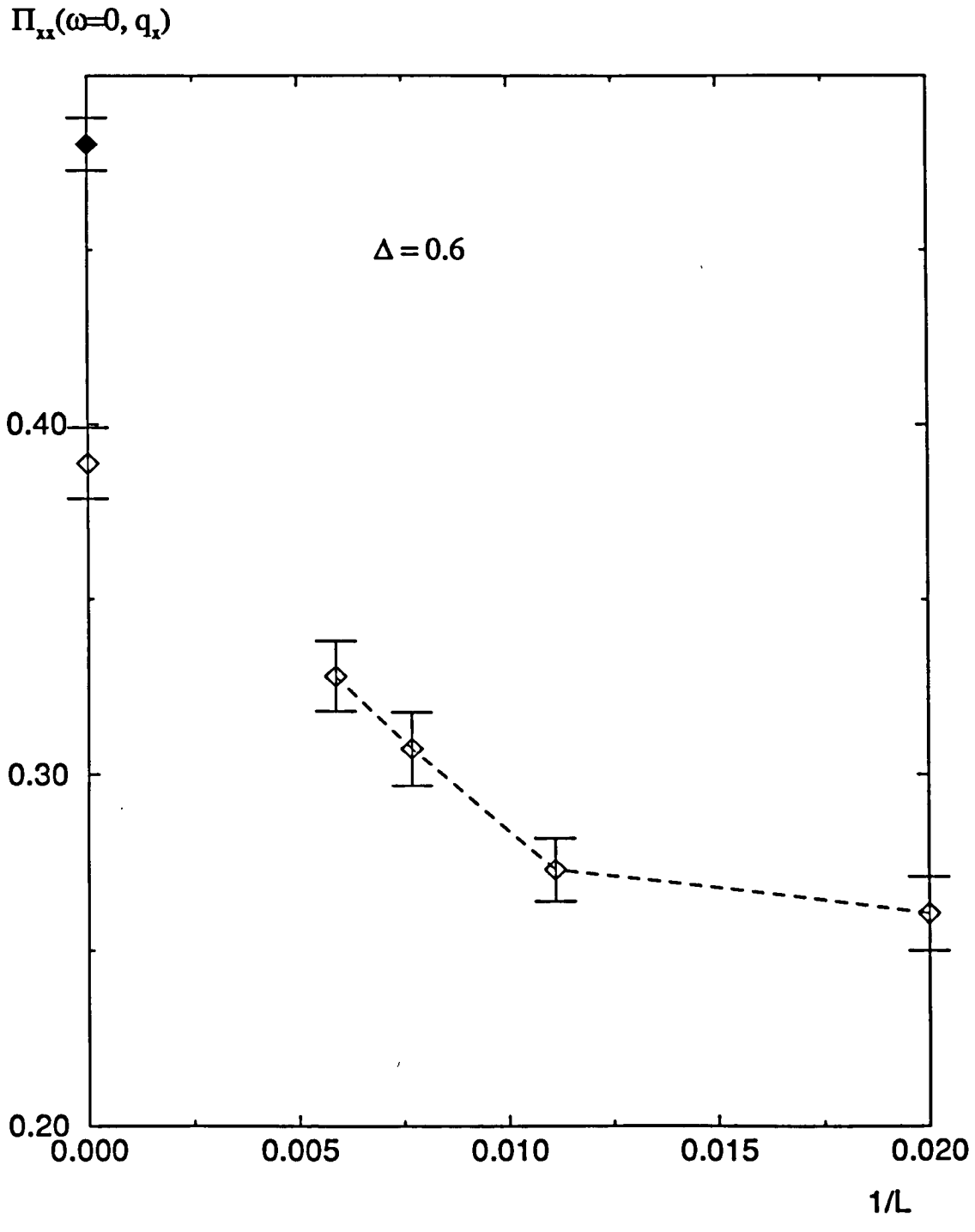

Figure 4.4: Similar plot to figs. 4.2 and 4.3, for $\Delta = 0.6$. ρ_s is reduced to 0.091 ± 0.011.

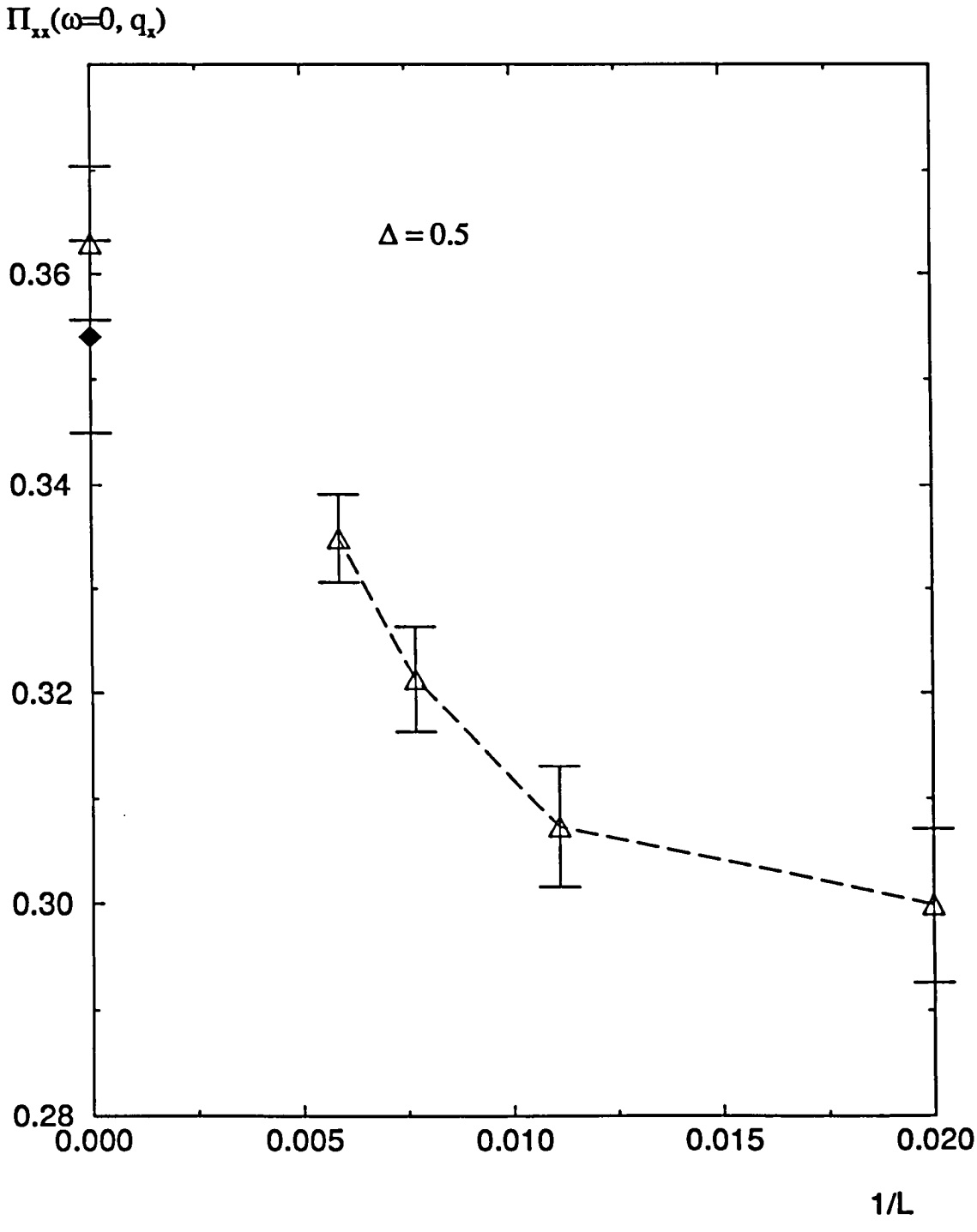

Figure 4.5: For Δ=0.5, the extrapolation of $\Pi_{xx}(q_x = 0)$ as $L \rightarrow \infty$ cancels out within accuracy of the diamagnetic term (the total superfluid density, ρ_s=0 (-0.009±0.011)).

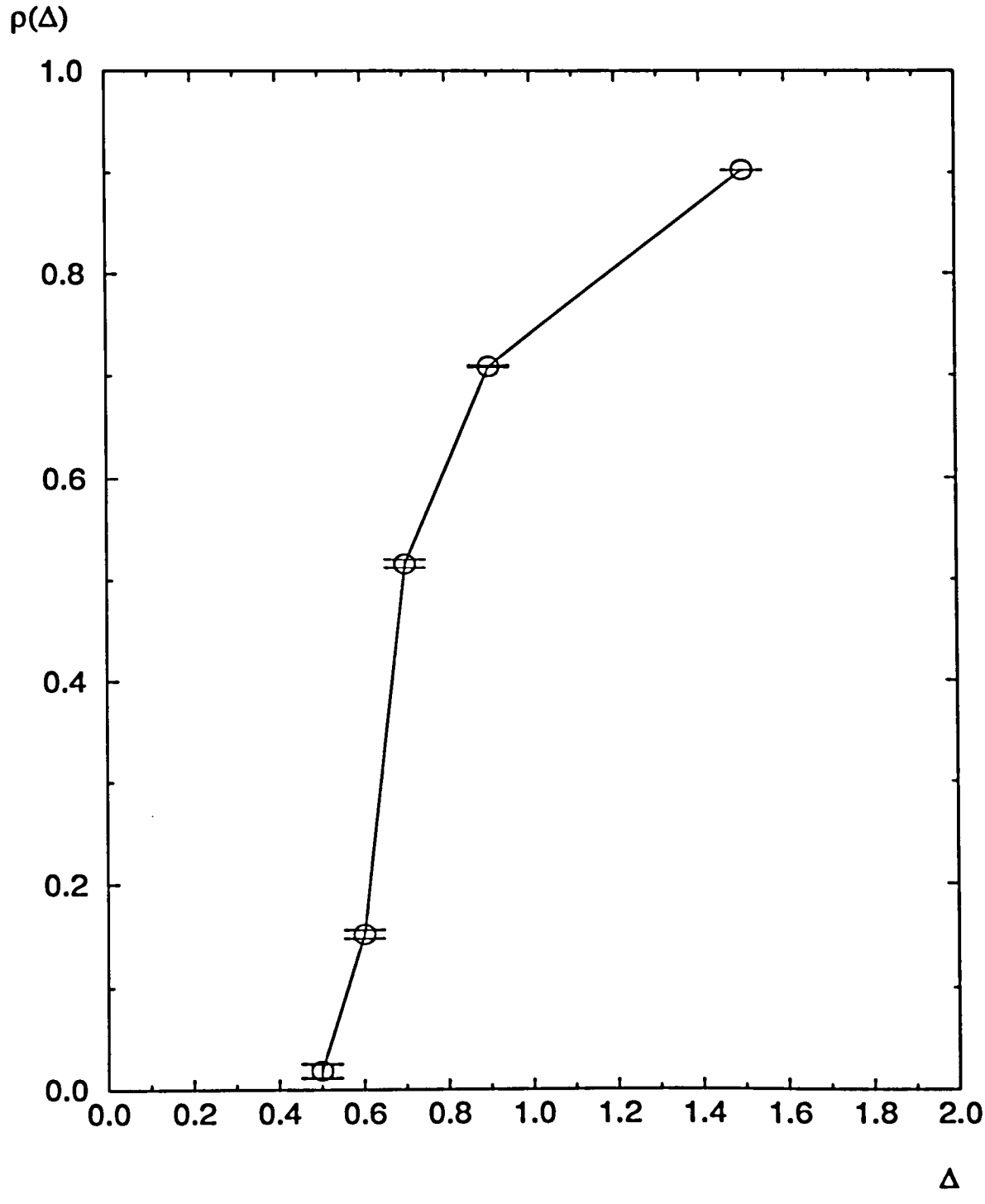

Figure 4.6: Plot of total superfluid density from linear response theory for size N=170, ρ_s v.s. Δ. ρ_s drops somewhat abruptly as $\Delta \rightarrow 0.5$ and vanishes in the vicinity of Δ=0.5.

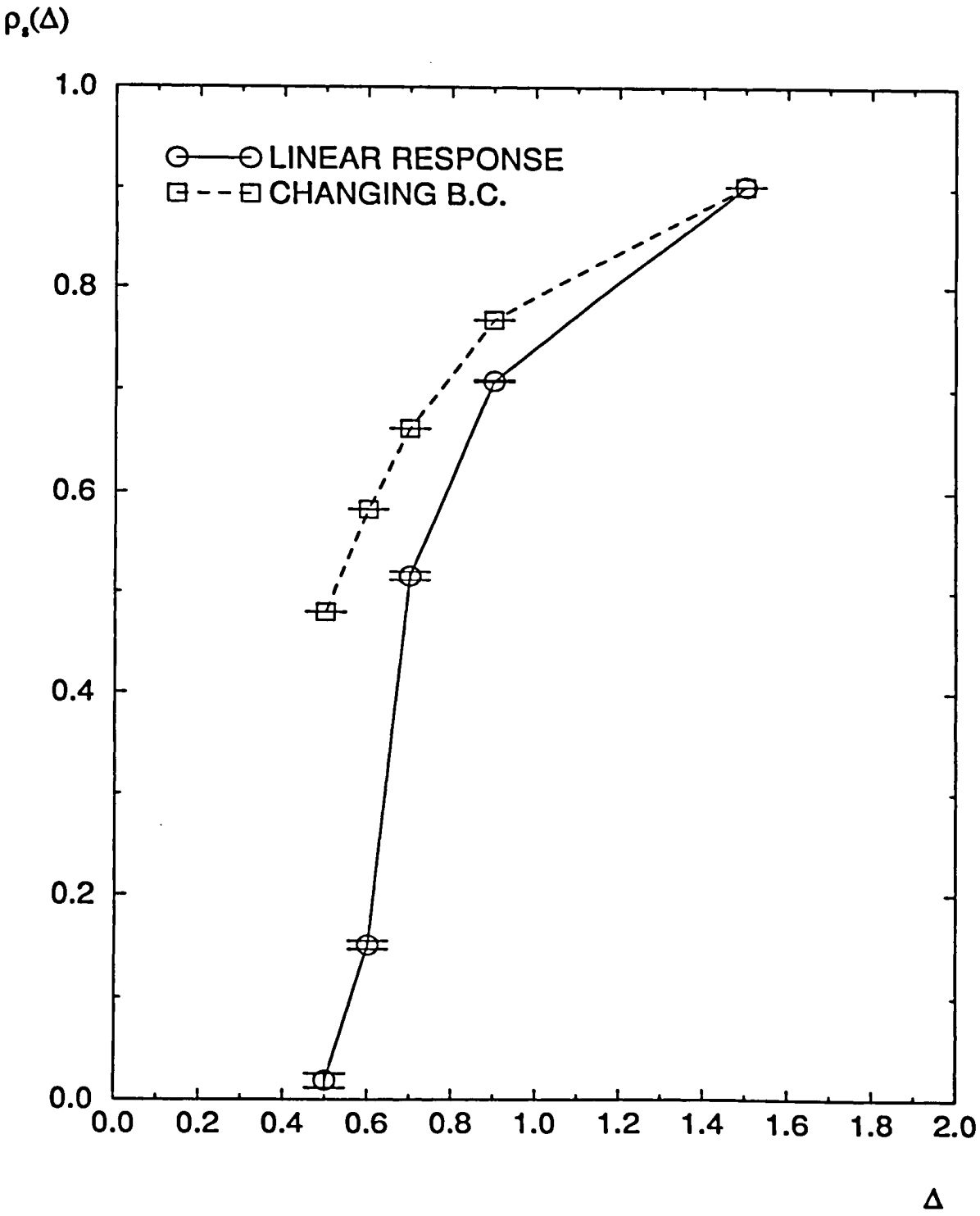

Figure 4.7: The total superfluid density, ρ_s v.s. Δ for 1D (N=170). The superfluid density calculated from linear response theory gives a differrent result from the calculation via changing boundary condition.

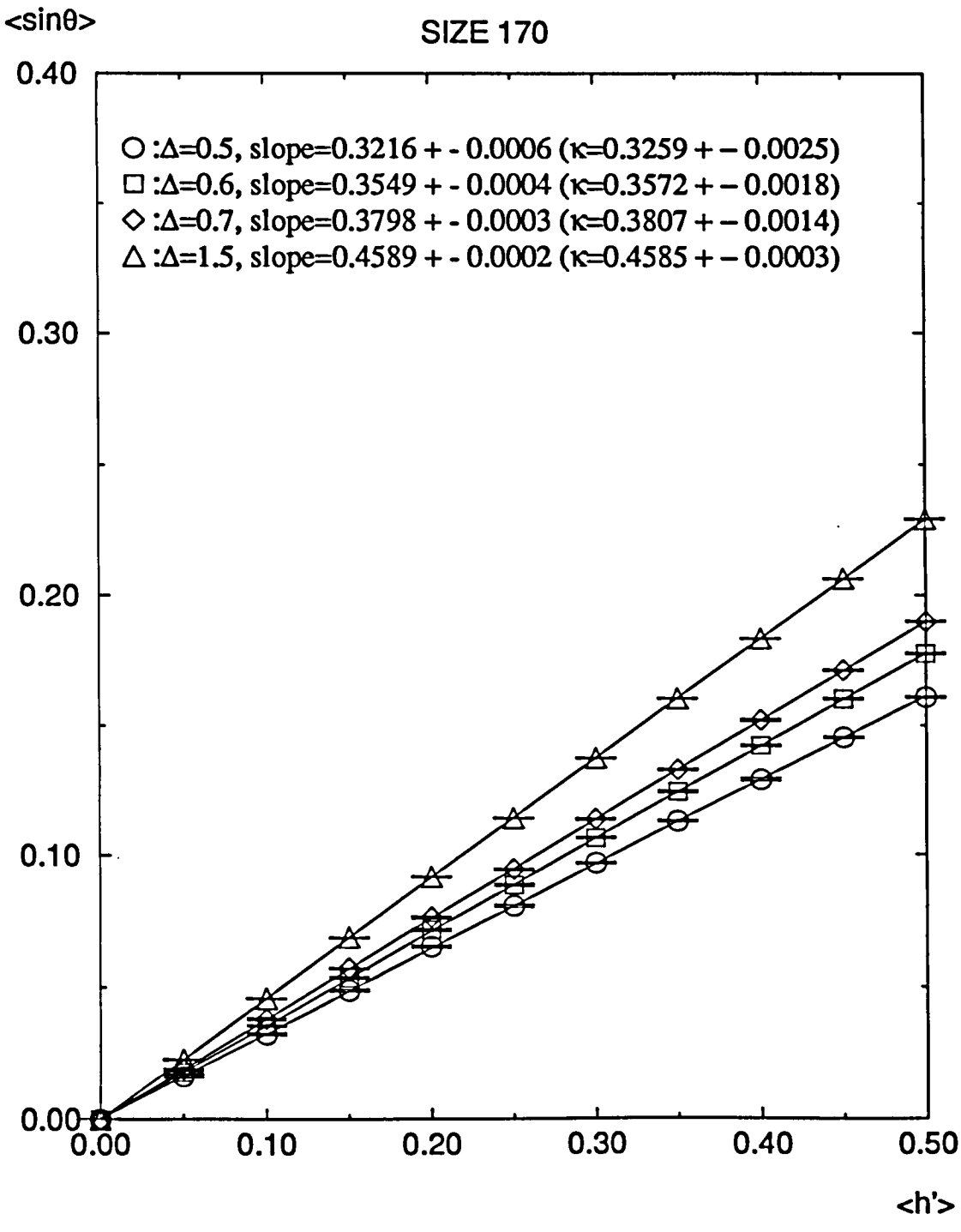

Figure 4.8: Show the plot of $< sin\theta >$ v.s. $< h' >$. The thermodynamic compressiblity (calculated from the classical equation of motion) is given by the slope of this graph for different disorder. The compressibility calculated from the linear response are shown in the bracket for each disorder.

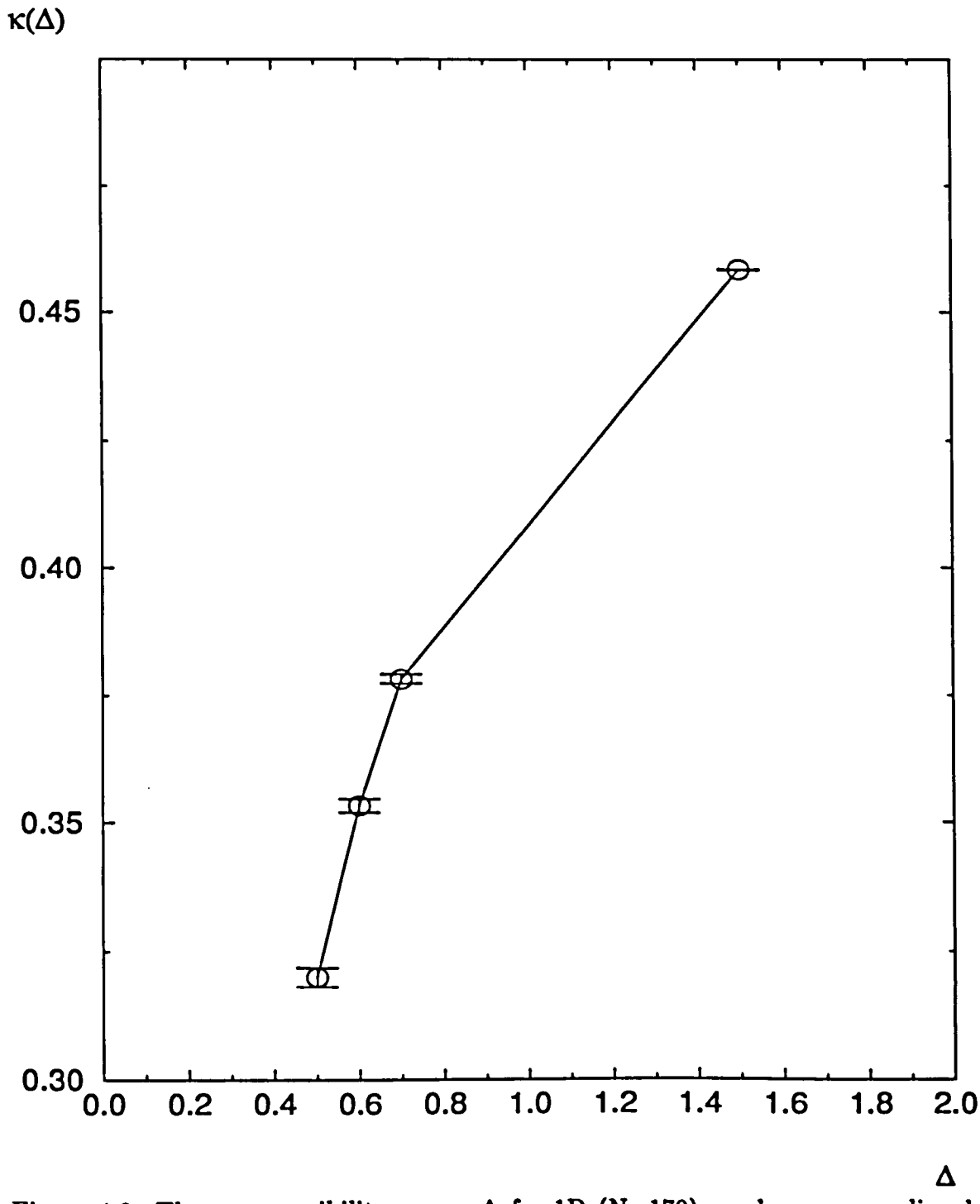

Figure 4.9: The compressibility κ v.s. Δ for 1D (N=170). κ decreases as disorder increases.

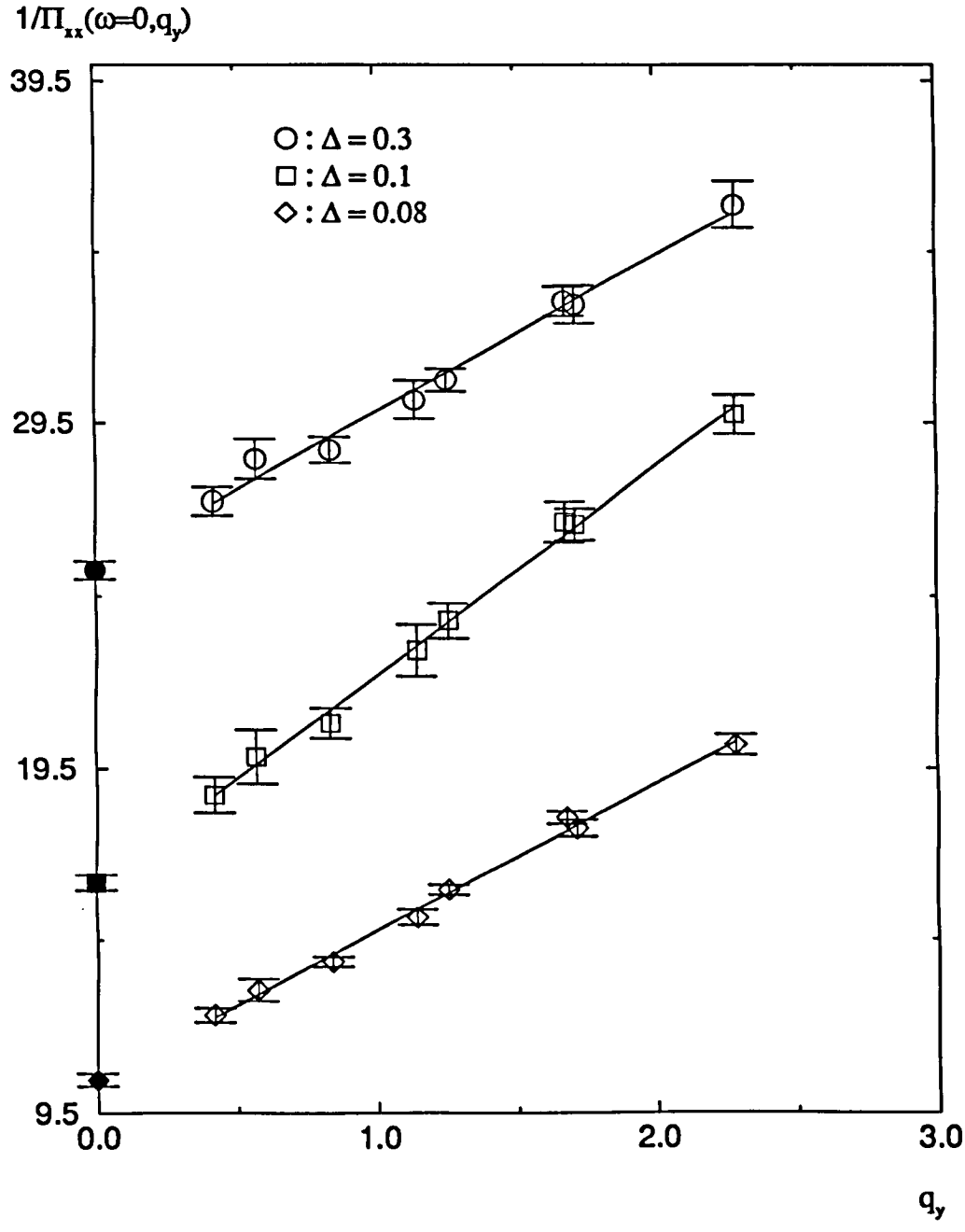

Figure 4.10: The plot of $\frac{1}{\Pi_{xx}(\omega=0,q_x=0,q_y)}$ v.s. q_y ($q_y=\frac{2\pi N}{L}$, N=1,2,3,4) for Δ = 0.3, 0.1, and 0.08 for various system sizes (11×11 and 15× 15) are plotted in the same graph. The extrapolation to $q_y \rightarrow 0$ gives the infinite size (L→ ∞) value of $\Pi_{xx}(\omega=0,q_x=0, q_y \rightarrow 0)$. The filled symbols in this figure are the value from the extrapolation for different disorder (Δ). The extrapolation to $q_y \rightarrow 0$ values of Π_o are $\Pi_o(\Delta=0.3)=25.3\pm 0.3$, $\Pi_o(\Delta=0.1)=16.0\pm 0.2$, and $\Pi_o(\Delta=0.08) =10.5\pm 0.2$.

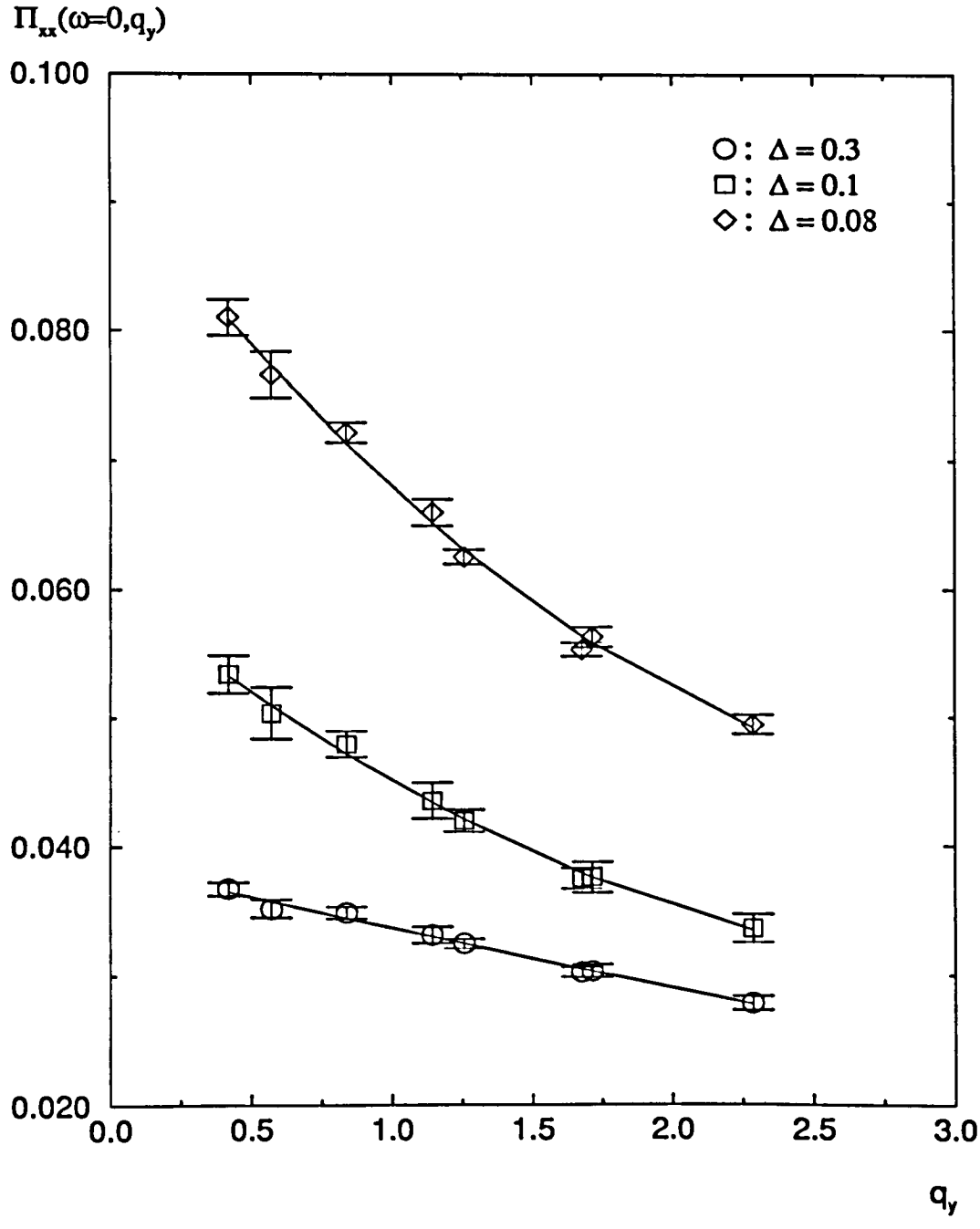

Figure 4.11: A similar plot to fig.4.10 showing Π_{xx} v.s. q_y for different disorder (Δ = 0.3, 0.1, 0.08).

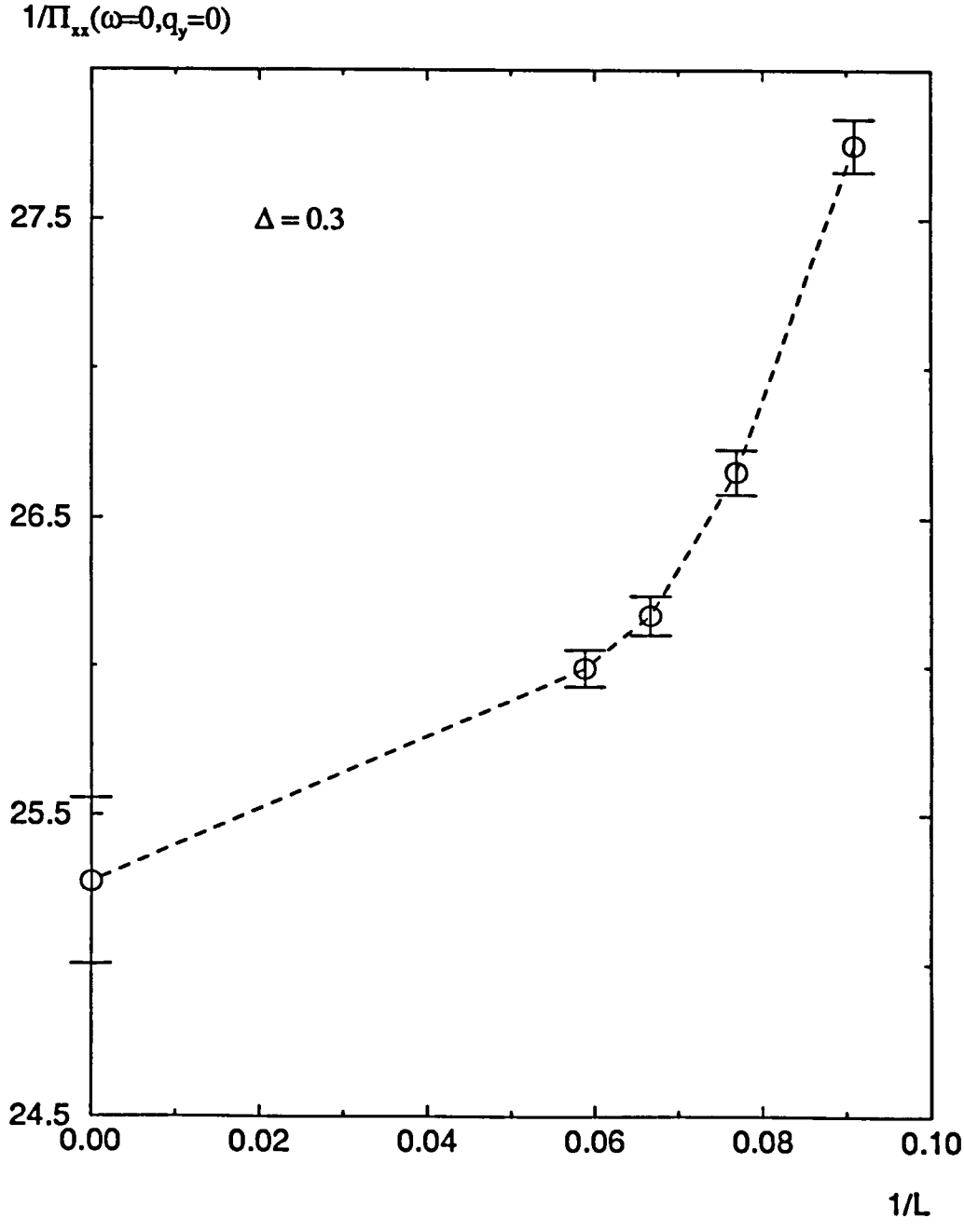

Figure 4.12: Finite size scaling plot of $\frac{1}{\Pi_{xx}(q_y=0)}$ v.s. $\frac{1}{L}$ for $\Delta = 0.3$. The dashed line in this fig. is a guide to the eyes. $\Pi_{xx}(q_y = 0)$ is calculated by taking q_y=0 and averaging over 400 different configurations (for size 11 × 11, 13 × 13, 15 × 15 and 17 × 17). The y-intercept point in this figure is given by the extrapolation of $\Pi_{xx}(q_y \to 0)$ (25.3±0.3) obtained in fig.4.10.

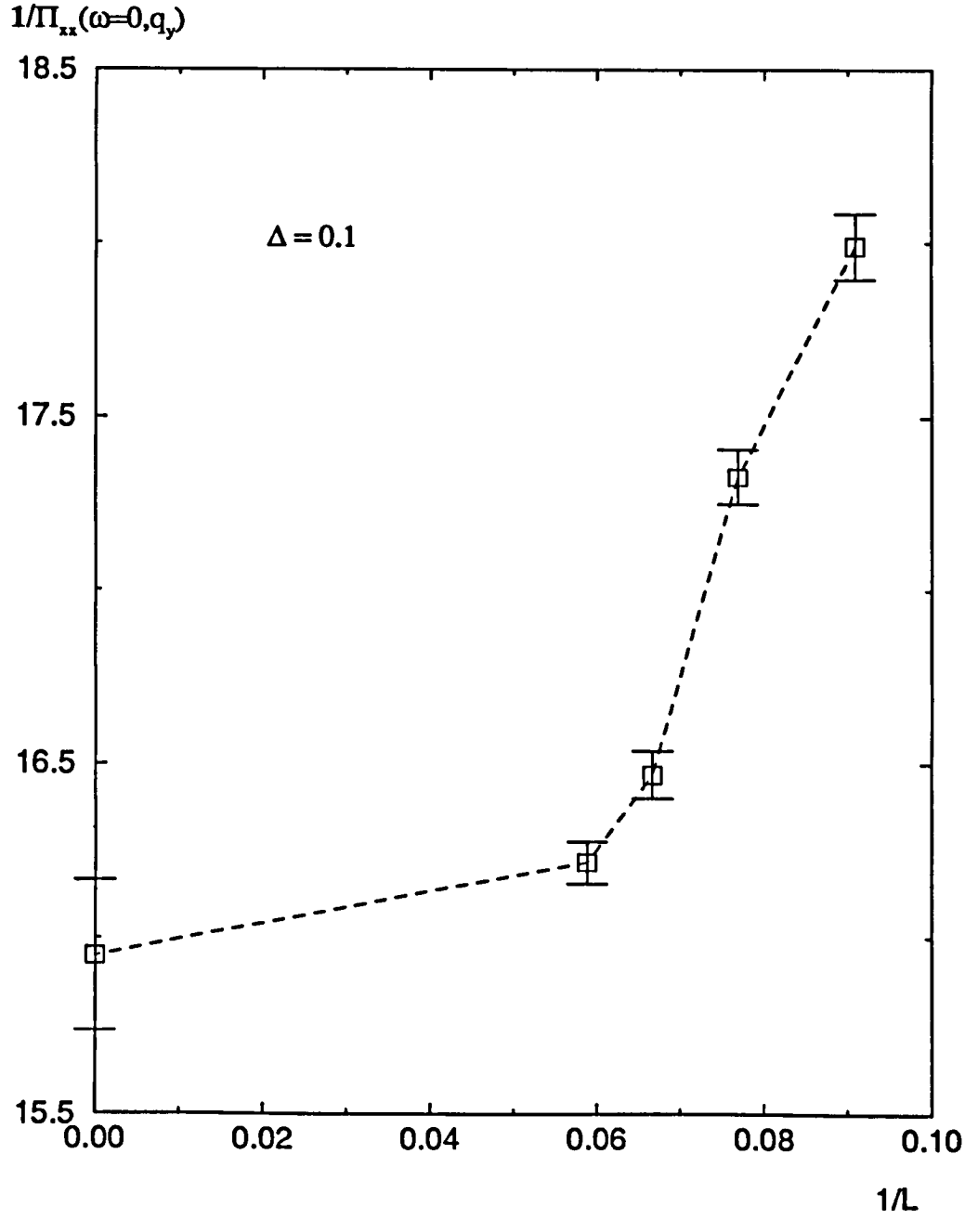

Figure 4.13: Similar to fig.4.12, for $\Delta = 0.1$. The line joining between points is a guide to the eye. The y-intercept point (16.0±0.2) in this figure is from fig. 4.10.

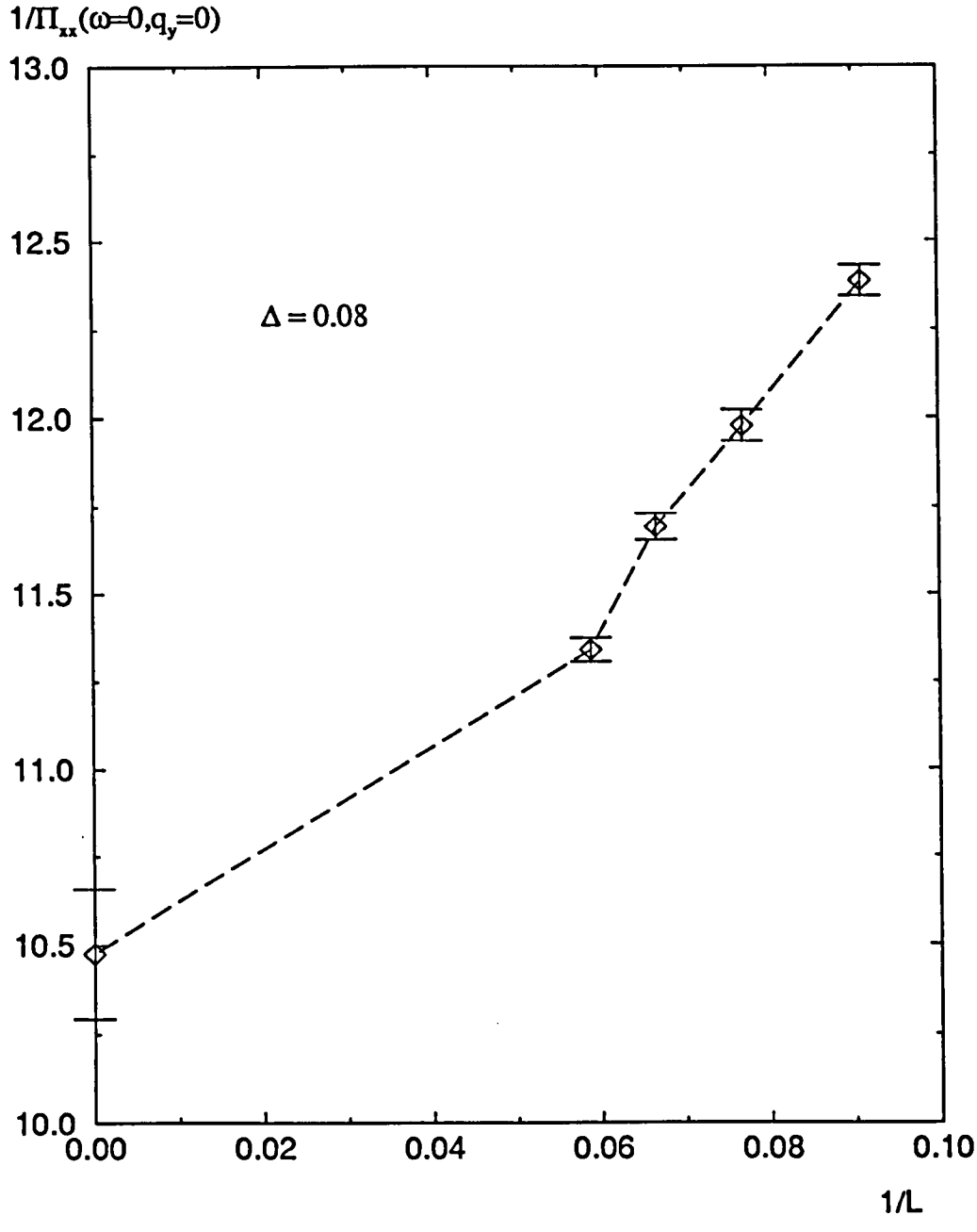

Figure 4.14: Similar plot to fig.4.12, for $\Delta = 0.08$. The y-intercept point (10.5 ± 0.2) is from fig. 4.10.

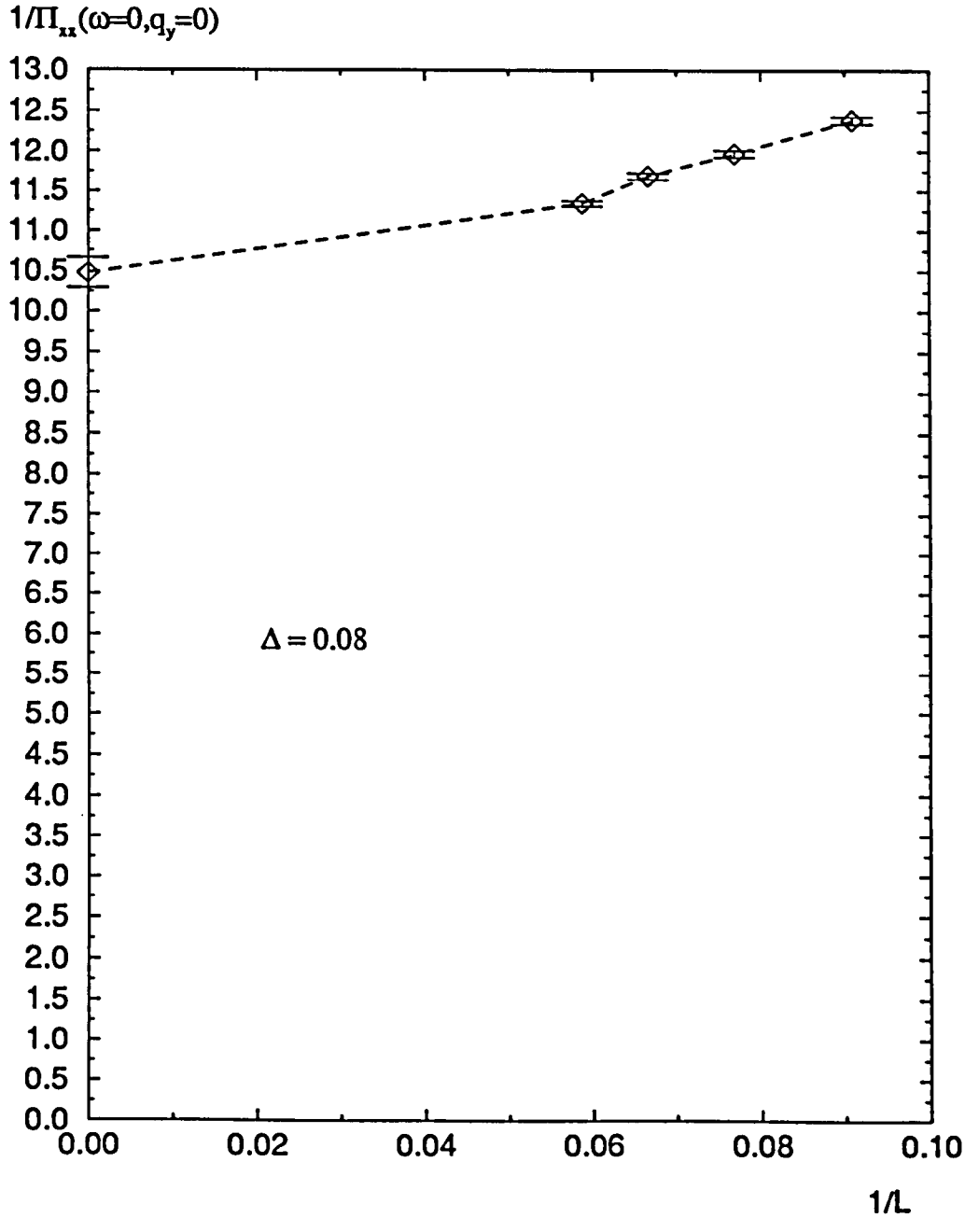

Figure 4.15: Here is the same plot as fig.4.14 on another scale.

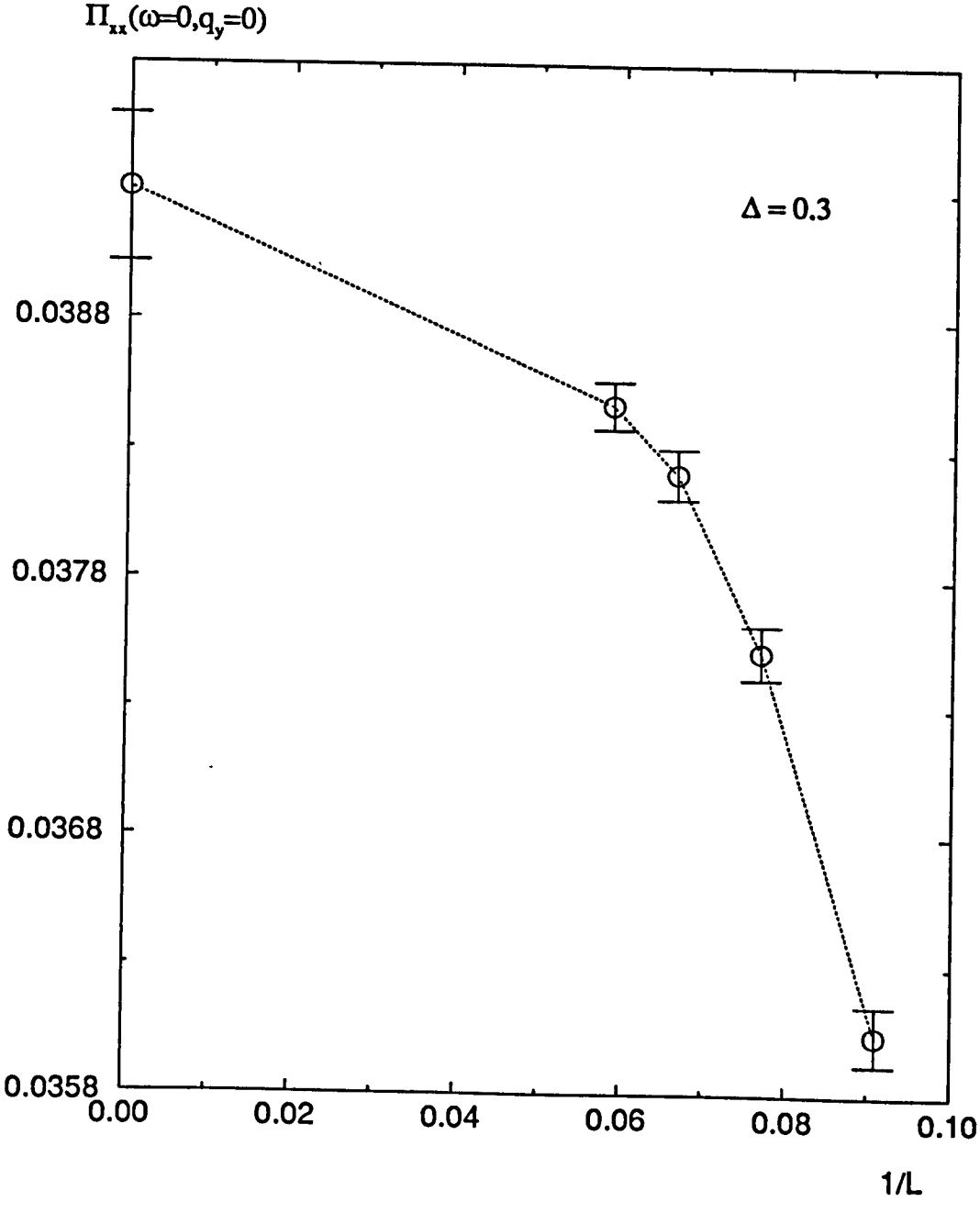

Figure 4.16: Same as fig. 4.12, but for $\Pi_{xx}(\omega = 0, q_y = 0)$ v.s. $\frac{1}{L}$ ($\Delta = 0.3$).

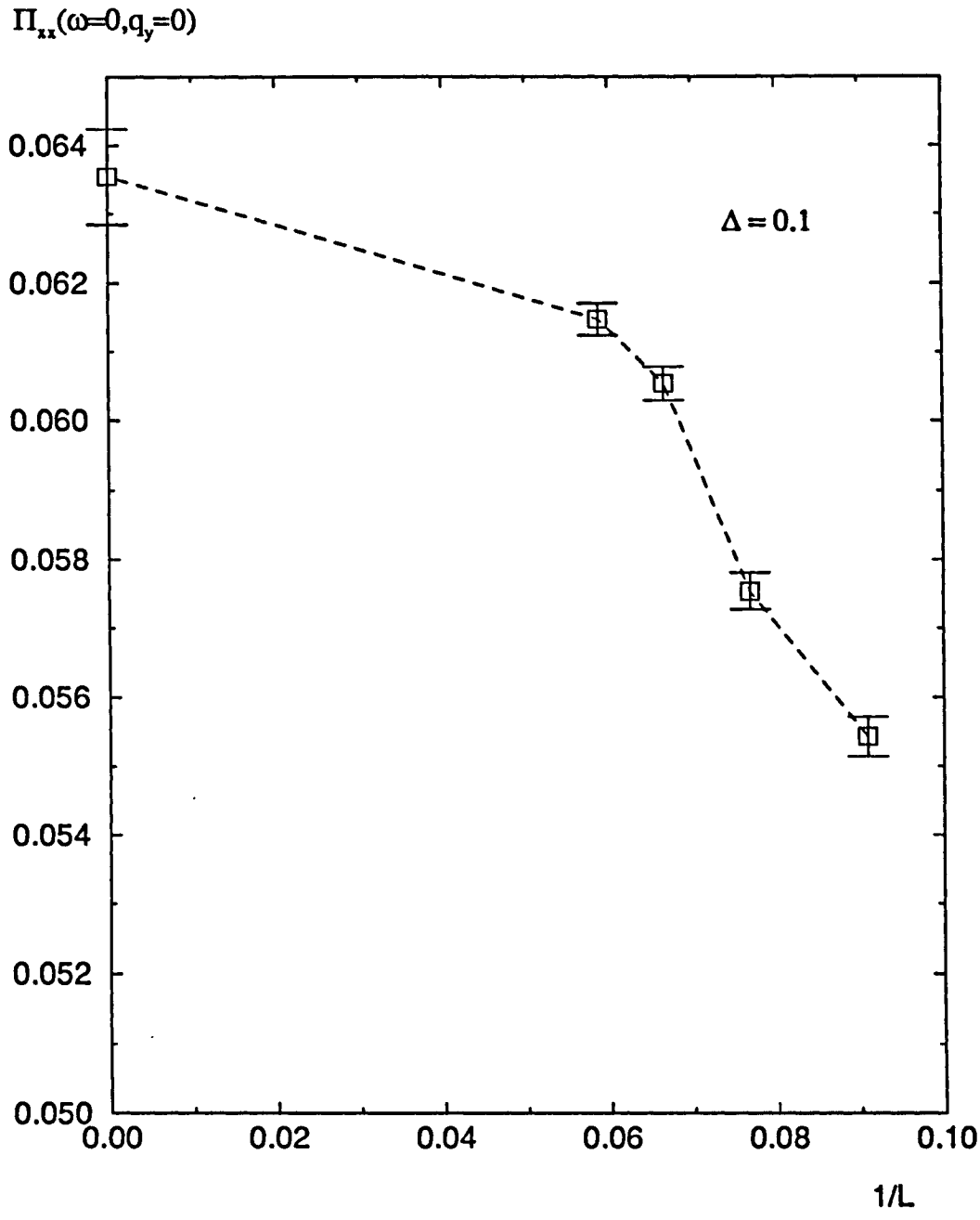

Figure 4.17: $\Pi_{xx}(\omega = 0, q_y = 0)$ v.s $\frac{1}{L}$ for $\Delta = 0.1$.

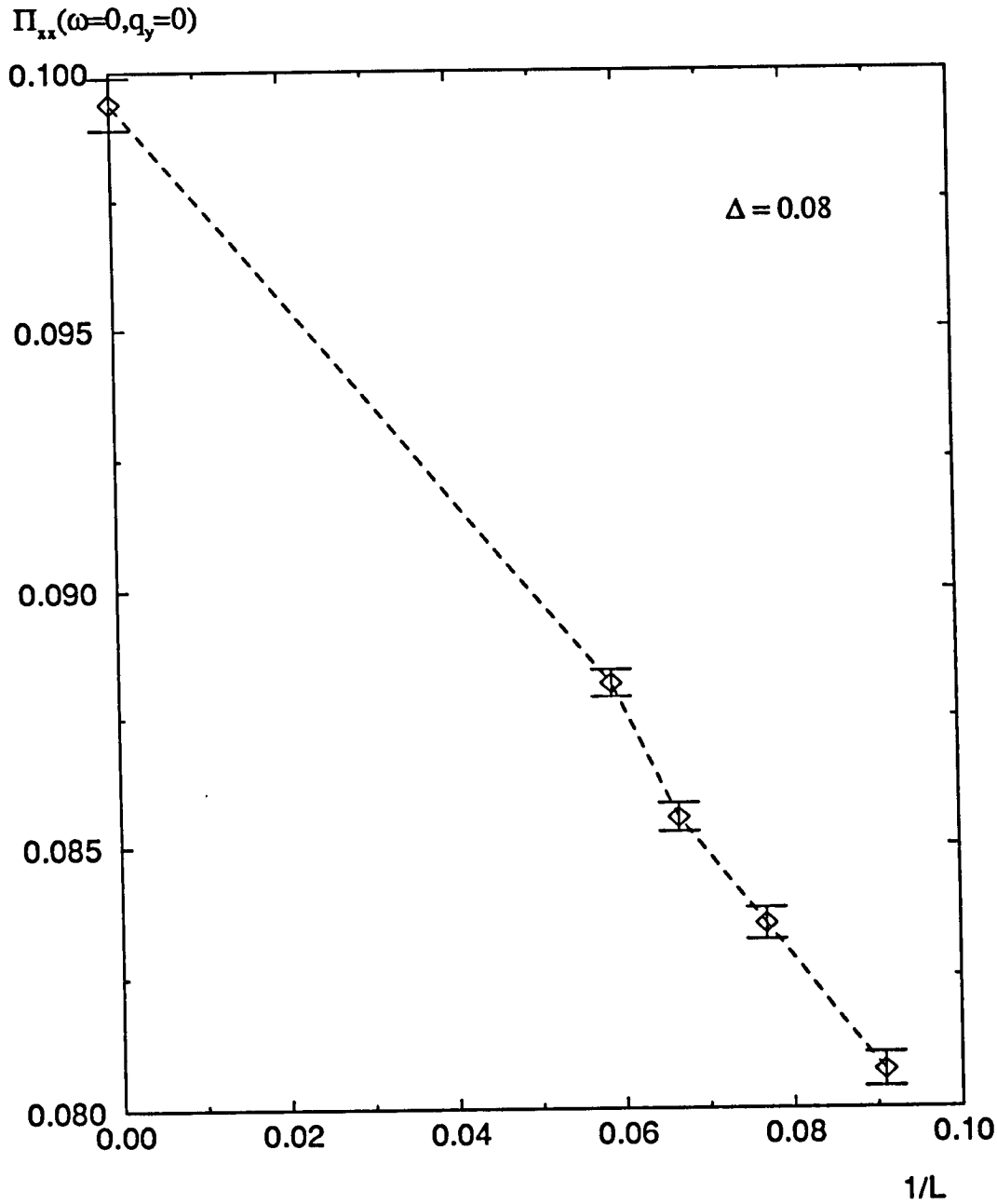

Figure 4.18: $\Pi_{xx}(\omega = 0, q_y = 0)$ v.s. $\frac{1}{L}$ for $\Delta = 0.08$.

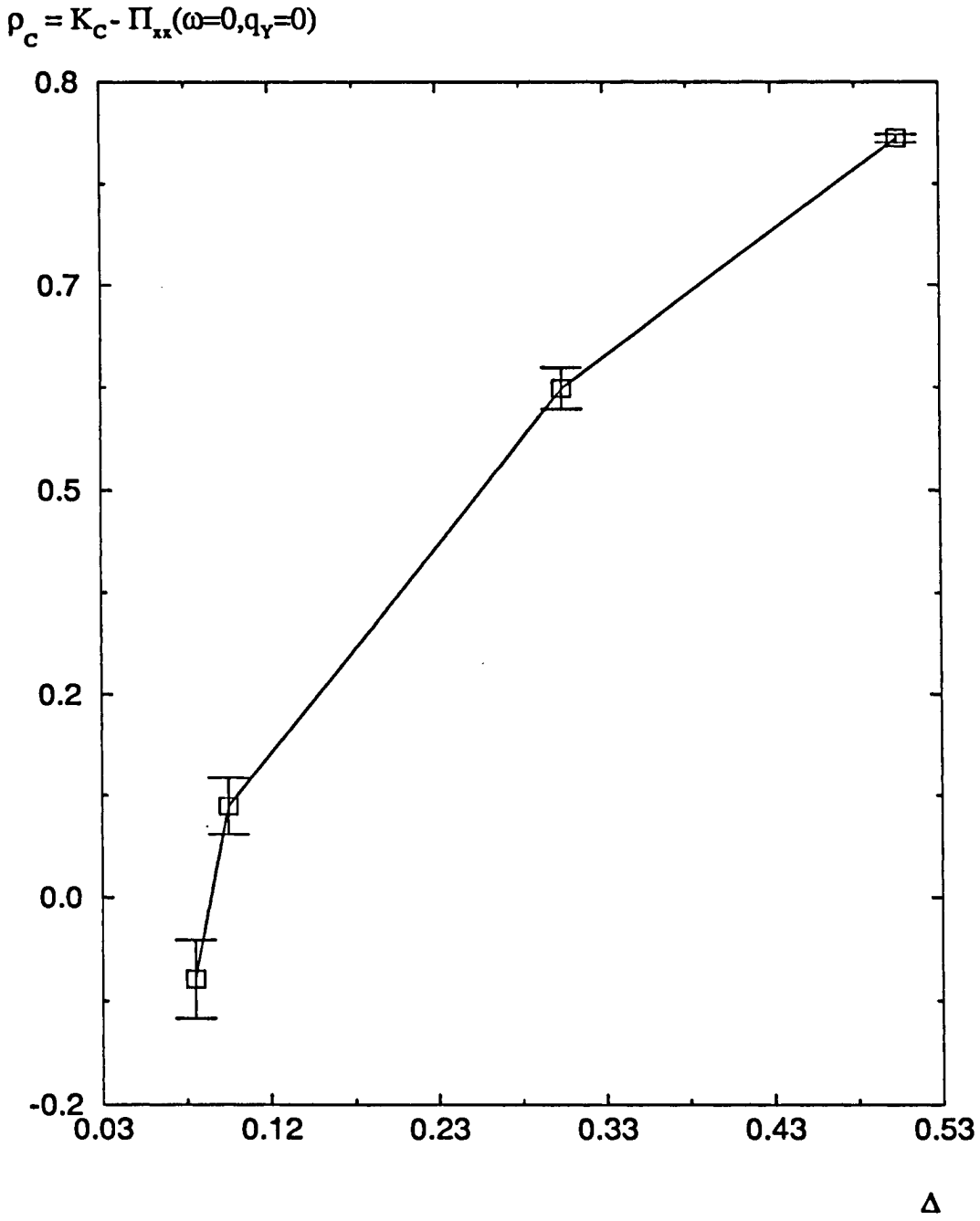

Figure 4.19: The total semiclassical superfluid density (ρ_s) as a function of disorder (Δ). In this figure, ρ_s decreases as disorder increases (Δ decreases) but remains positive for $\Delta > 0.1$. ρ_s becomes unstable at $\Delta \leq 0.08$ ($\rho_s(\Delta = 0.08) = -0.03 \pm 0.04$).

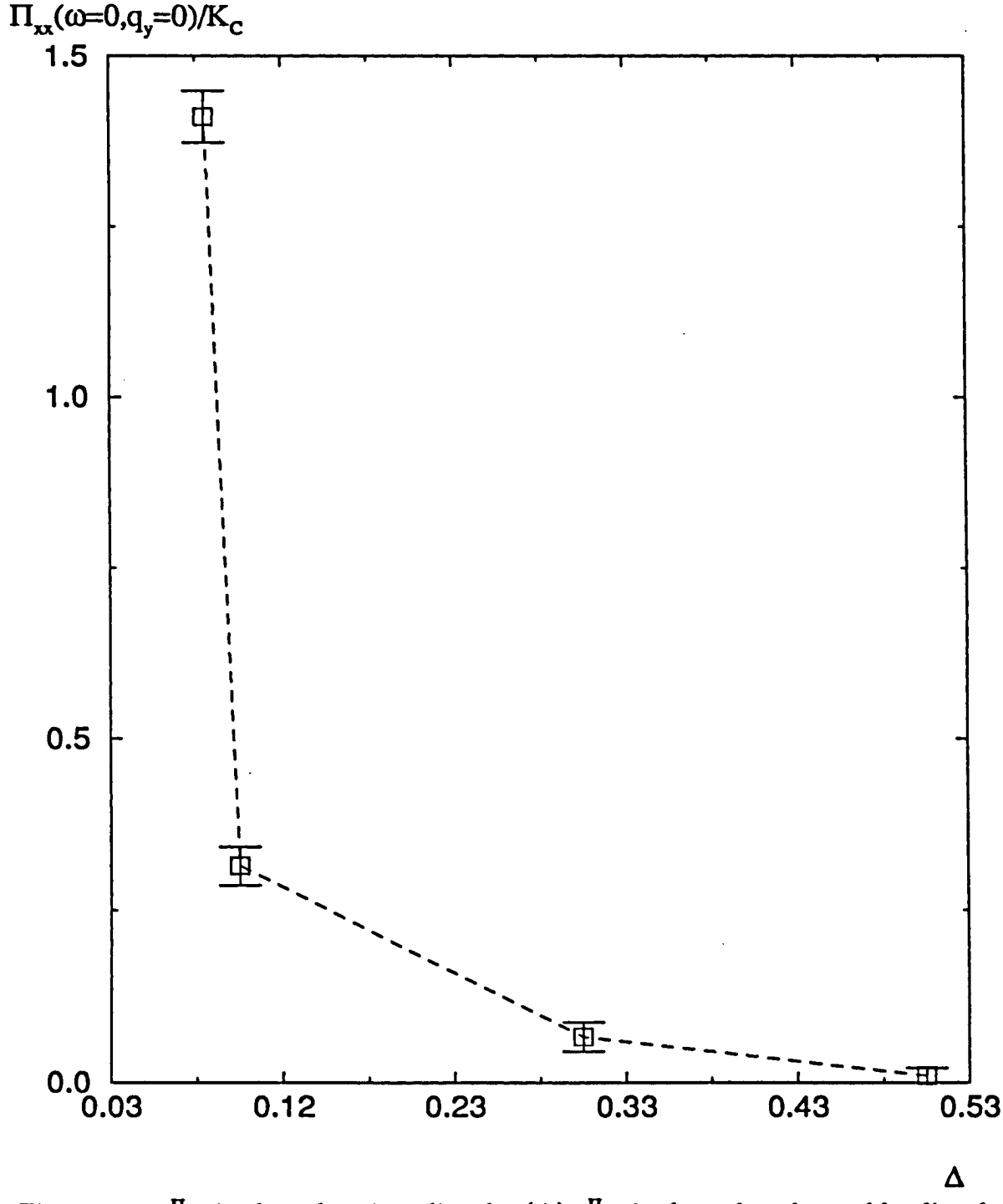

Figure 4.20: $\frac{\Pi_{xx}}{K_c}$ is plotted against disorder (Δ). $\frac{\Pi_{xx}}{K_c}$ is abruptly enhanced by disorder near the critical point (Δ=0.08).

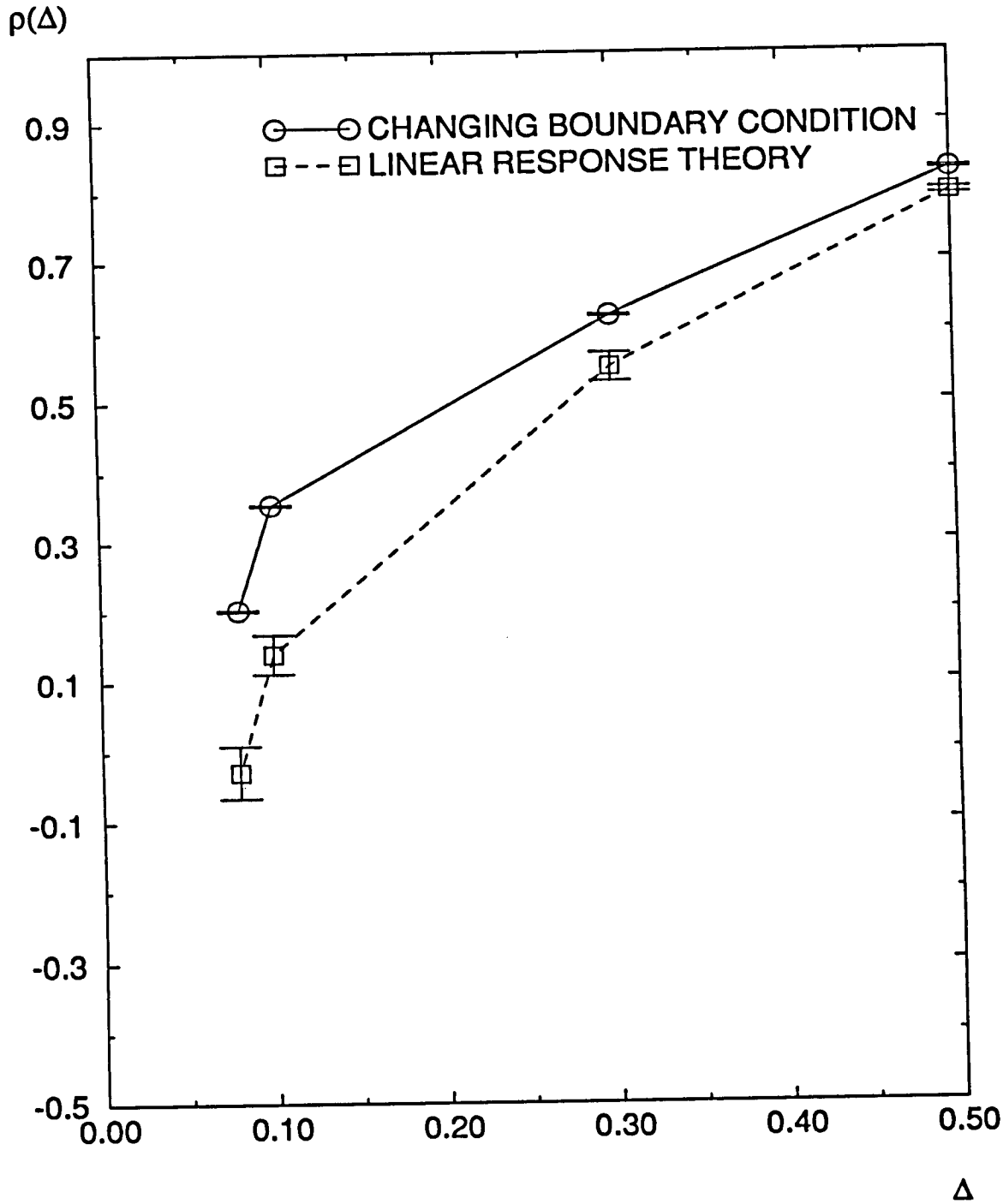

Figure 4.21: ρ_s v.s. Δ in 2D. The results from linear response theory and changing boundary condition give different results.

Bibliography

[1] L. Zhang and M.Ma, Phys. Rev. **37**, 960 (1988)

[2] T. Giamarchi and H.J. Schulz, Phys. Rev.**B37**, 325 (1988)

[3] W. Krauth and N. Trivedi, *Europhys. Lett.* **14**, 627 (1991); N. Trivedi, D.M. Ceperley, and W. Krauth and N. Trivedi, *Phys. Rev. Lett.*, **67**, 2307 (1991); R.T. Scalettar, G.G. Batrouni, and G.T. Zimanyi, *Phys. Rev. Lett.*, **66**, 3144 (1991); E.S. Sorensen, M. Wallin, S.M. Girvin and A.P. Young, *Phys. Rev. Lett.*, **69**, 828 (1992).

[4] B.C. Cooker, E. Hebard, E.N. Smith, Y. Takano and J.D. Reppy, *Phys. Rev. Lett.*, **51**, 666 (1983); M.H.W. Chan, K.I. Blum, S.Q. Murphy, G.K.S. Wong and J.D. Reppy, *Phys. Rev. Lett.* , **61**, 1950 (1988); D. Finotello, K.A. Gillis, A. Wong and M.H.W. Chan, *Phys. Rev. Lett.* , **61**, 1954 (1988); G.K.S. Wong, P.A. Crowell, H.A. Cho and J.D. Reppy, *Phys. Rev. Lett.* , **65**, 2410 (1990); M. Larson, N. Mulders and G. Ahlers, *Phys. Rev. Lett.*, **68**, 3896 (1992).

[5] D.K.K. Lee and J.M.F. Gunn, J. Phys. **C2**, 7753(1990).

[6] K. Huang and H.F. Meng, Phys. Rev. Lett., **69**, 664(1992).

[7] K.G. Singh and D.S. Rokshar, to be published.

[8] F. London, Superfluids (Wiley, New York, 1950), Vol. I, p. 27-95.

[9] For a recent discussion of the various criteria of superfluidity, see D. J. Scalapino, S. R. White and S. C. Zhang, Phys. Rev. Lett., **68**, 2830 (1992).

[10] T. Kennedy, E.H. Lieb and B.S. Shastry, *Phys. Rev. Lett.* , **61**, 2582 (1988).

[11] P. Nozieres and D. Pines, *The Theory of Quantum Liquids*, V.II, Addison-Welsley Publishing Company, INC.

[12] E.M. Lifshitz and L.P. Pitaevskii, *Statistical Physics (Part 2)*, Pergamon Press (1980); G.D. Mahan, *Many Particle Physics* Plenum, 2nd Edition, (1990).

[13] L. Zhang, Phys. Rev. **B47**, 14364 (1993).

Chapter 5

EXCITED STATES OF DISORDERED BOSON SYSTEMS

As disorder is increased, it enhances quantum fluctuations and causes an instability in the superfluid phase. And if the disorder is strong enough, the system will be driven into a localized phase of disordered bosons, so called Bose-glass phase. In the Bose-glass phase, both LRO and superfluid density will be destroyed. In addition, single particle-hole excitations will supplant the collective phonon mode as the low-lying excitations.

In this chapter, I discuss the excited state properties of the dirty boson model in the gaussian theory. As remarked in chap.3, the low-lying excitations of a uniform Bose condensate are phonons. For the pure case, the excitation spectrum is given by $\omega_k^0 = \frac{zJ}{S}\sqrt{1-\gamma_k}$. The speed of sound for this case is $c^0 = \frac{\sqrt{z}J}{S}$. For weak disorder, the perturbative result[1] shows that the speed of sound is given by $c = c^0[1-\frac{1}{2}(\frac{h}{zJ})^4]A(0)$, where

$$A(0) = \frac{3z+3}{2z} + \mathcal{P}\int \frac{d^dk}{(2\pi)^d} \frac{\frac{1}{d^2}\sum_{j=1}^{d} sin^2 k_j}{1-\gamma_k} \quad . \tag{5.1}$$

The speed of sound at low temperature is reduced with increasing disorder. The phonon has a mean free path that diverges at low frequency as $\omega^{-(d+1)}$.

5.1 DENSITY OF STATES AND ITS LOW LYING EXCITATIONS

As shown in chapter 3, the classical ground state always has LRO. However, when quantum fluctuations are included by means of the gaussian theory, there is a transition from an algebraic in 1D and a true long-ranged order in 2D superfluid phase to a disordered phase. Since in a gaussian theory, the ground state is just the classical state modified by the zero point motion of the the excitations, it is of interest to ask whether the transition is due to a change in the DOS ($g(\omega)$), or the nature of the excitations (charaterized by $v^2(\omega) = \frac{1}{N}\frac{\sum_\alpha \sum_i v_{i\alpha}^2 \delta(\omega-\omega_\alpha)}{\sum_\alpha \delta(\omega-\omega_\alpha)}$), or both.

In the pure case, $v^2(\omega) \propto \frac{1}{\omega}$ for small ω, while the linear phonon spectrum implies $g(\omega) \propto \omega^{d-1}$. For the infinitely strong disorder ($J = 0$) case, the Hamiltonian is given by $\mathcal{H} = \sum_j h_j S_j^z$. The excitations are single spin flips (the addition (removal) of a boson to unoccupied (occupied) site) with excitation energies $|h_j|$. Hence $g(\omega)$ is simply given by the distribution of random field $\{h_j\}$, and is finite at low energies. Since $g_o = g(\omega \rightarrow 0)$ is finite in the zero and infinite disorder limit in 1D, it seems reasonable to expect it is finite in 1D for all $\Delta = \frac{J}{h}$, and the transition must be due to $v^2(\omega)$ diverging faster than $1/\omega$. This picture is confirmed by the numerical calculations. Fig.5.1 shows the DOS in 1D for $\Delta = 0.5$ and size N=100. As one can see in this figure, the DOS resembles the gaussian random field distribution, with a finite g_o at low energy. The DOS plot (g(ω) is normalized by system size) is obtained by counting the number of states in each bin (energy interval). The DOS in 1D for the superfluid phase for $\Delta = 1.5$ is shown in fig.5.2, and for $\Delta = 0.6$ (near the transition) in fig.5.3. As one can see in both fig.5.1 and fig.5.3, g_o is finite. Thus, for 1D, the DOS is constant across the transition. Since the calculation is for a finite size, there is some ambiguity in deciding g_0 for the infinite system. To clarify this, I have checked that the scaling of g_0 with size N is consistent with a non-zero DOS at zero energy. As one can see in fig.5.4, g_o scales linearly with size N implying g_o is finite.

For $\Delta < \Delta_c$, $\delta m \propto N^\theta$, with $\theta = \theta(\Delta)$ (see chap. 3). My results show that the exponent θ is consistent with the exponent of $v^2(\omega) \sim \frac{1}{\omega^\delta}$, with $\delta = 1 + \theta$. This last relation is in fact consistent with finite g_o. This conclusion can be easily seen from eq.(5.2) and eq.(5.3) as follows. From the definition of $v^2(\omega)$, assuming g_0 finite, one has

$$\delta m = \int_{\omega_0} d\omega g(\omega) v^2(\omega) \sim \omega_0^{-\delta+1} \quad . \tag{5.2}$$

The lower cutoff ω_0 is the smallest excitation energy for a given size N. Since the DOS

is defined as the number of states per unit volume per unit energy, for 1D one has

$$\int_0^{\omega_0} g(\omega) N d\omega = 1 \ . \tag{5.3}$$

Hence for finite g_o, $\omega_0 \sim \frac{1}{N}$. Comparing to $\delta m \propto N^{\theta}$, one thus sees that a finite g_o is consistent with $\delta = 1 + \theta$. The numerical results give $\delta \approx 1.5$ (1.50± 0.01) and $\theta \approx 0.5$ (0.58±0.04) for $\Delta = 0.5$. The plot of $v^2(\omega)$ v.s. ω for $\Delta = 0.5$ is shown in fig. 5.5 with the exponent $\delta \approx 1.5$.

In two dimensions, without disorder, $\omega = c_0 k$ for small k. Thus for small ω, DOS $g(\omega) = \frac{1}{2\pi}\frac{1}{c_0^2}\omega$. With disorder, k is no longer a good quantum number, but if phonons are still the low-lying excitations, then presumably $g(\omega) \sim \omega$. One can define an effective speed of sound c as $g(\omega) = \frac{1}{2\pi}\frac{1}{c^2}\omega$, and one would expect it to decrease with increasing disorder. $g(\omega)$ on the superfluid side for two values of disorder is shown in fig. 5.6 and fig. 5.7, confirming $g(\omega)$ is linear in ω, with the the slope increasing with decreasing Δ. In the localized phase, I argued before that g_o should be finite. Fig 5.8, shows the the DOS in the disordered phase ($\Delta = 0.08$), indicating a finite g_0. In fact, even at this value of Δ, $g(\omega)$ is well approximated by the DOS in the $\Delta \to \infty$ limit, i.e. by the random field distribution $P(\{h_i\})$. In fig. 5.9, I show the Δ dependence of the speed of sound normalized to the pure case, $\frac{c(\Delta)}{c_0}$. As one can see in this figure the speed of sound decreases with the increasing disorder. Two possible scenarios for the behaviour of $c(\Delta)$ as the transition is approached from the superfluid side are

i) The speed of sound is reduced continuously with increasing disorder and vanishes right at the transtion. In this case the DOS changes continuously, $g_o(\Delta_{c+}) = g_o(\Delta_{c-}) = 0$.

ii) $c(\Delta_{c+})$ is finite and the DOS is discontinuous, $g_o(\Delta_{c+}) \neq g_o(\Delta_{c-})$. However, $\frac{dg(\omega)}{d\omega}|_{\omega=0}$ is discontinuous.

Although I cannot rule out c dropping very abruptly to zero as $\Delta \to \Delta_{c+}$, fig. 5.8 strongly suggests that $c(\Delta_{c+})$ is finite, and the DOS is discontinuous across the transition.

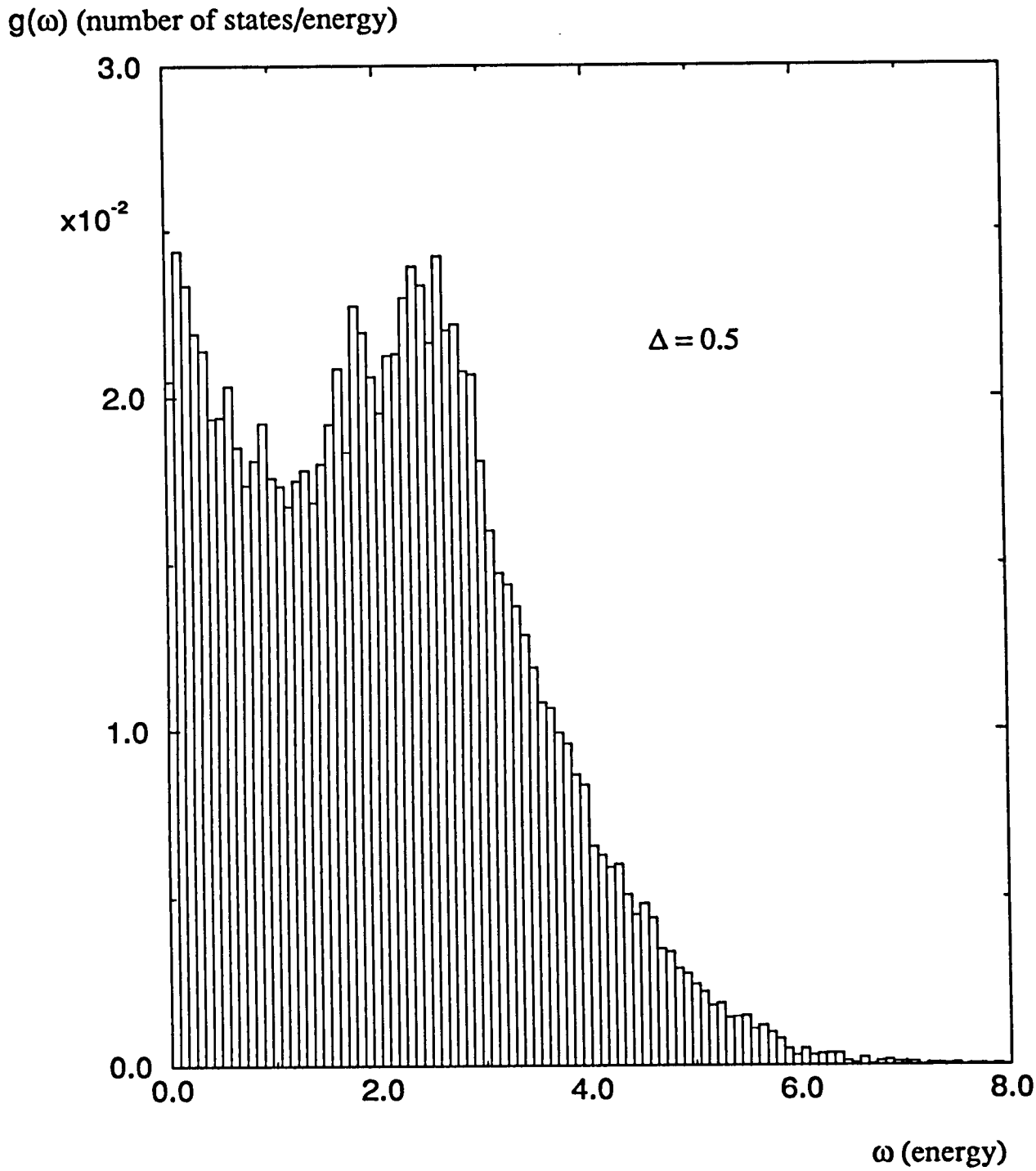

Figure 5.1: Density of states of the insulating phase ($\Delta = 0.5$) in 1D for N=100

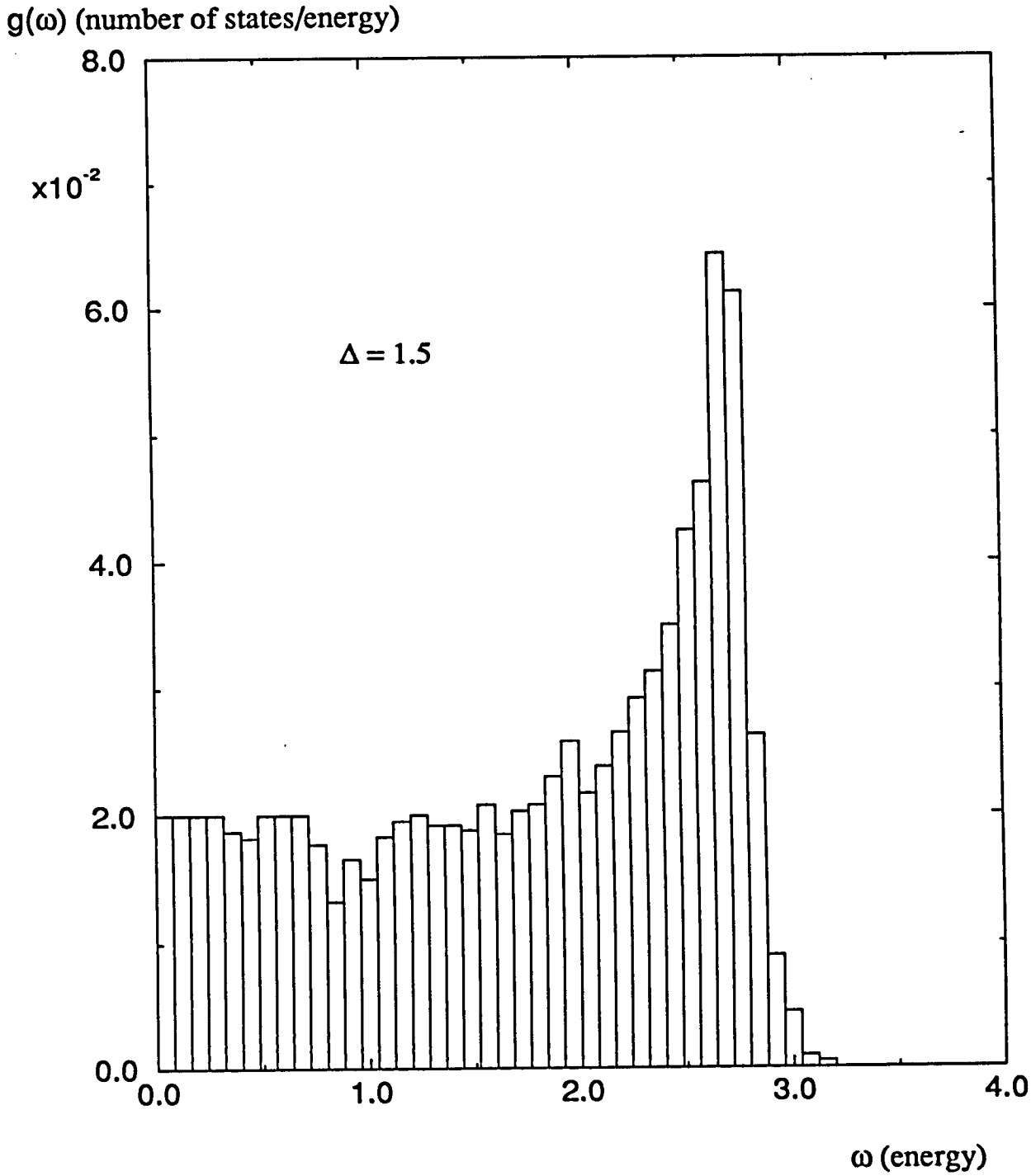

Figure 5.2: DOS of the superfluid phase ($\Delta = 1.5$) for $N = 100$.

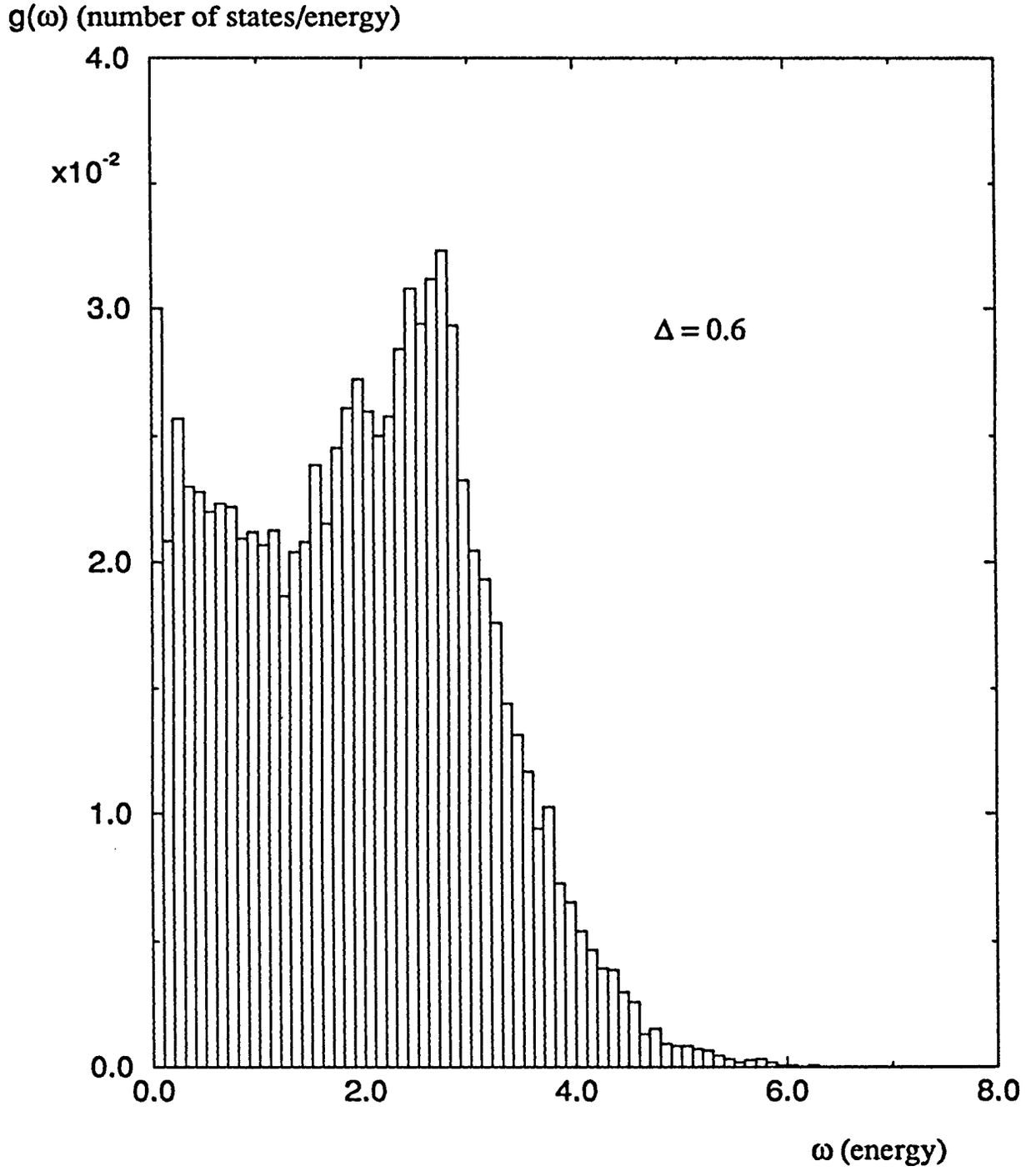

Figure 5.3: DOS for $\Delta = 0.6$ (near the transition on the superfluid side) with system size N=100.

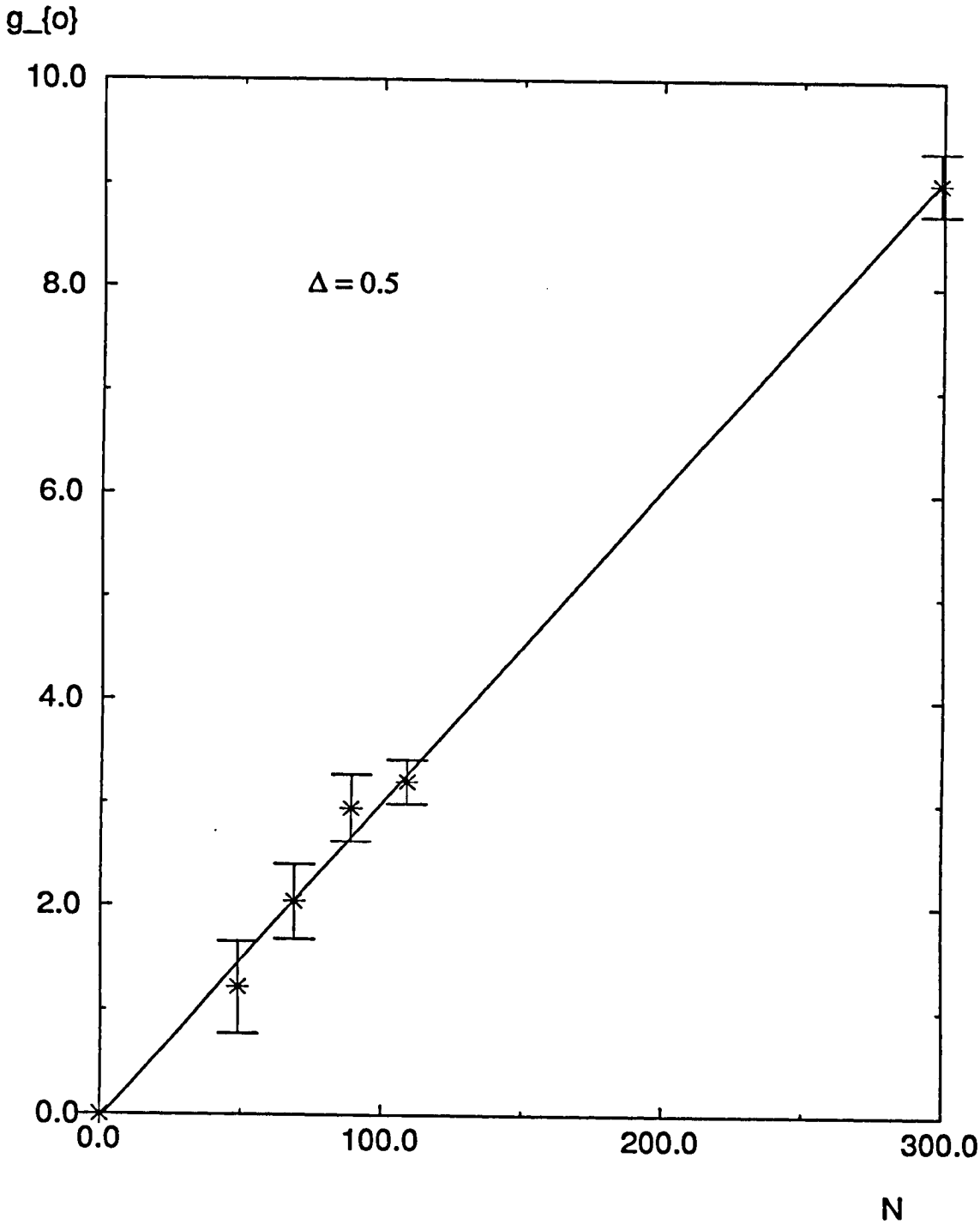

Figure 5.4: Plot supporting the DOS is finite at low energy in 1D for $\Delta = 0.5$. By fixing the y-intercept equal to zero, one can see that g_0 (defined as the first bin of DOS times the systems size) is linear proportional to N with the accuracy within the error bars.

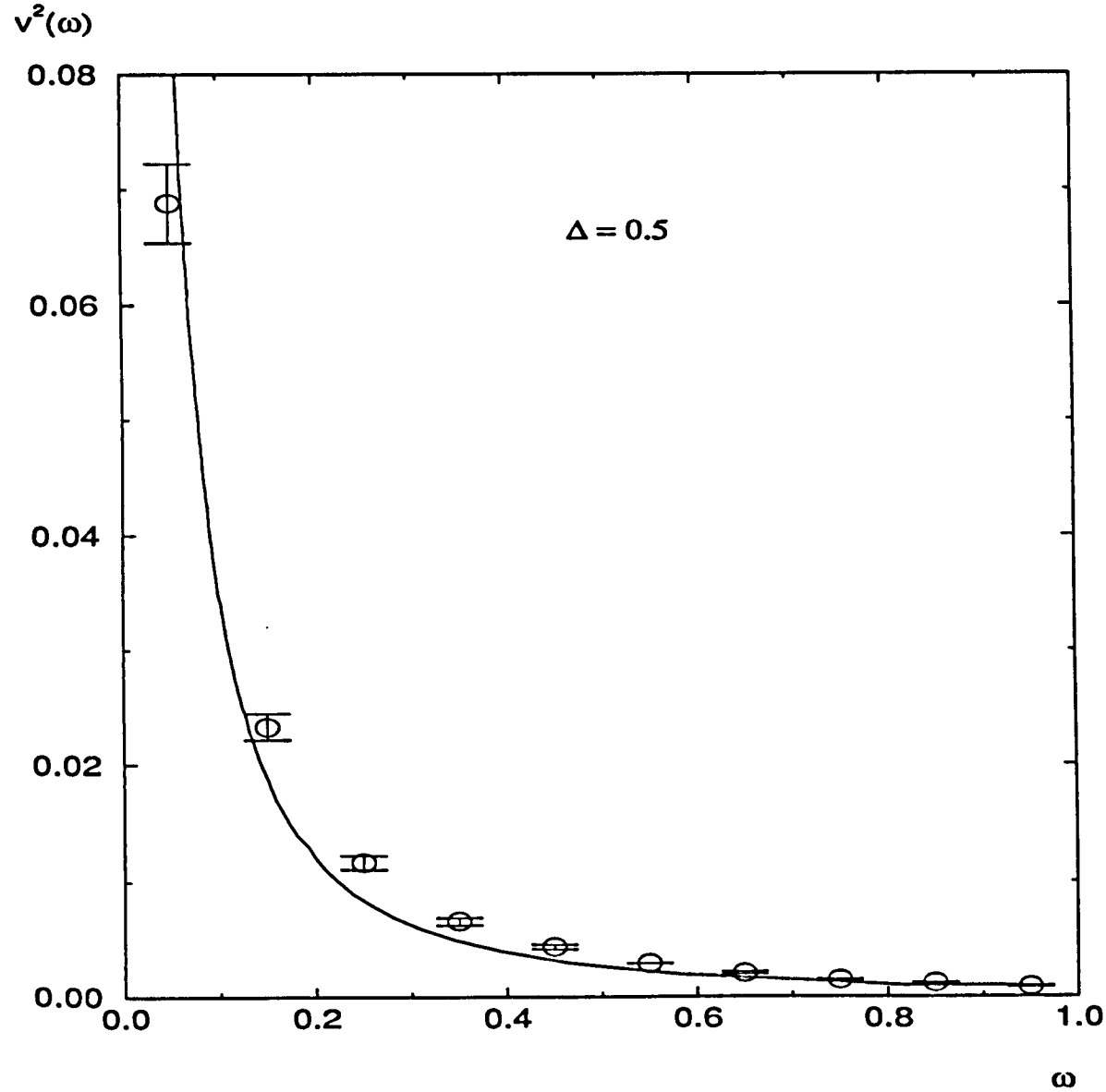

Figure 5.5: The plot of $v^2(\omega)$ v.s. ω for $\Delta = 0.5$ (N=100).

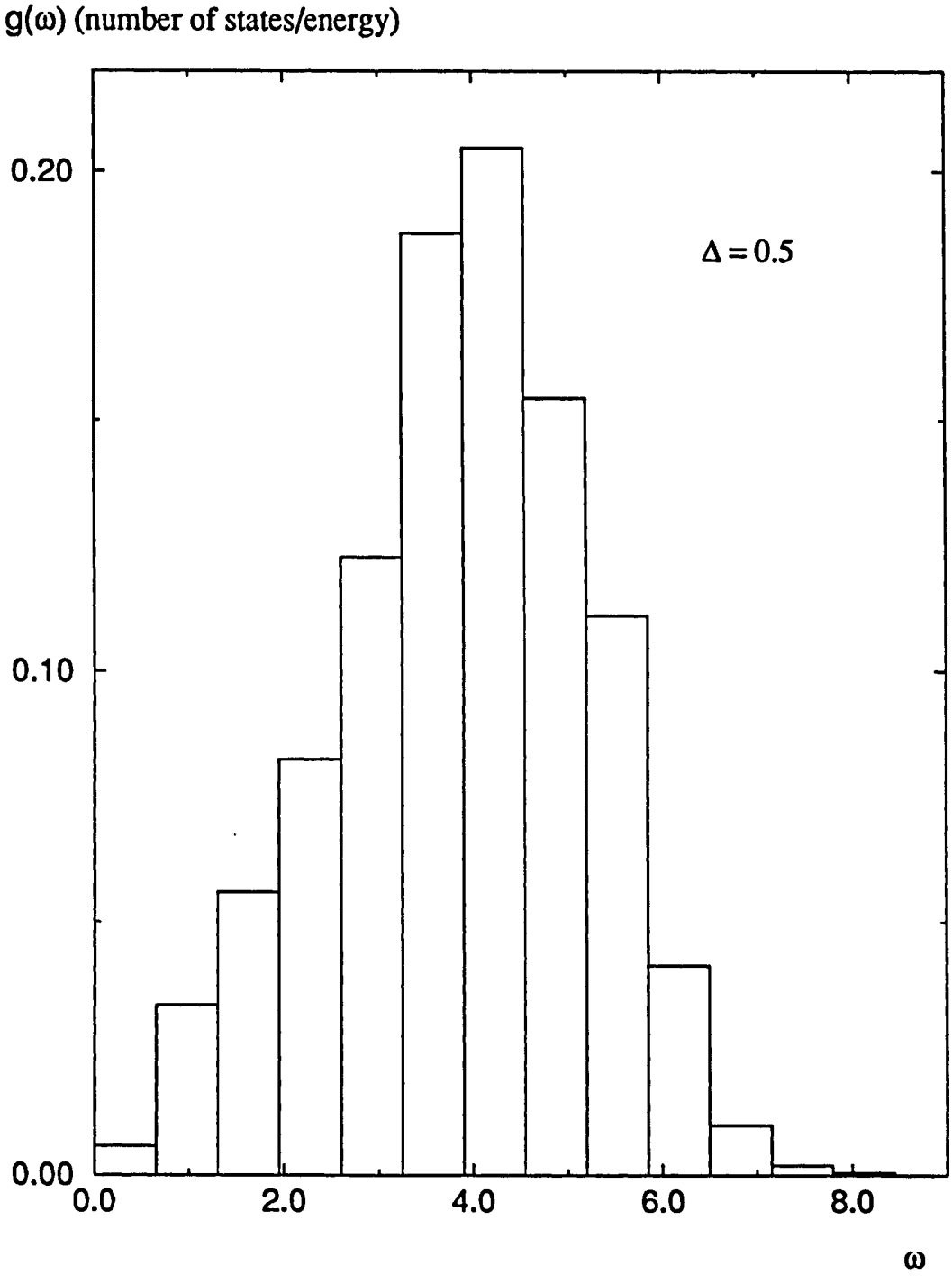

Figure 5.6: DOS of the superfluid phase ($\Delta = 0.5$) in 2D with size 13× 13. Note the linear slope (α=5.86± 0.34) for low energy excitations.

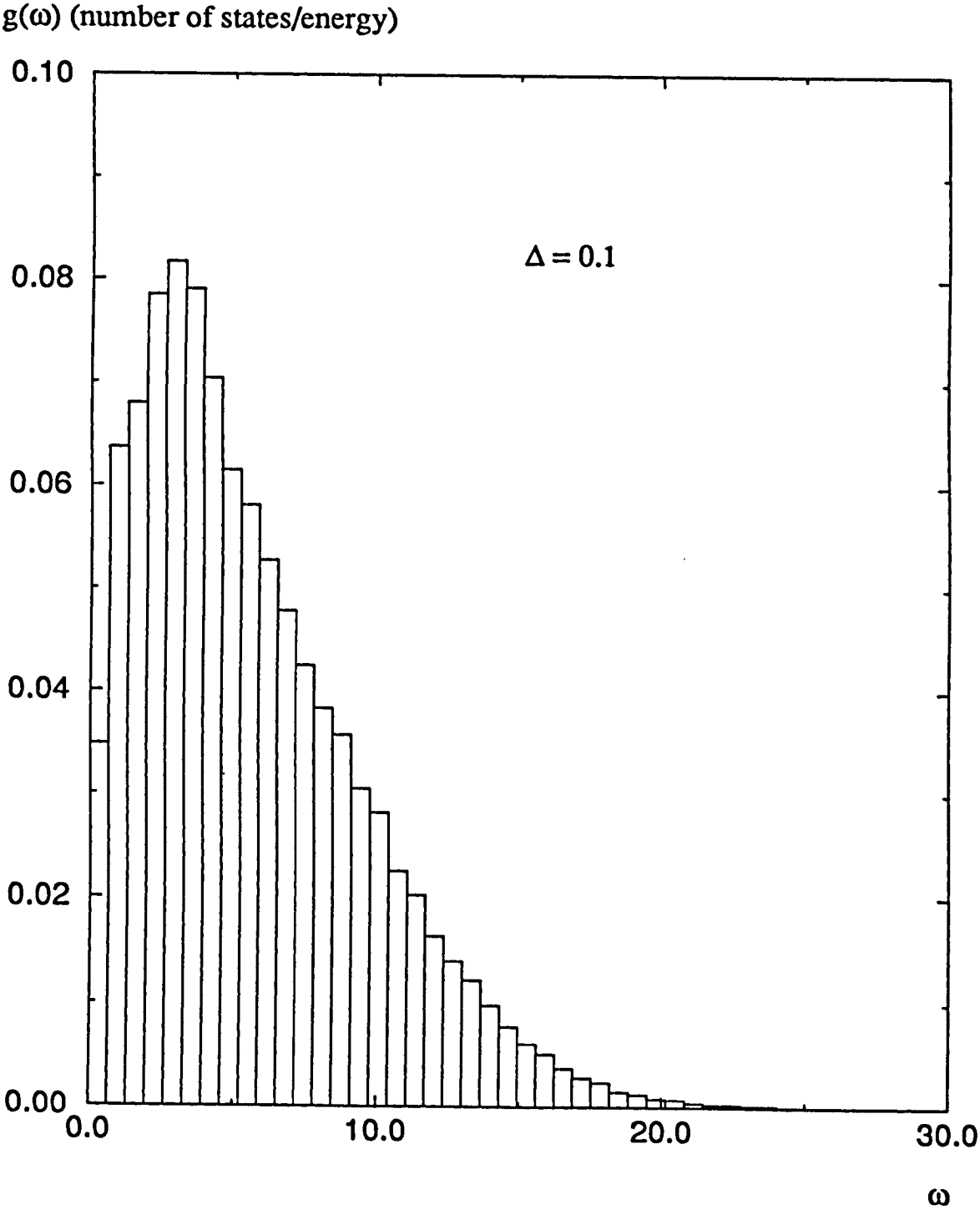

Figure 5.7: DOS for size 13×13 ($\Delta = 0.1$).

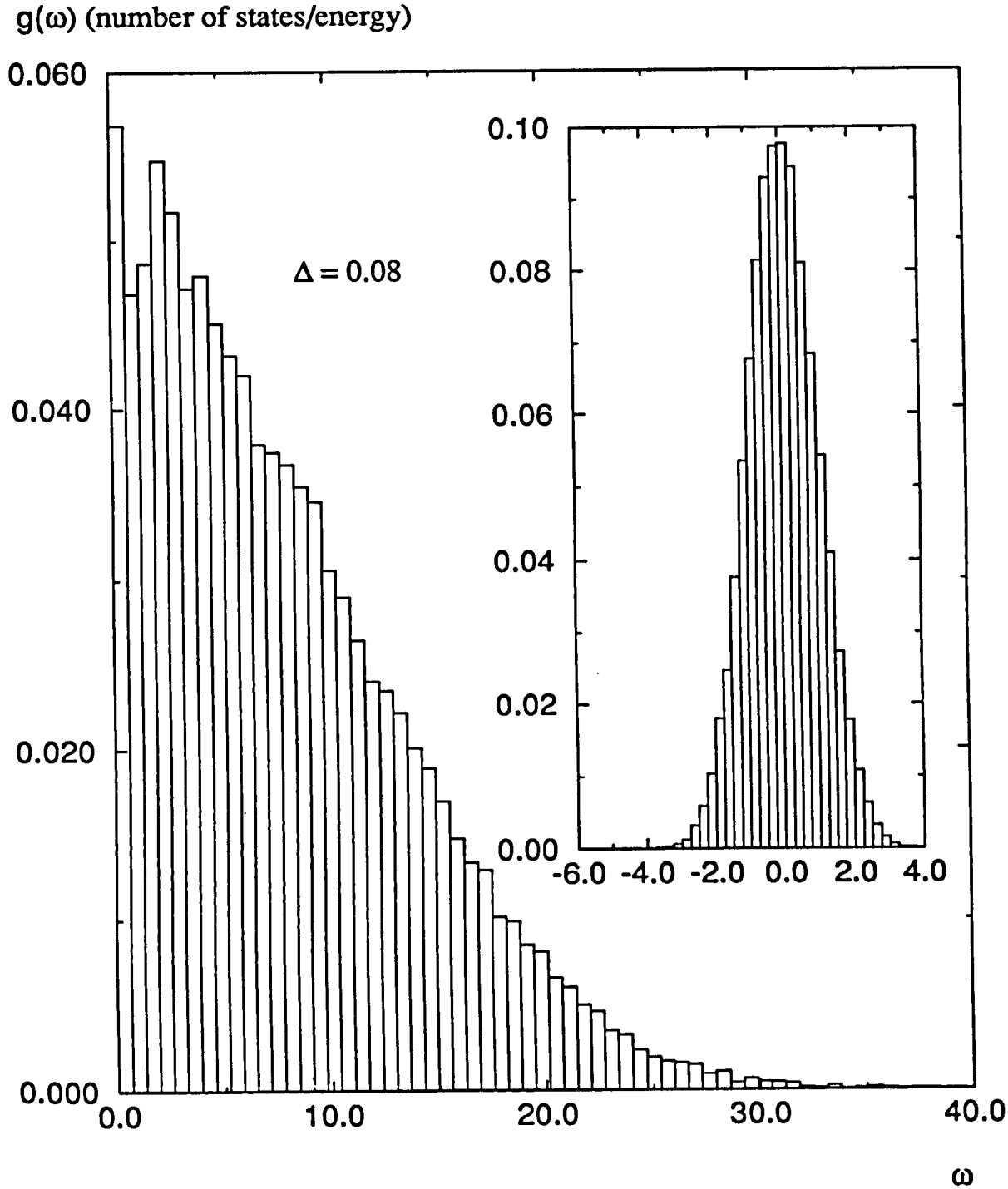

Figure 5.8: DOS for size 13×13 on the insulating side($\Delta = 0.08$). The linear slope disappears. The DOS is dominated by the random field distribution $P(\{h_i\})$, with finite DOS at zero excitation. The inset frame shows the DOS of the random field distribution, $P(\{h_i\})$.

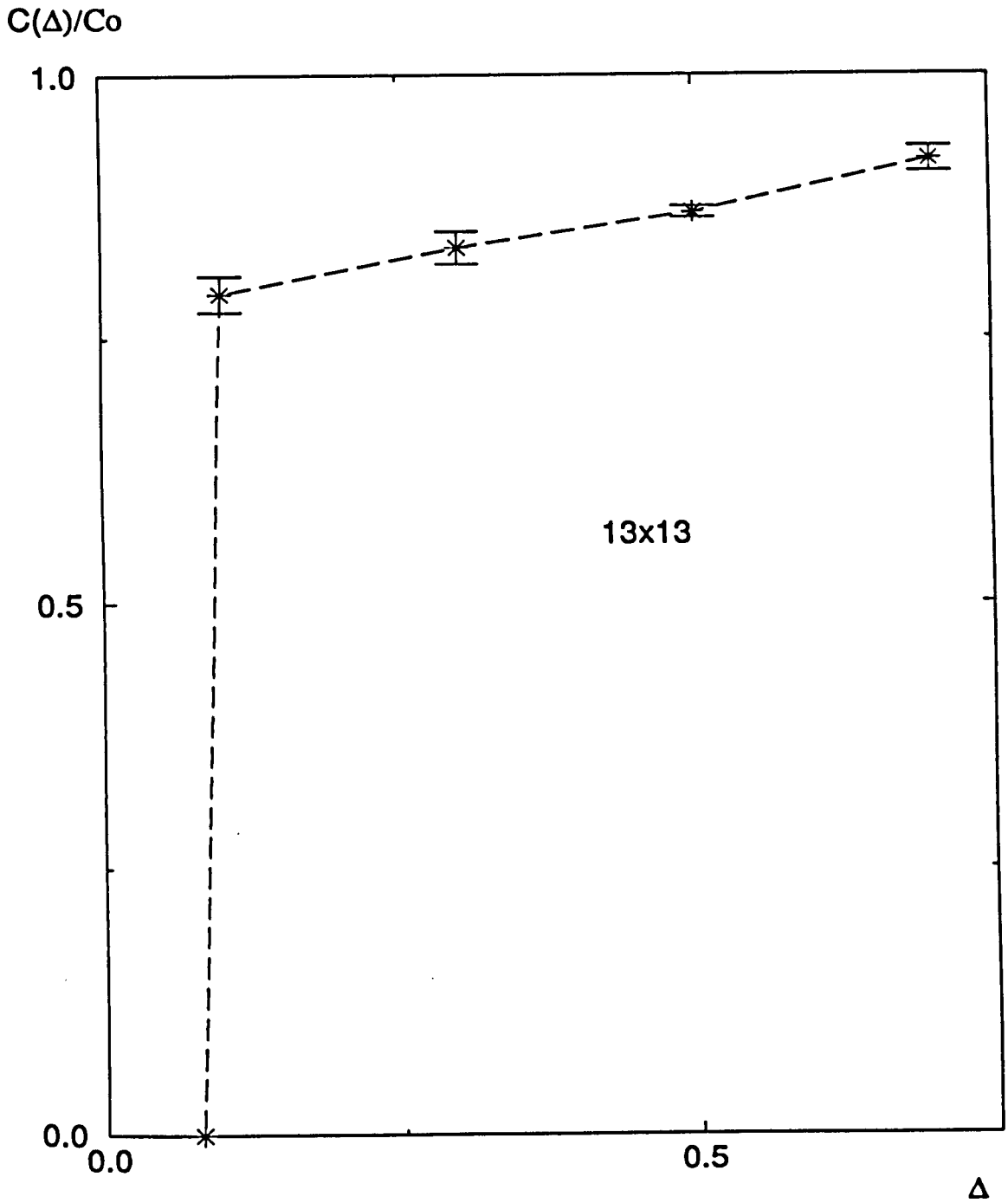

Figure 5.9: The plot of the speed of sound $\frac{c(\Delta)}{c_0}$, v.s. Δ. The speed of sound defined through the shape of the DOS reduces with increasing disorder. Apparently, $c(\Delta_{c+})$ is finite.

Since $g(\omega) \propto \omega$ in the superfluid phase and g_o is finite in the Bose-Glass phase away from the transition, one expects the specific heat to be $\propto T$ and $\propto T^d$ respectively. Unfortunately, I cannot definitely conclude whether the DOS transition exactly occurs at the order parameter transition due to the inability of pinpointing Δ_c.

5.2 LOCALIZATION OF THE EXCITATIONS

The low-energy excitations discussed in the previous section are particularly significant in the SF phase, as they are approximations to the collective modes (phonons). In principle, these states can be extended or localized. The zero-energy mode is a Goldstone mode and corresponds to uniform phase rotation, it therefore must be extended. Assuming the localization length has a monotonic and smooth dependence on energy, for a given amount of disorder, one expects to have a transition from extended states to localized states with increasing energy at a mobility edge energy E_c. And with sufficient disorder , $E_c \rightarrow 0$. Then, all states except the Goldstone mode will be localized. One obvious question is if the the ground state transition relates to the localization transition of the excited states, with perhaps $E_c \rightarrow 0$ as $\Delta \rightarrow \Delta_{c+}$. The quantity I calculate as a measure of localization is the inverse participation ratio $\mathcal{P}(\omega)$ defined as the mean of the fourth power of the eigenstates,

$$p(\omega_\alpha) = \frac{\sum_{i=1}^{M} u_{i\alpha}^4}{(\sum_{i=1}^{M} u_{i\alpha}^2)^2} \ , \tag{5.4}$$

which I assume for localized states scale as the inverse localization length ξ^{-1}, and is zero for extended states in infinite systems. The mobility edge energy, E_c, is defined as the energy where p first vanishes. However, for finite size, p scales as the greater of ξ^{-d}, L^{-d}. Hence, at low energy, where $\xi > L$, $p(E)$ is energy independent, and only for $E > E_c(L)$, where $p(E_c(L)) = L^{-1}$ for 1D. Does $p(E)$ give the behavior of an infinite system ? One way to obtain E_c is by extrapolating that part of the curve of $p(\omega)$ v.s. E to $\mathcal{P} = 0$. An improved method is to extrapolate $E_c(L)$ to $L \rightarrow \infty$ [2].

Since eqn.(2.27) guarantees that $u_{j\alpha}$ and $v_{j\alpha}$ are either both extended or localized, it suffices to calculate $p(E)$ for $u_{j\alpha}$.

First consider the 1D case. In fig. 5.10 and 5.11, I show $p(E)$ for various L's in 1D for $\Delta = 1.5$ (SF side) and $\Delta = 0.5$ (insulating side). The former seems to show clearly a finite E_c. For the latter, I ascertain E_c to be very small, probably zero (the extrapolation actually gives an unphysical small negative value). This seems to support the ground state and excited localization are related.

Upon reflection, I have serious reservations. In the perturbative (for disorder) calculation of ref.[1], the phonon mean free path is found to diverge as $E^{-(d+1)}$. From the known result of phonon localization in 1D, the localization length and the mean free path are essentially identical, since any scattering is backscattering. Moreover, since the low-lying excitations in our problem are phonons, this problem should be equivalent to other known results of phonon localization model. Hence, one expects the relatively slow $\xi^{-1}(E) \propto E^2$ for small E, crossing over to a more rapid E dependence at a higher cross-over energy E_x. This is known to be the case for classical vibrational modes in 1D [3], and all states except the uniform translation mode are localized. The problem is that the divergence of the localization length ξ is not a true critical phenomena with a critical exponent. In this calculation, if the size $L < \xi(E_x)$, then one cannot probe the weak E dependent regime, and one will mistake E_x for E_c. Hence, I believe $E_c = 0$ for any disorder in 1D.

For comparison, in fig. 5.12 and 5.13 I look at a finite system of random masses connected by springs in 1D and find $p(E)$ curves similar to fig. 5.11 and 5.10. While these results do not constitute evidence for all eigenstates of eq.(2.24) to be localized in 1D, I believe this is in fact the case, and what fig. 5.10, 5.11 show is E_x decreasing as the disorder is increased, vanishing at or close to the superfluid-insulator transition.

For 2D, on less firm ground, it is believed that all classical vibrational waves are also localized[4]. I find similar features to the 1D case. Fig. 5.14 - fig. 5.16 show the plots of the participation ratio for 2D. As one can see in fig. 5.14, for

weak disorder ($\Delta = 0.5$), apparently there is a finite pseudo-moblity edge energy, E_x. As the disorder becomes stronger, E_x becomes smaller(or even close to zero) as presented in fig. 5.15 and fig. 5.16. However, I cannot say for certain if $E_x \rightarrow 0$ at the transition. Although my result does not constitute proof that all the excited states are all localized in 2D, I believe that is the case. A physical consequence of this is that there are no propagating sound modes. Thus, unlike the pure case, the speed of sound calculated from the slope of the density of states (section 5.1) is very much a dream. Experimentally, the absence of propagating sound modes can be tested on ^4He absorbed on disordered substrates.

In conclusion, I believe $E_c = 0_+$ for any disorder in 1D and 2D, and the localization transition of the excitations are unrelated to that of the ground state. My calculation, however, indicates that there is an energy scale, E_x which does seem to be correlated to the ground state localization. The significant of this is not yet clear. In 3D, general localization theory predicts a mobility edge for weak disorder. Thus, presumably $E_c \rightarrow 0_+$ at a finite critical disorder unrelated to Δ_c for the ground state.

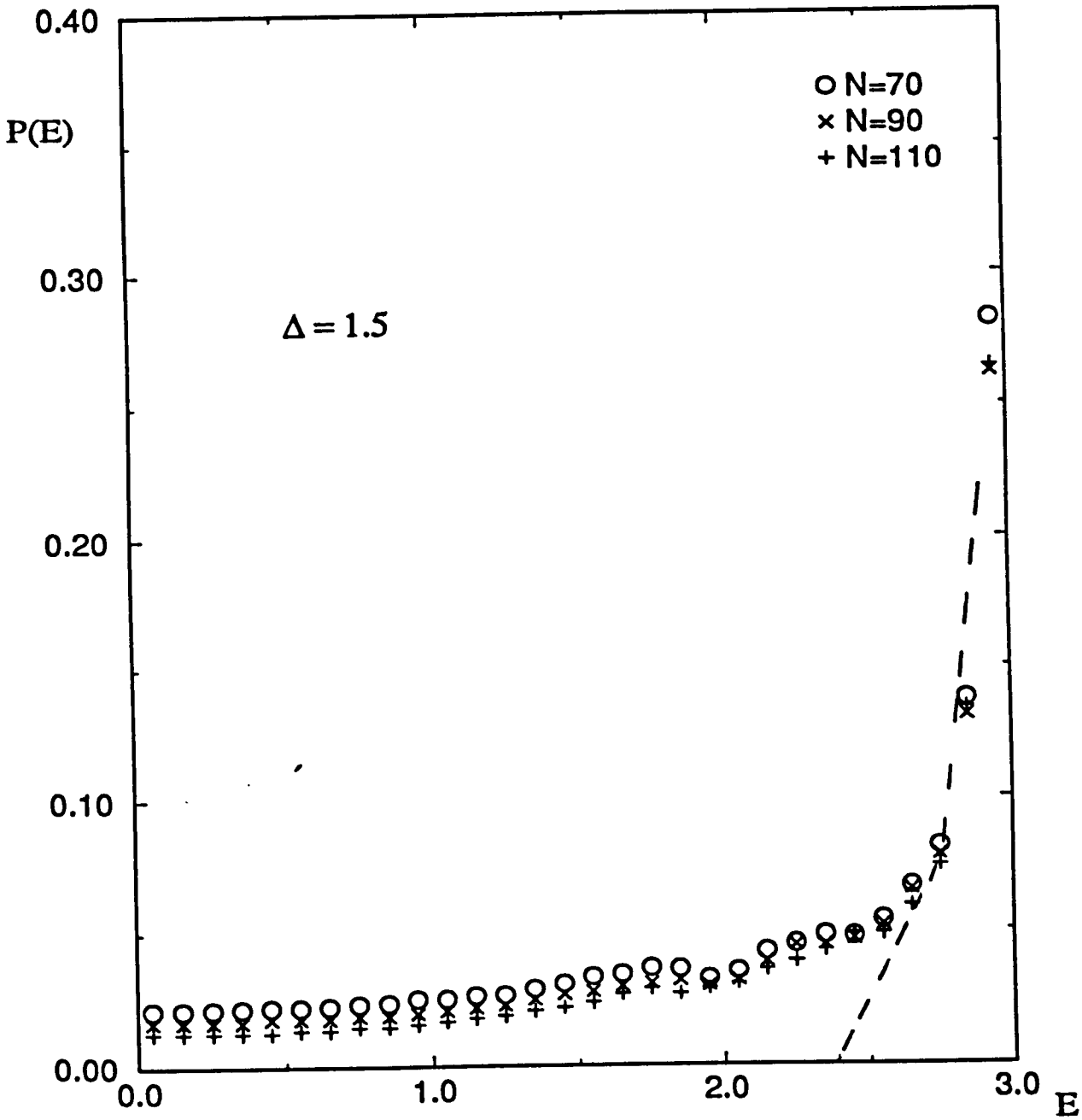

Figure 5.10: Inverse participation ratio $p(E)$ in 1D is plotted for several values of N. The pseudo-mobility edge E_x is obtained from these plots through the extrapolation procedure decribed in the main text. Here I show the plot for superfluid phase ($\Delta = 1.5$) with finite E_x.

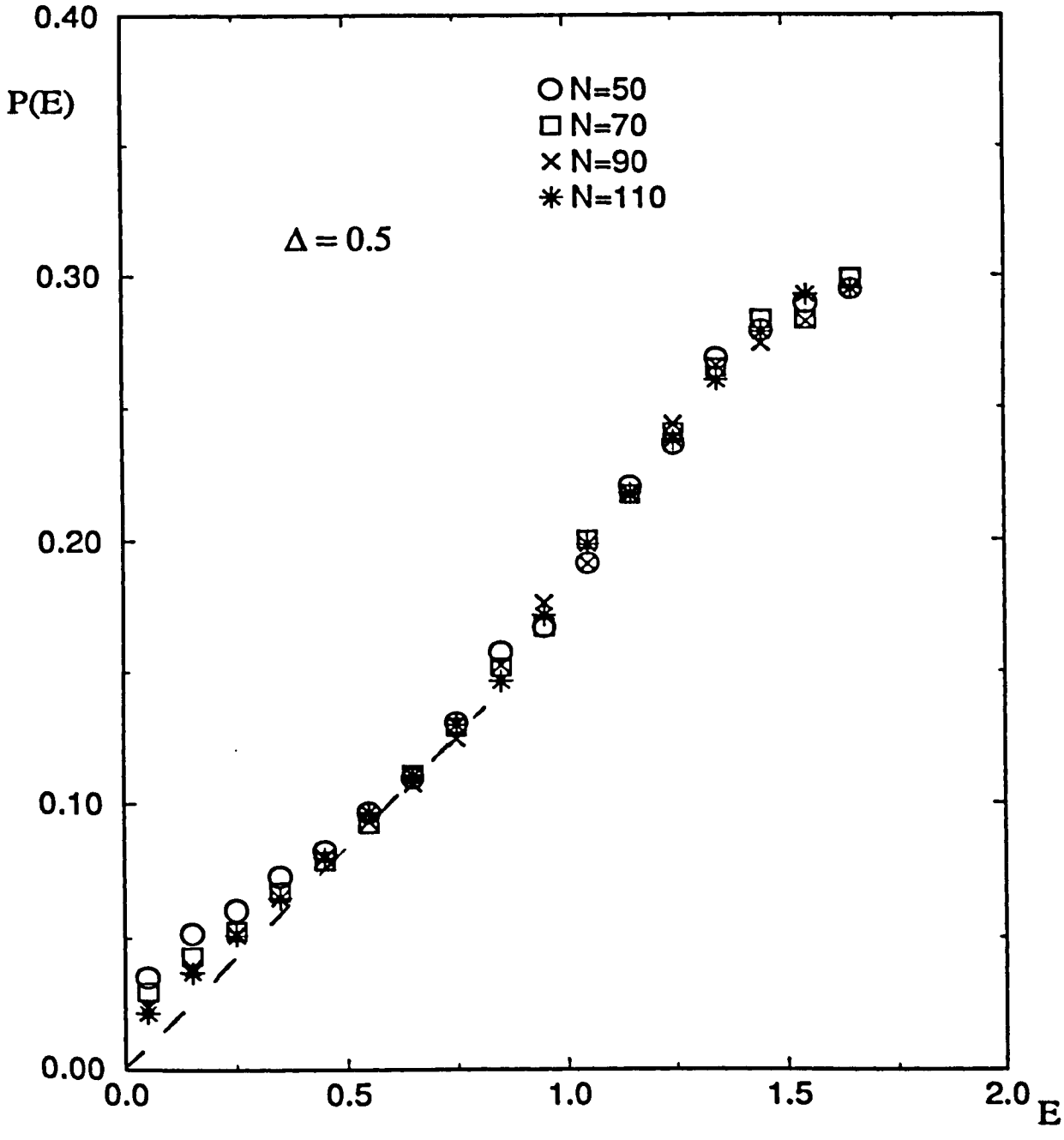

Figure 5.11: p(E) v.s. E in the insulating phase ($\Delta = 0.5$), E_x is close to zero.

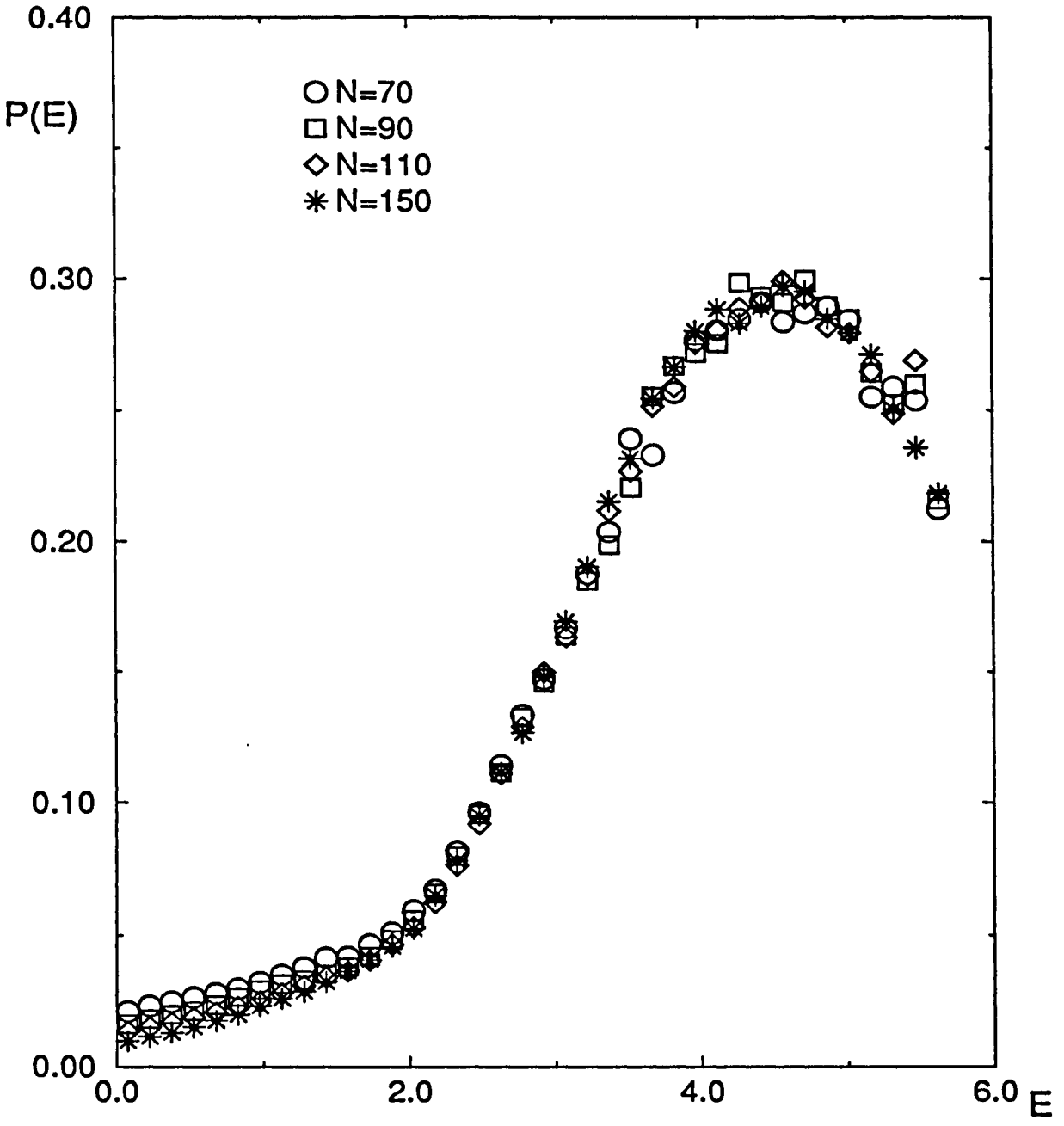

Figure 5.12: The finite size scaling of inverse participation ratio P(E) v.s. E for a finite system of random masses for the strong localization case ($E_x = 0$).

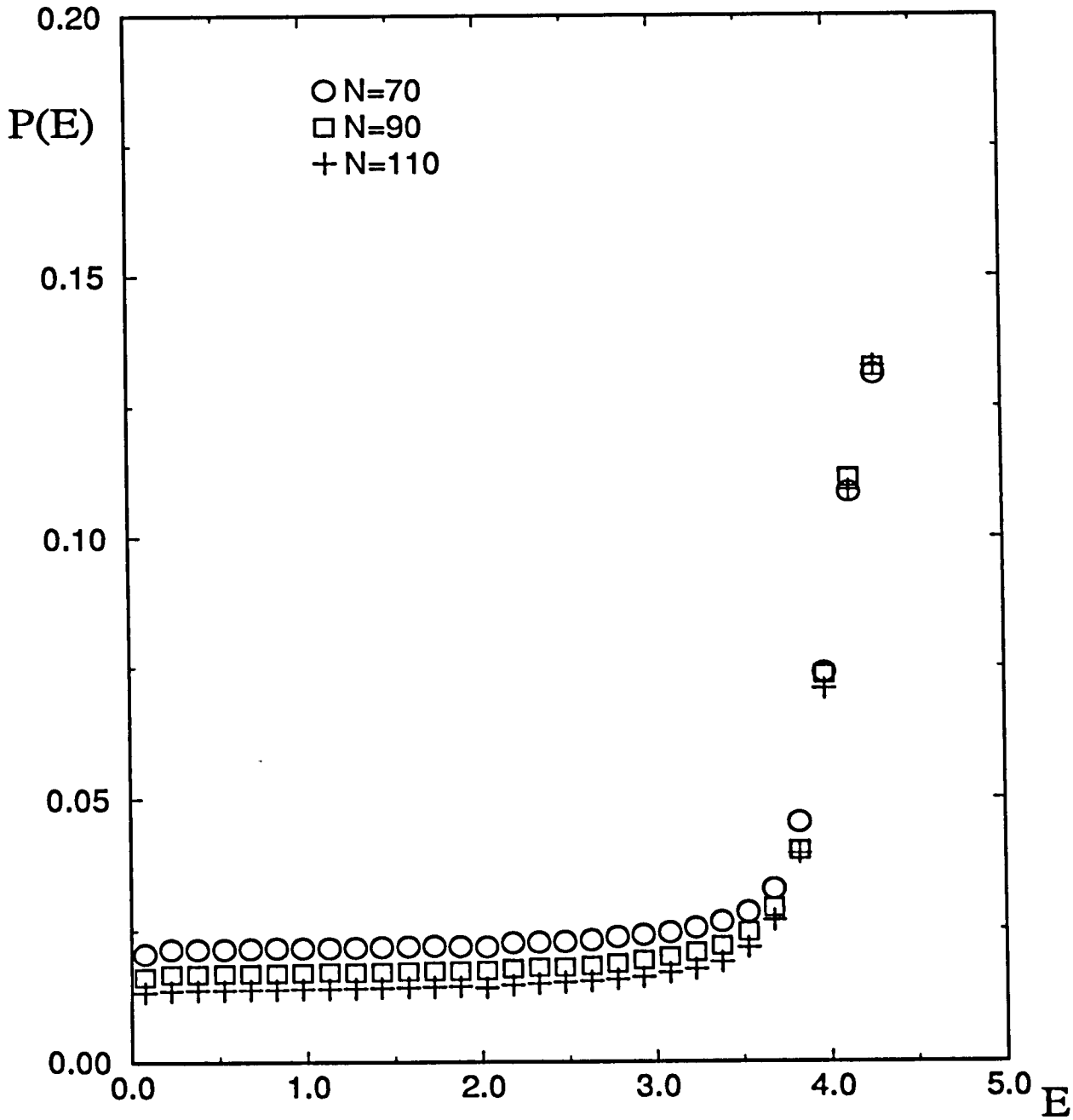

Figure 5.13: Plot of inversed participation ratio P(E) v.s. E for a finite system of random masses for the weak localization case with finite pseudo-mobility edge energy E_x.

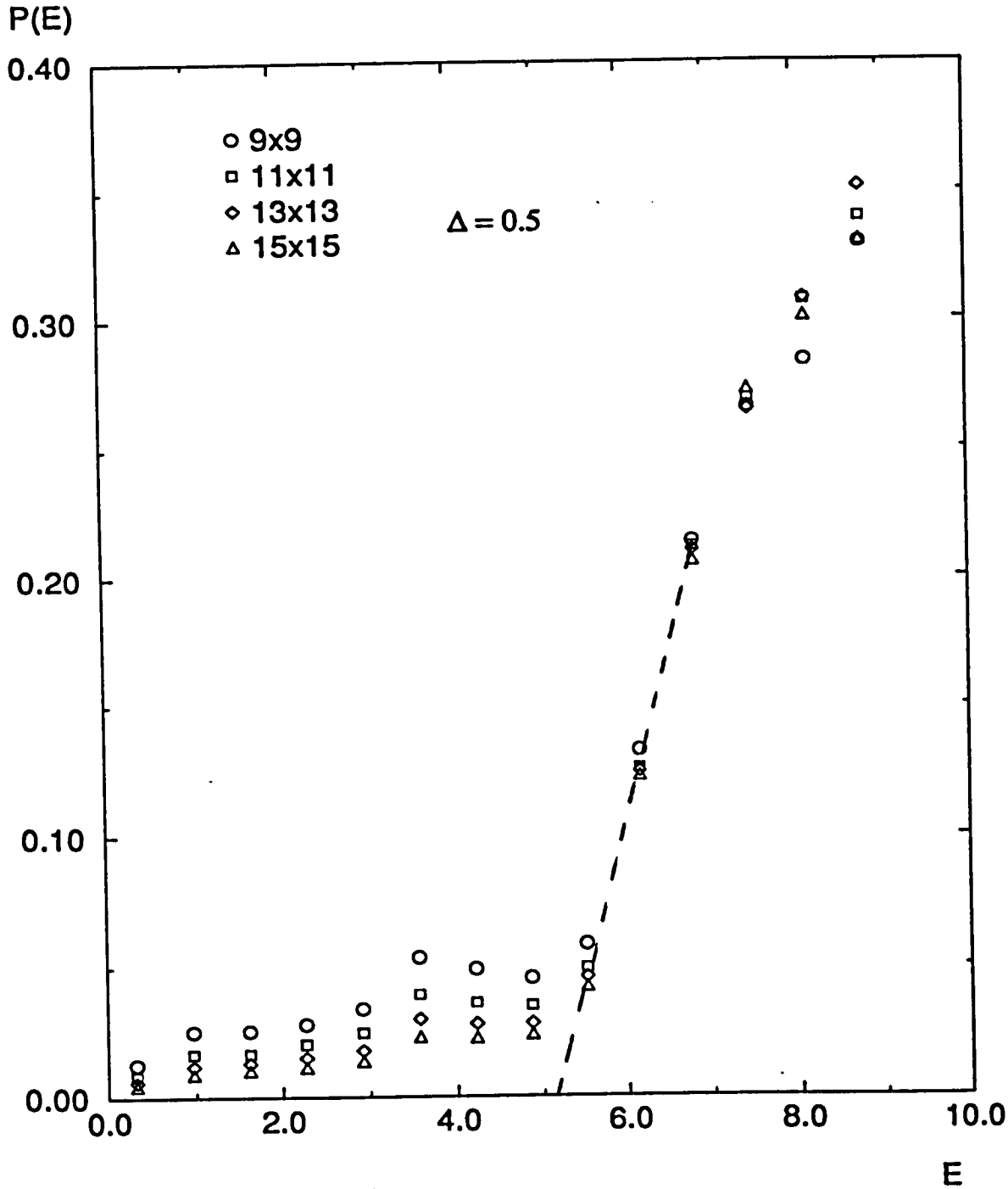

Figure 5.14: P(E) v.s. E in 2D for $\Delta = 0.5$ shows an apparent finite mobility edge energy.

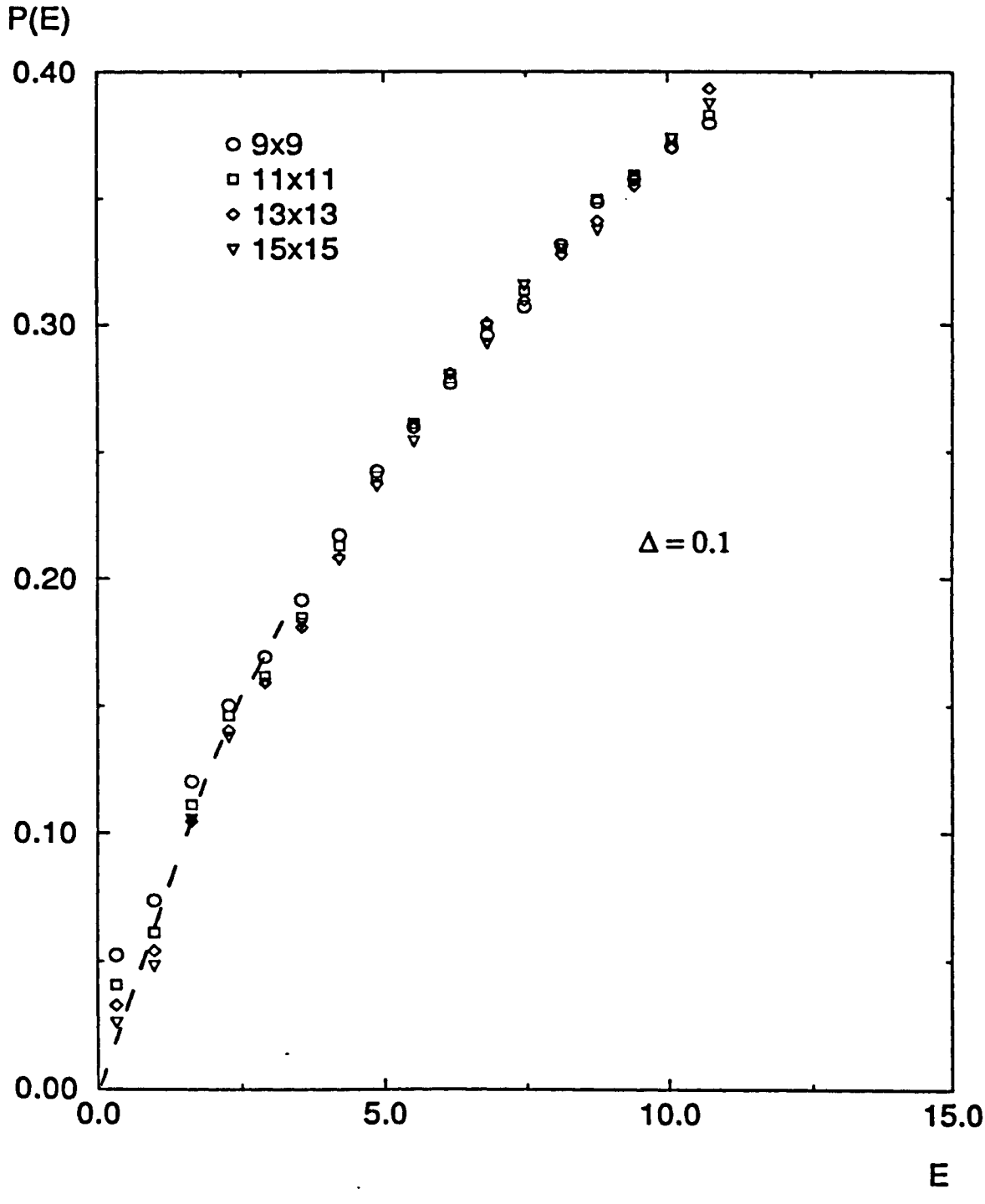

Figure 5.15: Similar to fig. 5.13 but for Δ=0.1. As the disorder is increased, the pseudo-mobility edge energy E_x becomes smaller and vanishes near or at the ground state transition.

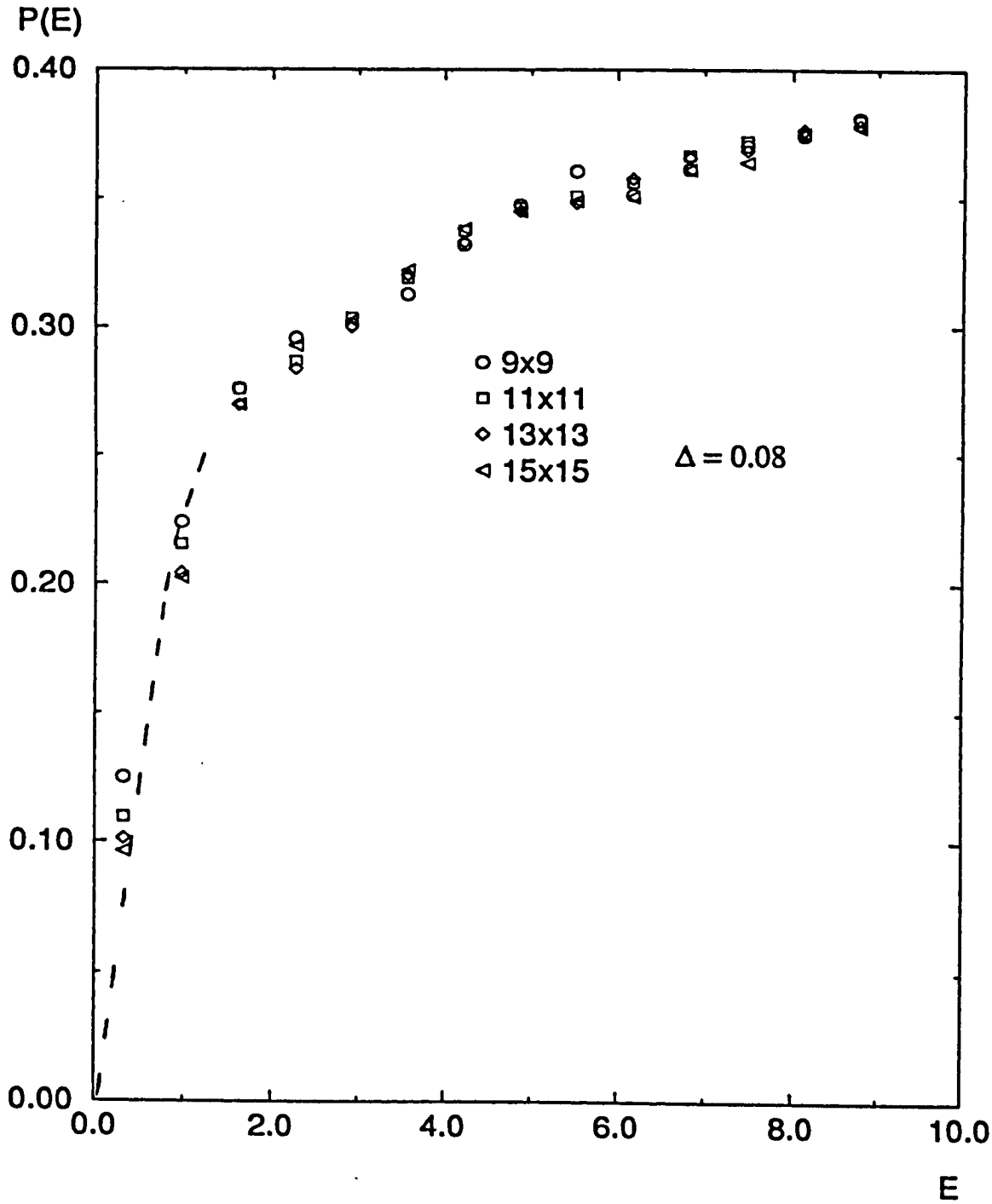

Figure 5.16: The inverse participation ratio for 2D on the insulating side ($\Delta = 0.08$).

Bibliography

[1] L. Zhang, *Phys. Rev.B*, **47**, 14364, (1993).

[2] Y. Huo and R.N. Bhatt, *Phys. Rev. Lett.*, **68**. 1375 (1992).

[3] K. Ishii, *Suppl. of the Theor. Phys.*, **53**, 77 (1973).

[4] S. John and M. Stephen, *Phys. Rev. B*, **28**, 6358 (1983).

[5] M. Makivic, N. Trivedi and S. Ullah, *unpublished*

Chapter 6

COULOMB GAP FOR BOSONS

6.1 INTRODUCTION

The previous chapters are restricted to the study of neutral bosons (bosons with short-ranged interaction). To address superconductivity, one must study charged bosons. In this chapter, I will consider the issue of the density of states of the excitations of a charged Bose glass.

The previous decade has withnessed advances in our understanding of the metal-insulator transition (MIT) in disordered systems[1]. These advances have been made possible not only by new experimental results, but through novel theoretical ideas. On the other hand, due to the complexity of the problem, little is understood about superconductor- insulator-transition (SIT) in disordered systems. In recent years, a number of extensive studies have focused on the destruction of superconductivity in 2D thin films[2].

The concept of Anderson localization[3] forms the basis of the modern theory of electrons in strongly disordered systems. Sufficiently strong disorder introduced into a metallic system leads to the localization of electronic states at the Fermi level[1, 4]. At the same time, if there exists an attraction between electrons in the vicinity of the Fermi level, the metallic system becomes superconducting due the formation (and Bose condensation) of Cooper pairs at low temperature [5]. However, when sufficient disorder is introduced to the system, superconductivity will disappear. This transition is still not well understood, since it occurs when the system is strongly disordered. Thus, it is interesting to investigate the interplay of localization and superconductivity. One relevant fundamental question is whether superconductivity still survives as one crosses the mobility edge into the localized phase, and if so, when and how does superconductivity break down? To address this issue, Ma and Lee[6] suggested a criteria showing that superconductivity may persist even if the normal state is in the insulating phase, provided the localization length ξ is sufficiently long. A sufficient criteria is given by $\xi^d N_0 \Delta_0 > 1$, where N_0 is the single particle DOS, d is spatial dimension, and Δ_0 is the zero- temperature superconducting energy gap for

the pure systems.

Experimentally, a number of systems are observed to undergo superconductor-insulator transition[7]. Fig.6.1 shows one of the experiments on Bi films. In this experiment[8], the system undergoes zero temperture superconductor-insulator transition from insulator with infinite resistance to superconductor with zero resistance by systematically varying the thickness of the film. Furthermore, the result of the transport properties on the insulating side of SIT shows some characteristics of variable range hopping conductivity[4]. An interesting observation is that the film at the critical thickness has a finite resistance when the temperature is extrapolated to zero. The value of this critical resistance is close to $\frac{h}{(2e)^2}$, and may be universal in the critical phenomena sense.

Since conventional superconductivity is due to the Bose condensation of Cooper pairs, it is tempting to apply the dirty boson model to the superconductor-insulator transition. This problem is investigated in reference[9] by assuming charge-2e bosons moving in the random potential. Universal conductance at criticality is predicted. However, the theory assumes that bosons, rather than fermions, are the elementary charge carriers even in the insulating phase. Whether the insulating phase is characterized by Fermi glass, Bose glass or the coexistence of both , is still inconclusive.

One possible way to distinguish a Fermi glass from a Bose glass is through a study of their elementary excitations. It is known that due to the interplay between disorder and the long-ranged Coulomb interactions, the density of states of excitations of the Fermi glass exhibits the so called *Coulomb gap*. In this chapter, I will present the results of a system of localized charge bosons with a long-ranged $\frac{1}{R}$ Coulomb interaction and establish if there is a Coulomb gap in the density of states (DOS) and if so, how it may differ from that of localized fermions.

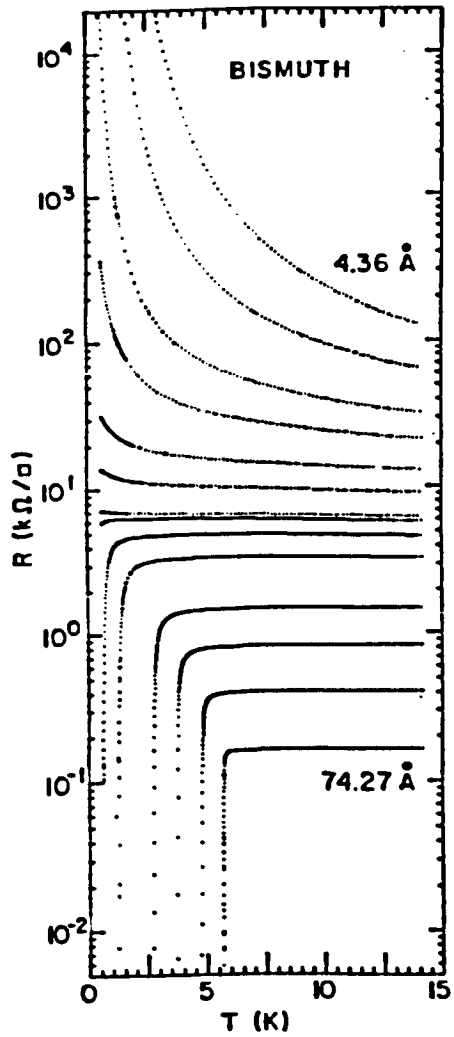

Figure 6.1: Shows the curves of the temperature dependence $R(T)$ of Bi film [7]. In this figure shows the possibility of zero temperature superconductor-insulator transition with a critical thickness, d_c=6.73 Angstrom. The critical resistance, R_c, was found to be close to $\frac{h}{4e^2}$ or 6.5 kΩ.

6.2 COULOMB GAP FOR FERMIONS

The Coulomb gap, a vanishing of DOS at zero excitation energy, was first pointed out by Efros[10] based on the interplay between disorder and the long-ranged $\frac{1}{r}$ Coulomb interaction. In the Efros model, one considers the extremely localized case where the localization length is much smaller than the distance between lattice sites, so that the overlap between localized wavefunctions is negligible. The hamiltonian of such a system is then,

$$\mathcal{H} = \sum_i \phi_i n_i + \frac{1}{2} \sum_{i \neq j} \frac{e^2}{|r_{ij}|} n_i n_j \ , \tag{6.1}$$

where n_i is the number operator on the i^{th} site, ϕ_i is a random energy on the i^{th} site with a flat uniform distribution in the range from 0 to A; and the last term describes the long-ranged Coulomb interaction between electrons on different sites. Ignoring spins, n_i is then restricted to 0 or 1 only due to Pauli exclusion principle. The one-electron excitation energy consists of the initial random energy ϕ_i and the potential energy created at i^{th} site due to all other electrons;

$$\epsilon_i = \phi_i + \sum_{i \neq j} \frac{n_j}{r_{ij}} \ . \tag{6.2}$$

Now imagine an excitation of the ground state where no new particle is introduced. Instead, an electron is transfered from an occupied site i to an unoccupied site j. The energy of this excitation (particle-hole excitation) is the difference in the single-particle energies, $\epsilon_j - \epsilon_i$, minus the interaction of the newly placed electron on site j with the now charged donor site i.

Since we started in the ground state, this energy transfer, Δ_{ij} must be positive,

$$\Delta_{ij} = \epsilon_j - \epsilon_i - \frac{e^2}{r_{ij}} > 0 \ . \tag{6.3}$$

The Coulomb gap can be understood by simple self-consistent argument as follows. From the inequality (6.3), if we take $\epsilon_i = \mu$, then, $\epsilon = \epsilon_j - \mu > \frac{e^2}{r_{ij}}$. Since DOS is

defined as the probability to find a state per unit energy and volume, to find a state within energy ϵ and distance R, one must have

$$\int_0^{\epsilon} R^d g(\epsilon')d\epsilon' \sim 1 \ . \tag{6.4}$$

If the DOS is constant at low energy, $g(\epsilon) = g_o$. From the above equation, this will give $\epsilon \sim \frac{1}{R^d}$ for large R.

Therefore, the assumption of constant DOS contradicts the fact that $\epsilon > \frac{1}{R}$. Now assume the DOS goes as ϵ to some power, $g(\epsilon) \sim |\epsilon|^{\alpha}$. From, eq.(6.3) and (6.4), this requires $\alpha = d - 1$, thus $g(\epsilon) \sim |\epsilon|^{d-1}$. In particular, $g(\epsilon) \sim |\epsilon|$ for 1D and 2D, and g(ϵ)$\sim$ $|\epsilon|^2$ in 3D. This form of the DOS implies a soft gap with the DOS vanishing only at the chemical potential. In 1D, the self-consistent argument is inconclusive, the functional form of g(ϵ) being consistent with either no gap or a logarithmic gap. However, if the interaction is modified to go as $\frac{1}{\sqrt{r}}$, then a linear gap $g(\epsilon) \sim |\epsilon|$ would result in 1D. Rigorously, $g(\epsilon)$ from eq.(6.4) is an upper bound since the ground state must be stable not only respect to single electron-hole excitation but also any number of electron-hole excitations,

$$\Delta^{j_1,j_2,...,j_n}_{i_i,i_2,...,i_n} = \epsilon_{j_1} + ... + \epsilon_{j_n} - \epsilon_{i_1} - ... - \epsilon_{i_n} - \frac{e^2}{r_{i_1 j_1}} - ... - \frac{e^2}{r_{i_n j_n}} > 0 \ . \tag{6.5}$$

However, numerical simulations using the two particle-hole excitation condition (6.5) see a DOS similar to that obtained from the single electron-hole excitation condition (6.3) only.

6.2.1 VARIABLE-RANGE HOPPING CONDUCTIVITY

In 1968, Mott[4] pointed out that the dc conductivity of amorphous materials at very low temperature can be achieved through phonon-assisted hopping of electrons between localized states. Consider two localized states, one filled and at or slightly below the Fermi energy E_F, and the other empty and above E_F. Their energy and

spatial separations are Δ and R, respectively. The hopping transition rate γ will be determined by three factors: (i) the probability of the existence of a phonon of energy Δ, given by the Boltzman factor $e^{\frac{-\Delta}{k_B T}}$ (the presence of the phonon is necessary to conserve energy in the process), (ii) the probability of electron transfer between sites. If it is assumed that each state is exponentially localized, with the same localization length α^{-1}, $\psi \sim e^{-\alpha r}$, and if an electron transfer is by means of tunnelling, the probability is given by the overlap, i.e. $p \propto e^{-2\alpha R}$ and (iii) a rate term which can be regarded as an attempt frequency ν_0, and which depends on the strength of the electron-phonon coupling and the phonon density of states, but will be only weakly dependent on R or Δ. The hopping transition rate is then given by

$$\gamma = \nu_0 e^{-2\alpha R - \frac{\Delta}{k_B T}} \quad . \tag{6.6}$$

At low temperatures, where the number and energy of phonons are both small, hopping to nearest neighbours (thereby maximizing the $e^{-2\alpha R}$ term) is unfavourable because of the large energy separations encountered on average. Instead, it is more favourable for the electron to tunnel to more distant sites, at the expense of the $e^{-2\alpha R}$ term, but at a saving of the $e^{\frac{-\Delta}{k_B T}}$ term since there is a higher probability that more distant sites will have smaller transfer energies. By optimizing the hopping probability eq.(6.6) subject to the condition that there is at least one state at a given spatial and energy separation

$$g_0 \Delta R^d \approx 1 \ , \tag{6.7}$$

where g_0 in the above equation is a DOS at zero excitation energy, assumed to be finite, and R is the hopping distance , over which a state will be found within the energy interval Δ, the hopping conductivity is given by

$$\sigma \approx e^{(-\frac{T_M}{T})^{\frac{1}{d+1}}} \ , \tag{6.8}$$

in which $\sigma \approx e^{[\frac{T_M}{T}]^{\frac{1}{4}}}$ in 3D, where $k_B T_M \approx \alpha^d / g_o$. Here α is the rate of decay of the wavefunction, that is

$$\alpha \approx \frac{1}{\xi} \ , \tag{6.9}$$

where ξ is the localization length.

The hopping conductivity eq.(6.8) derived by Mott neglects the effect of electron-electron interaction. When this effect is taken into account, as described in the previous section in the Efros model, it will lead to the appearance of Coulomb gap in the DOS near Fermi level. That is for 3D,

$$g(E) \approx \frac{\epsilon^3 E^2}{e^6}, \qquad |E| < \Delta_{CG} \tag{6.10}$$

and

$$g(E) \approx g(0), \qquad |E| > \Delta_{CG} \ , \tag{6.11}$$

where ϵ in eq.(6.10) is defined as a dielectric constant and Δ_{CG} denotes the width of the Coulomb gap which is

$$\Delta_{CG} \approx e^3 [\frac{g(0)}{\epsilon^3}]^{\frac{1}{2}} \ , \tag{6.12}$$

and the excitation energy E is measured from the Fermi level. Using the DOS in Efros model eq.(6.10) in the variable-range hopping derivation by Mott, I find that eq.(6.7) should be replaced by

$$R^d \int_0^{\Delta} g(\epsilon) d\epsilon \simeq 1 \ . \tag{6.13}$$

Hence, the hopping conductivity with a Coulomb gap is found to be

$$\sigma \approx e^{[-\frac{T_E}{T}]^{\frac{1}{2}}} \ , \tag{6.14}$$

where $k_B T_E \approx \frac{\alpha e^2}{\epsilon}$, and now the hopping exponent $\frac{1}{2}$ is independent of the dimension. As was pointed out by Efros, a necessary condition for eq.(6.14) to hold is that the

energy involved in the hopping should be smaller than the width Δ_{CG}. In other words, the temperature-dependent hopping distance in Efros model,

$$R_E(T) \approx (1/\alpha)(T_E/T_M)^{\frac{1}{2}} \tag{6.15}$$

should be longer than the temperature-dependent hopping distance of Mott;

$$R_M(T) \approx (1/\alpha)(T_M/T)^{\frac{1}{4}} \ . \tag{6.16}$$

This imposes an upper limit on the temperature below which the Efros formula eq.(6.14) is expected. We denote this temperature by T_c,

$$k_B T_c \approx \frac{e^4 g(0)}{\alpha \epsilon^2} \ . \tag{6.17}$$

At T_c, the conductivity is expected to cross-over from the Efros to the Mott law. This is supported by the experiments[12] on heavily doped gallium asenide. On the other hand, we expect that the Mott law will break down once the temperature-dependent hopping deistance $R_M(T)$ becomes comparable with some characteristic length of the system ξ_L. This implies a temperature T_c' which makes the lower limit of the range of validity of Efros law

$$k_B T_c' \approx \frac{1}{\alpha \xi_L^4 g(0)} \ . \tag{6.18}$$

It follows that a necessary requirement to observe the Mott law is that $T_c' > T_c$, i.e.,

$$\frac{e^2 g(0)}{\epsilon} < \frac{1}{\xi_L^2} \ . \tag{6.19}$$

In other words, the Mott law should not be observed when the highest possible hopping energy is in the order of Coulomb gap width Δ_{CG}.

The characteristic length ξ_L introduced above is identified as the smallest possible hopping distance. In a granular system, when the system is well below the metal-

insulator transition, i.e., $\alpha \approx \frac{1}{\xi}$ is not small, this distance is of the order of the typical length of the granular system, say a grain size(in the order of tens angstroms). On the other hand , $\frac{\epsilon}{e^2 g(0)}$ the right hand side of eq.(6.19) , which is the square of Thomas-Fermi screening length (Coulomb gap is inversely proportional to the screen length as one can clearly see from eq.(6.12) and eq.(6.19). This implies Coulomb gap decreases as the screening length increases), yields a much shorter length, a few angstroms[13]. Thus, we expect eq.(6.19) not to be applicable for high-resistivity granular samples. Moreover, deep inside the insulating phase, there will be a wide range which eq.(6.14) can be observed. Hence, for granular samples well below the metal-insulator transition the Mott law should be replaced by Efros formula eq.(6.14).

Next, I will discuss the situation near the MIT. As the transition is approached, the localization length $\alpha^{-1} \approx \xi$ increases and diverges at the vicinity of the transition[14].

$$\alpha^{-1} \approx \xi \approx |E_F - E_c|^{-\nu} \ , \tag{6.20}$$

where E_F is the Fermi energy and E_c denotes the mobility edge. In this regime, the static dielectric also diverges[15],

$$\epsilon \approx \frac{\xi^2}{\lambda^2} \ , \tag{6.21}$$

where $\lambda \approx (g(0)e^2)^{1/2}$ is the Thomas-Fermi screening length. Eq.(6.21) was derived in the context of Anderson localization, i.e., neglecing electron-electron interaction. When the exchange part of electron-electron interaction is included, $\epsilon \approx \xi^{2-\eta}$ [16], but experimental data indicates that η is small.

Eq.(6.12) and (6.21), suggest that the Coulomb gap Δ_{CG}, should decrease as the transition is approached from the insulating side. This implies that Efros hopping conductivity is applicable to the case where the localization length is small compared with the hopping distance[18], that is, from eq.(6.16), $T < T_E$. In the same way, we also can see that the cross over temperature T_c between Efros and Mott formulas decreases as the transition is approached. This might lead to the situation where T_c

will be low enough for Mott formula to be observed. However, in the vicinity of the transition, T_c' (the upper limit on the validity range of Mott formula) also becomes very small. That is because very close to the transition the shortest hopping distance L should be in the order of ξ, which implies that T_c' vanishes as ξ^{-3}. Indeed it is seen from eq.(6.17), (6.18) and (6.21) that at the transition, T_c and T_c' are in the same order of magnitude, and both tends to diverge as ξ^{-3}. Neither the Mott nor the Efros formula holds at the transition.

6.3 COULOMB GAP FOR BOSONS

Let us now discuss how the Efros model can be modified to study localized charged bosons. In the extremely site-localized limit, the hamiltonian describing a system of localized charged bosons can be written as

$$\mathcal{H} = \sum_i \phi_i n_i + \frac{1}{2}\sum_{i\neq j} \frac{e_B^2}{r_{ij}} n_i n_j + \frac{U}{2}\sum_i n_i(n_i - 1) \ , \tag{6.22}$$

where the first term in eq.(6.22) describes the disordered potential energy of a boson on site i, (for granular system this site can be a localized state or a grain), the second term describes the long-ranged Coulomb interaction between charged bosons on different lattice sites, and the last term arises from the additional short- ranged interaction between bosons on the same site. This short-ranged interaction is required in order to prevent bosons from collapsing into the lowest energy localized state. In a granular system, the Hubbard U term can be interpreted as the charging energy of a grain, which is inversely proportional to the size of the grain. e_B is the charge of the boson.

From this hamiltonian, the energy of one particle excitations can be written as the sum of the random localization energy, the Coulomb interaction energy due to other bosons on different sites, and the on-site Hubbard interaction,

$$\epsilon_i = \phi_i + U n_i + \sum_{i\neq j} \frac{e_B^2}{r_{ij}} n_j \ . \tag{6.23}$$

Thus, compared to the expression for fermions (eq.6.2), the energy to transfer a boson from site i to site j here has an additional factor U; and for the ground state this energy must be greater than zero.

$$\Delta_{ij} = \epsilon_j - (\epsilon_i - U) - \frac{e_B^2}{|r_{ij}|} > 0 \ . \tag{6.24}$$

It may seem that because of the presence of U term in eq.(6.24), the simple an-

alytic argument for the Coulomb gap in fermion case is not applicable here, and perhaps there is no Coulomb gap. I argue below that in fact the argument still applies, and there will be a Coulomb gap independent of the value of U. Assume the probability distribution of the random localization energy, $P(\phi)$, is given by a flat uniform distribution,

$$P(\phi) = \begin{cases} \frac{1}{A}, & 0 \leq \phi_i \leq A \\ 0, & \text{otherwise.} \end{cases}$$

Without loss of generality, I consider the case where the total number of bosons is less than the total number of sites. Energies are measured from the chemical potential.

First consider the large U limit, $U >> A$. In this limit the number of bosons on each site is 0 or 1; the problem is identical to the fermion case since kinetic energy is neglected. Thus, without Coulomb interaction the DOS g_o is given by the probability distribution of ϕ, $P(\phi)$. While for finite $\frac{e_B^2}{a}$, a Coulomb gap exists. In particular for 2D, the gap is linear and the Coulomb gap size, $\Delta_{CG} = e_B^4 g_0$.

How does one deduce the Coulomb gap from eq.(6.24)? In eq.(6.24), i must be an occupied site. ϵ_i, being the energy to add a particle will involve the energy U. Thus, for $U >> A$, ϵ_i will always be large ($\sim U$), while $\epsilon_i - U$ can be small. The rationale for Coulomb gap is obtained from eq.(6.24) by choosing $\epsilon_i - U \approx 0$. The apparent discrepancy from the fermion inequality, where U is absent is that for eq.(6.3), ϵ_i there is actually the energy of the particle that already occupies site i, and not the energy to add another particle (not allowed for fermions).

In the small U limit, $U << A$, the situation is somewhat different from the case with large U. Without Coulomb interaction, the DOS is enhanced at low energy excitation ($\epsilon \leq U$) by the order of $\approx A/U$. This simply comes from the fact that all sites with random localization energy ϕ_i below the chemical potential, μ, need to be filled with enough number of bosons to give an excitation energy, $\epsilon_i > \mu$. In other words, let $\epsilon_i(n_i)$ be the value of ϵ_i with n_i bosons on the i^{th} site, then the ground

states must have $\epsilon_i(n_i - 1) < 0$, $\epsilon_i(n_i) > 0$. Since

$$\epsilon_i(n_i) - \epsilon_i(n_i - 1) = U \tag{6.25}$$

then

$$\epsilon_i \leq U \ . \tag{6.26}$$

Thus, all the occupied sites have excitation energies less than U. With finite $\frac{e^2}{a}$ there will be a Coulomb gap, but with U instead of A playing the role of the band width.

6.4 RESULTS AND DISCUSSIONS

The hamiltonian in eq.(6.22) can be solved via numerical simulations. Beginning with bosons in some arbitary state, I will attempt to find the ground state by redistributing bosons, one boson at a time, until the energy cannot be lowered any further. In other words, we attempt to find a set $\{n_i\}$(the occupation number of bosons which can be 0,1,2,...) which minimizes the hamiltonian and find the DOS corresponding to this set. The minimization procedure can summarized as following.

STEP 1. Using random number generator to produce random site energies.

STEP 2. For fixed number of bosons, randomly put bosons on the sites.

STEP 3. Sampling a pair site $\{i, j\}$ and transfer a boson from site i to site j.

STEP 4. If $\Delta_{ij} < 0$ accept the alteration, if not repeat STEP3. until the property of the ground state eq.(6.24), $\Delta_{ij} > 0$, is satisfied.

Eventually, this minimization procedure will produce a set of occupation number $\{n_i\}$ and the ground state $\{\epsilon_i\}$ which fulfils the inequality(6.24). While in principle, this procedure may result in a metastable rather than the true ground state. I have checked this for 100 different intial configurations for the same set of random potentials for size 100 and 1000 for both large U and small U. In all cases the system reaches the same final configuration independent of initial configurations, strongly implying the system has reached the ground state configuration. Furthermore, there is no obvious reason why the DOS of excitations from the ground state and a typical metastable state should differ in essential features.

The numerical results for both large U and small U are in agreement with the theoretical argument. For simplicity I set the total number of bosons equals to the half number of sites (this will not affect our result as long as the total number of bosons is not equal to an integer multiple number of sites). And the probability distribution of random localization energy is given by a uniform distribution in the range $(0 \leq \phi \leq A)$.

The DOS is calculated for size N=2500 in 1D with $\frac{1}{\sqrt{r}}$ interaction and 40x40, 50x50

in 2D with $\frac{1}{r}$ interaction. I perform the simulations for large U, (U=5, A=2) and small U limit, (U=0.5, A=2). I find that the Coulomb gap exists in both limits. The results are calculated for the same initial configuration and same random potential (single random configuration).

First, consider a large U limit ($\frac{U}{A} < 1$). As discussed before, without Coulomb interaction, the DOS is gapless. The DOS in this case is given by the uniform distribution ($P(\phi)$). While with finite $\frac{e_B^2}{a}$, there is a linear gap ($g(\epsilon) \sim \epsilon$) for low energy excitations. These results are shown in fig.6.2. In this fig., I present a plot of the DOS for 2D (50 × 50) in the large U limit (U=5 and A=2). The plot of the DOS without Coulomb interaction (dashed line) and with finite Coulomb interaction (solid line) are plotted in the same graph for comparision. Without Coulomb interaction (dashed line), the DOS is given by two block uniform distributions with the separation between these two energy band $\sim U$. The lower band corresponds to adding a boson to an unoccupied site, and the upper band to an occupied site. While for finite $\frac{e_B^2}{a}$ (solid line), shows a gap (linear slope in the DOS) at the low energy excitations. Except for the upper band, which corresponds to excitations forbidden for fermions due to Pauli Exclusion Principle, the results here are identical to those for fermions. This is to be expected since in the large U limit, each site is occupied by 0 or 1 particle in the ground state, making the problem identical to that of fermions.

Next consider the small U limit ($\frac{U}{A} < 1$). In this limit, without Coulomb interaction, there is no gap and the DOS is finite at the chemical potential. In particular, the DOS is greatly enhanced for low energy excitations with width U. The enhancement is of the order of A/U and hence $g(\epsilon < U) = \frac{1}{U}$. This result is shown in Fig.6.3 for 2D with system size 50x50. The plot of large U and small U limit are plotted in the same graph for comparision. The dotted line and solid line in this fig. represent large U ($\frac{U}{A} > 1$) and small U ($\frac{U}{A} < 1$) for $\frac{e_B^2}{a} = 0$ case. With a finite Coulomb interaction in the small U limit, there is a Coulomb gap at the low energy excitation. These results are shown in Fig.6.4 for 2D with system size 50x50. The linear slope of the DOS at

low energy increases with the decreasing Coulomb interaction. In other words, the gap width decreases as Coulomb interaction becomes weaker. These results are shown in fig.6.5 for 2D (40x40 sites) and fig.6.6 for (1D 2500 sites) large U. In fig.6.5, I show the plot of DOS in 2D (40x40) for differrent Coulomb interaction. The linear slope (α) increases as the Coulomb interaction is decreased. The gap width (Δ_{CG}) which is estimated through the slope increases with the increasing Coulomb interaction ($\Delta_{CG}(\frac{e_B^2}{a} = 0.5) = 0.289 \pm 0.052$, $\Delta_{CG}(\frac{e_B^2}{a} = 0.75) = 0.526 \pm 0.023$). Similar results are also shown in fig.6.5 for 1D (2500 sites) with gap width proportional to the Coulomb interaction ($\Delta_{CG}(\frac{e_B^2}{a} = 0.5) = 0.207 \pm 0.025$, $\Delta_{CG}(\frac{e_B^2}{a} = 0.7) = 0.415 \pm 0.019$).

In conclusion, the numerical results show that Coulomb gap exists for both small U and large U limit and are in agreement with the previous analytical argument. The size of the gap is proportional to the Coulomb interaction (increasing with the increasing Coulomb interaction), $\frac{e_B^2}{a}$ for both large and small U. There is also a large enhancement in the DOS of the excitation above the gap for the small U compared to large U.

Next I would like to discuss the validity of temperature range of Coulomb gap for large U and small U. For granular systems, the Hubbard U term can be interpreted as a charging energy of the grain, which is inversely proportional to the grain size. In that case, large U limit will imply small grain while small U limit will imply large grain. For low temperature, the Coulomb gap exists for $k_B T << \Delta_{CG}$. For small grains ($U/A > 1$) with $\frac{e_B^2}{a} < U$), the linear gap (occurs in 2D) at the low energy excitations is valid for the energy range within the gap width , Δ_{CG} (which is in the order of $\Delta_{CG} \approx e_B^4 g_0$). Here g_0 is a non-interacting DOS, assuming a flat uniform distribution of width A. In general, the width of the gap is in the order of $e_B^4 g_0$ for 2D, and $e_B^3 g_0^{\frac{1}{2}}$ for 3D. While for large grain ($\frac{U}{A} < 1$ with $\frac{e_B^2}{a} < U$) will be in the order of U (Δ_{CG} cannot be greater than the band width, as discussed in sec. 6.3 U plays a role as a band width instead of A for small U case). Therefore, for given A with $\frac{e_B^2}{a} < U$, the Coulomb gap for small grain will be observed in a larger temperature

range than that of large grain.

Within this model, an even more interesting question is how could ones distinguish the fermi glass from bose-glass in the insulating phase? On the bose-glass phase, one need an attractive force to form a boson of charge-2e. The quantum fluctuation even at zero temperature prevents the local pairing of charge-2e boson from bose condensation but will not break the pairing. As the disorder becomes stronger, the Ma-Lee criteria for mean field superconductivity will fail because the (fermion) localization length or the grain size will become too small. Cooper pairs will cease to form, and one expects a Bose glass-Fermi glass transition. A possible model for such a transition may be one where the Hubbard U is changed from negative (attractive) to positive (repulsion) as the disorder is increased.

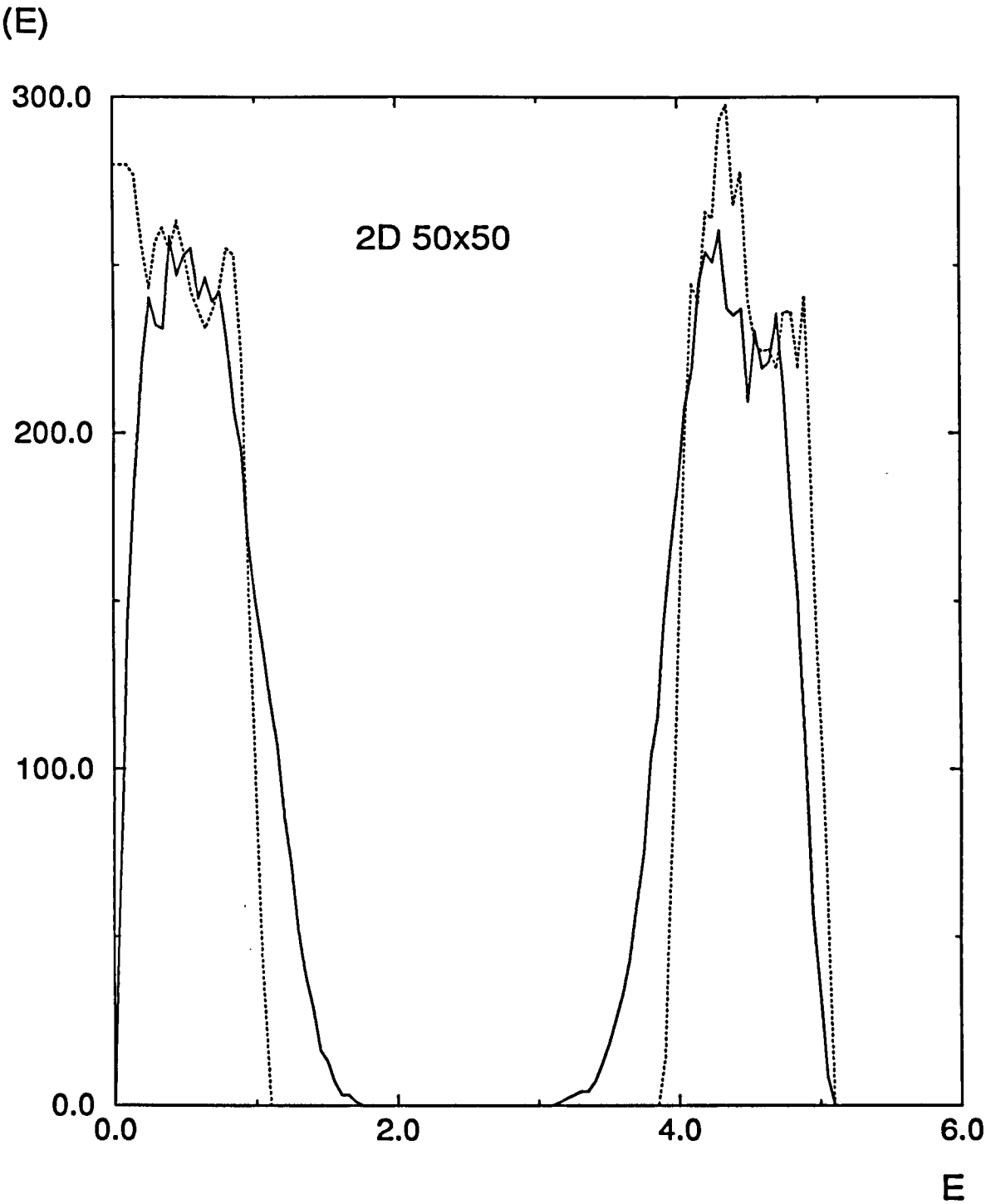

Figure 6.2: The DOS in 2D for size 50x50 and large U (U=5, A=2). Without Coulomb interaction (dashed line) and with Coulomb interaction (solid line , $\frac{e_B^2}{a} = 0.25$) are plotted in the same graph for comparision. Note the linear Coulomb gap at low energy for $\frac{e_B^2}{a} \neq 0$.

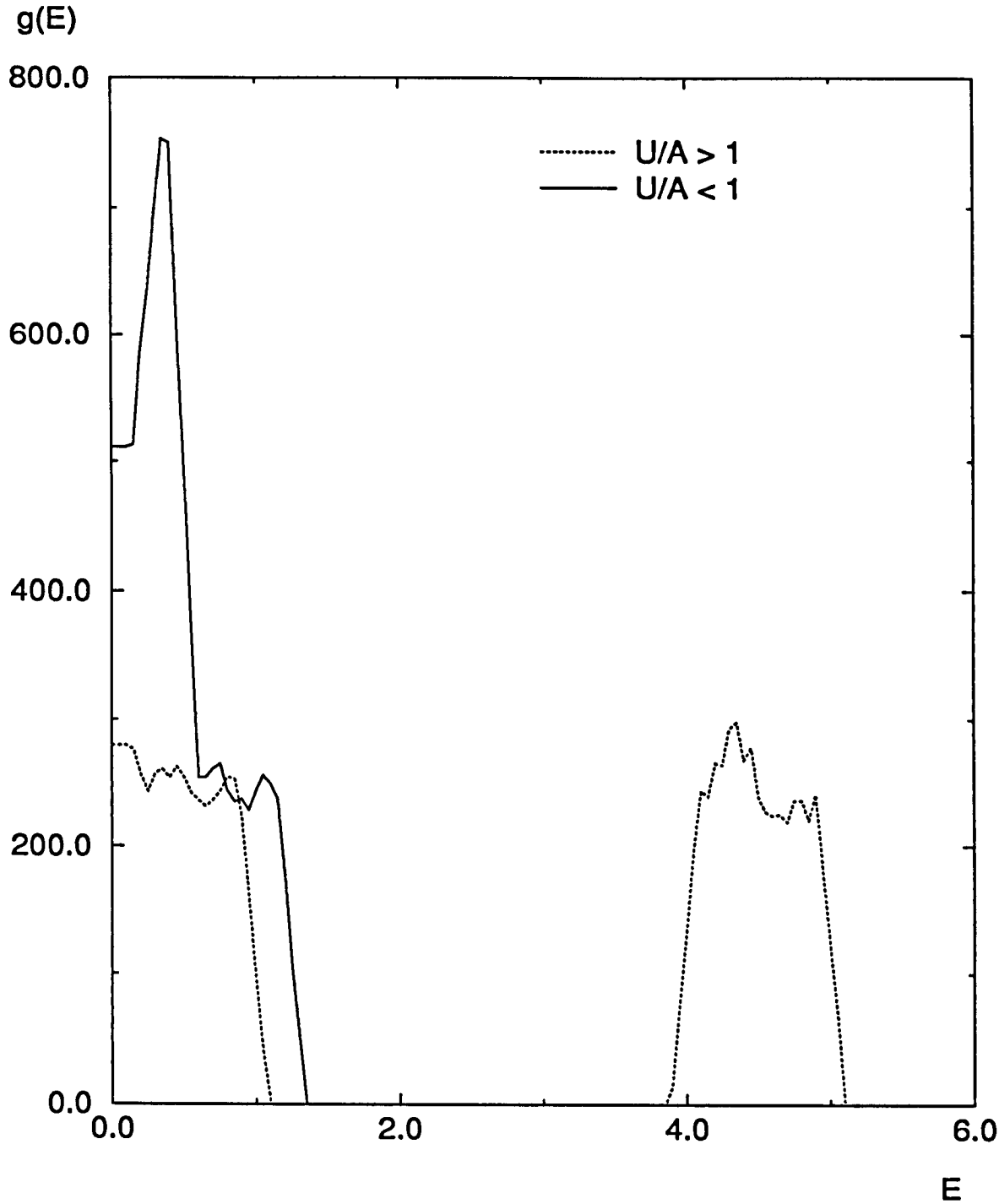

Figure 6.3: For small U (U=0.5, A=2), there is an enhancement of DOS of low energy excitation. Here I show the comparision between large U limit (U=5, A=2) and small U limit without Coulomb interactions in 2D (size 50 × 50 sites).

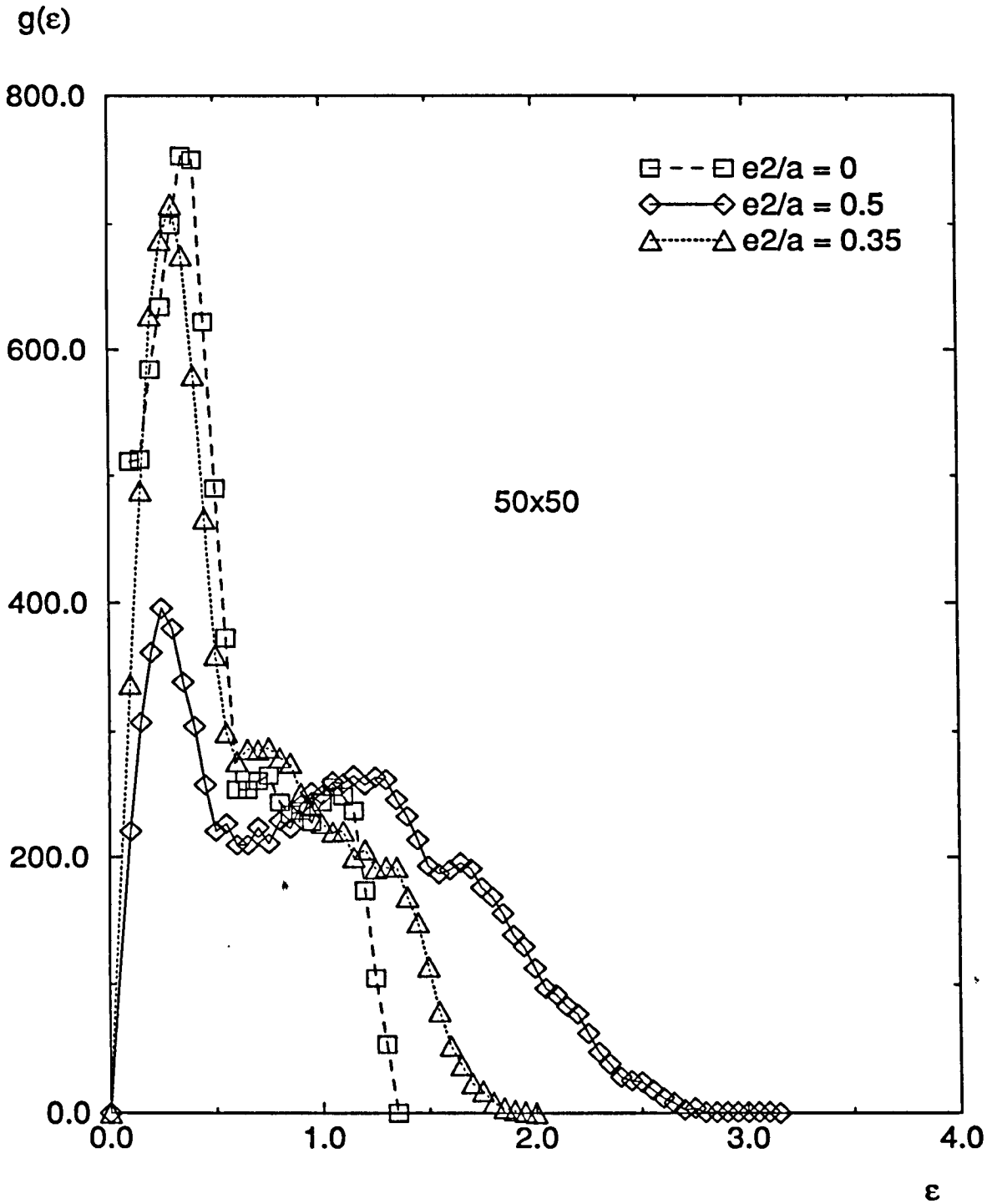

Figure 6.4: Here I show the Coulomb gap in 2D, size 50×50 sites for small U (U=0.5, A=2). In this figure, dashed line is for $\frac{e_R^2}{a} = 0$ and solid line for $\frac{e_R^2}{a} \neq 0$. The gap width (Δ_{CG}) is proportional to the Coulomb interaction. The gap width estimated from the slope of the linear part of the DOS ($\Delta_{CG}(\frac{e_R^2}{a} = 0.5) = 0.282 \pm 0.027$, $\Delta_{CG}(\frac{e_R^2}{a} = 0.35) = 0.166 \pm 0.005$).

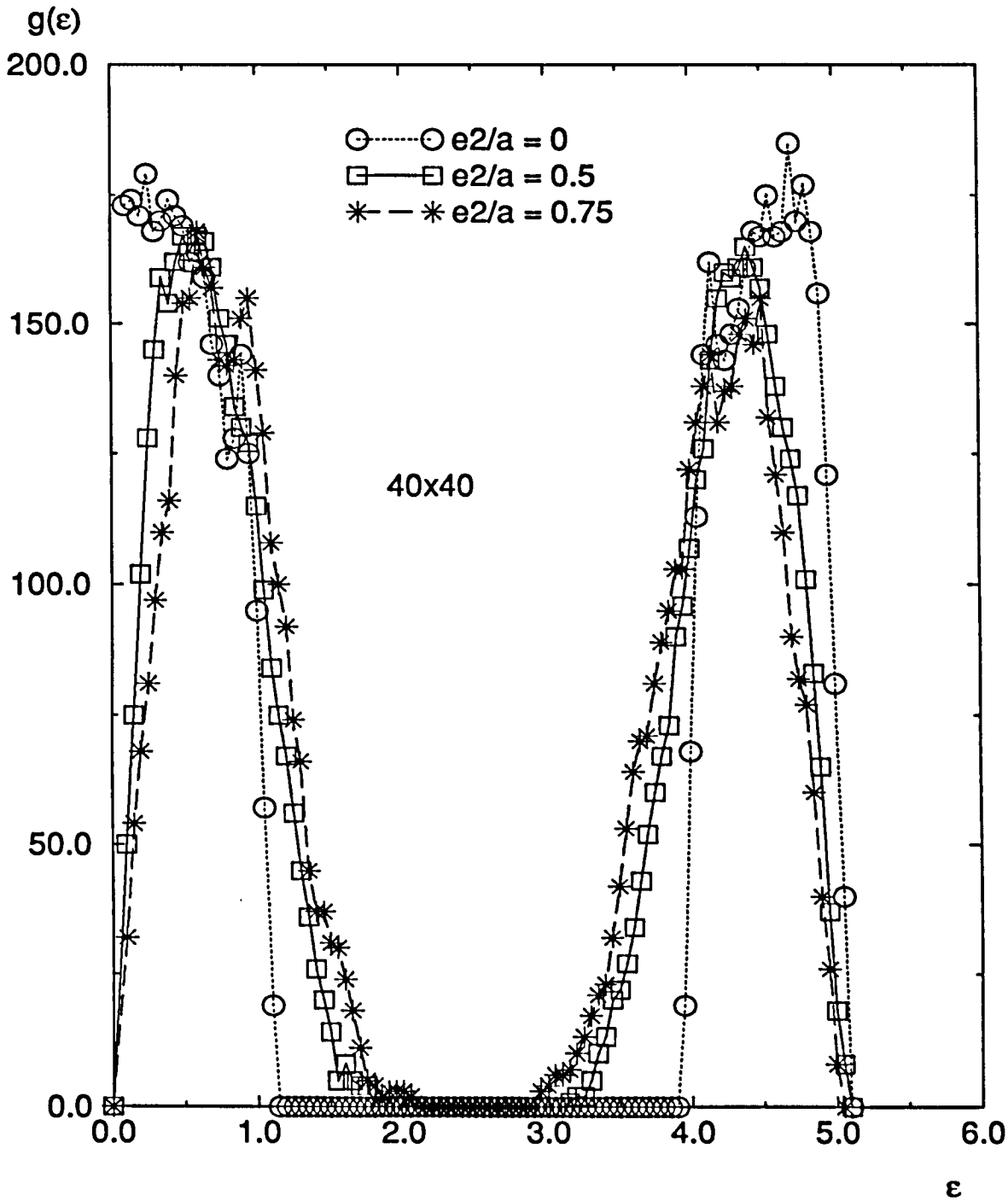

Figure 6.5: DOS in 2D, size 40×40 sites, is plotted for large U, (U=5, A=2). The gap at low energy increases with increasing $\frac{e_B^2}{a}$. $\Delta_{CG}(\frac{e_B^2}{a} = 0.5) = 0.289 \pm 0.052$, $\Delta_{CG}(\frac{e_B^2}{a} = 0.75) = 0.526 \pm 0.023$.

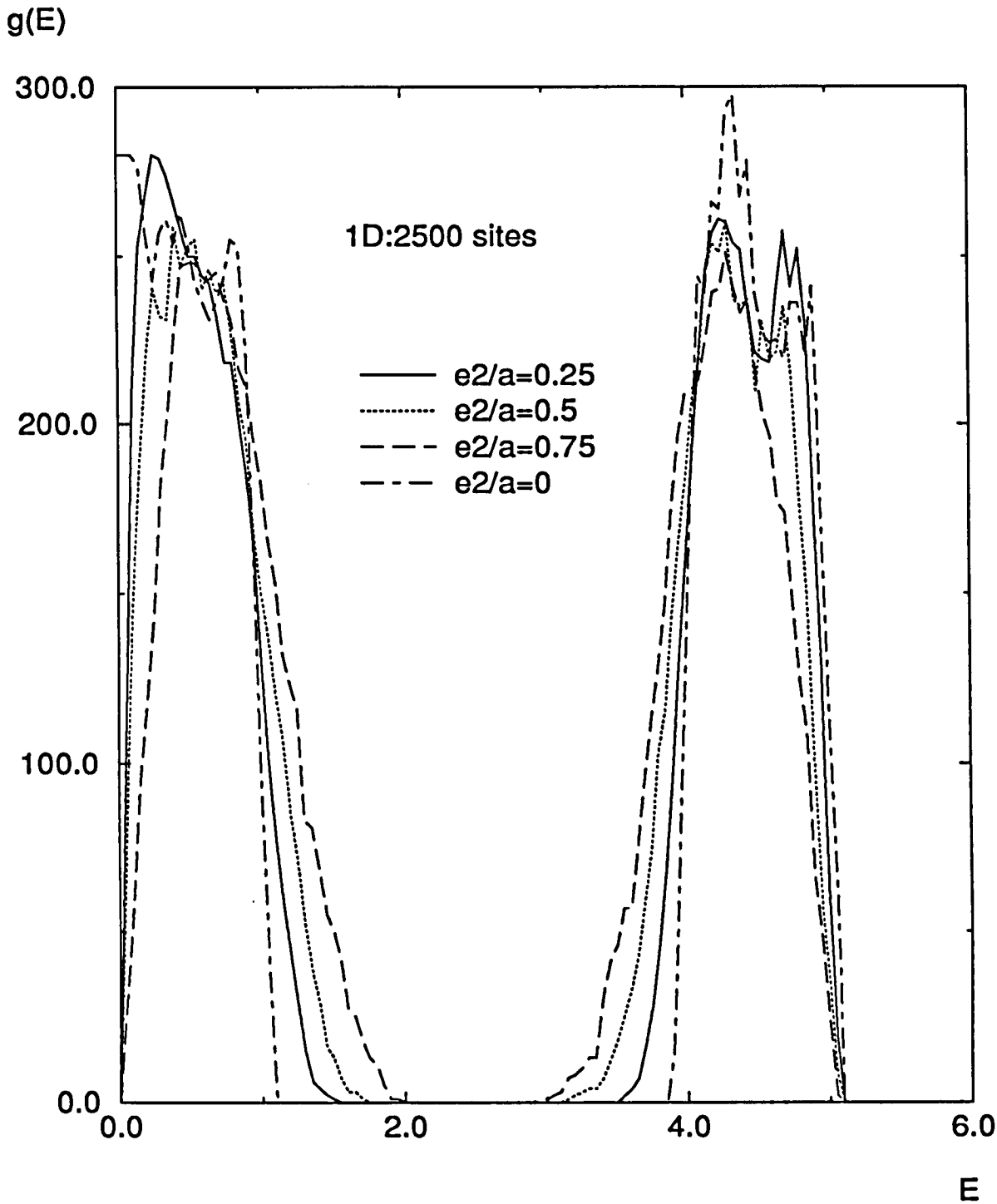

Figure 6.6: Similar to fig.6.5. Here I consider 1D with system size 2500 sites. The size of the gap varies with the interaction, as one can see in this figure. $\Delta_{CG}(\frac{e_R^2}{a} = 0.5) = 0.207 \pm 0.025$, $\Delta_{CG}(\frac{e_R^2}{a} = 0.75) = 0.415 \pm 0.019$. See text for the form of interaction used for 1D.

Bibliography

[1] P.A. Lee, and T.V. Ramakrishnan, Rev. Mod. Phys.,**57**, 287(1985).

[2] S. Chakravarty, G. Inglod, S. Kivelson, and A. Luther, Phys., Rev. Lett., **56**, 2303 (1986). M.P.A. Fisher, Phys. Rev. B**36**, 1917 (1987). M.C. Cha, M.P.A. Fisher, S.M. Girvin, M. Wallin and A.P. Young, Phys. Rev. B**44**, 6883 (1991). A. Kampf and G. Schon, Phys. Rev. B**36**, 3651 (1987). W. Zweger, J. Low Temp. Phys. **72**, 291 (1988). B. Abeles, PinchR.A. Ferrell and B. Mirhashem, Phys. Rev. B**37**, 648 (1988). A. Gold, Z. Phys. B**81**, 155 (1990).

[3] P. W. Anderson, Phys. Rev., **109**, 1492 (1958).

[4] N.F. Mott, J. Non-Cryst. Solid, **1**, 1 (1968). N.F. Mott. Metal-Insulator Transition. Taylor and Francis, London, 1974.

[5] J. Bardeen, L.N. Cooper, and J.R. Schrieffer, Phys. Rev. **57**, 287 (1985).

[6] S. Maekawa and Fukuyama, Physica **107B**, 123 (1981); J. Phys. Soc. Jpn., **51**, 1380 (1982); H. Fukuyama, Physics **126B**, 306 (1984). P.W. Anderson, K.A. Muttalib, and T.V. Ramakrishnan, Phys. Rev. **B21**, 117 (1983). M. Ma and P.A. Lee, Phys. Rev. **B32**, 5658 (1985). A. Kapitulnik, G. Kotliar, Phys. REv. Lett., **54**, 473 (1985). L.N. Bullaevskii, M.V. Sadovskii, JETP Lett., **43**, 76 (1986).

[7] A.F. Hebard and M.A. Paalanen, Phys. Rev.B**30**, 4063 (1984). L.J. Geerligs, M. Peters, L.E.M. de Groot, A. Verbruggen, and J.E. Mooij, Phys. Rev. Lett. **63**,

326 (1989). H.M. Jaeger, D.B. Haviland, B.G. Orr, and A.M. Goldman, Phys. Rev. B40, 182 (1989). T. Wang, K.M. Beauchamp, D.D. Berkely, B.R. Johnson, J.X. Liu, J. Zhang, and A.M. Goldman, Phys. Rev. B43, 8623 (1991).

[8] D.B. Haviland, Y. Liu, and A.M. Goldman, Phys. Rev. Lett., 62, 2180 (1989).

[9] M.C. Cha, M.P.A. Fisher, S.M. Girvin, M. Wallin and A.P. Young, Phys. Rev. B44, 6883 (1991).

[10] A.L. Efros, J. Phys. C: Solid State Phys., 9,2021 (1976).

[11] S.D. Baranovskii, A.L. Efros, B.L. Gelmont, and B.I. Shklovskii, Solid State Com., 27, 1 (1978).

[12] D. Redfield, Phys. Rev. Lett., 30, 1319 (1973).

[13] B. Abeles, H.L. Pinch and J.Y. Gittleman, Phys. Rev. Lett., 35, 247 (1975). B. Abeles, P. Sheng, M.D. Coutts, and Y. Arie, Adv. Phys., 24, 407 (1975).

[14] E. Abrahams, P.W. Anderson, D.C. Licciadello and T.V. Ramakrishnan, Phys. Rev. Lett., 42, 673 (1979).

[15] Y. Imry, Y. Gefen, and D.J. Bergman, Phys. Rev. B5, 3609 (1972).

[16] Y. Gefen and Y. Imry, Phys., Rev., B28, 3569 (1983).

[17] S.D. Baranovskii, A.L. Efros, B.L. Gelmont and B.I. Shklovskii, J. Phys. C, 12, 1023 (1978).

[18] N.F. Mott, J. Phys. C: Solid State Phys., 8, L239 (1975).

Chapter 7

SUMMARY

In this dissertation, I have studied the ground state and excited states of the dirty boson system. I investigated the effect of quantum fluctuations on the destruction of superfluidity in 1D and 2D. The superfluid-Bose-glass phase transition was studied via mapping the hard-core dirty boson model to the quantum spin XY model with transverse random field. From this mapping, the superfluid phase corresponds to the spin LRO in the XY plane. The classical spin ground state ($S = \infty$) in our model corresponds to Gutzwiller projection of a non-uniform condensate. Gaussian quantum fluctuations are included by using the spin wave approximation which is equivalent to order $1/S$ expansion and gives rise to a quadratic hamiltonian which can be diagonalized via Bogoliubov transformation.

I showed that a Bogoliubov-like theory for dirty bosons indicates there is an instability in the superfluid phase with a finite amount of disorder. This instability is signified by a divergence in the order parameter reduction due to quantum fluctuations. The properties of the ground state and the excited states given by this theory were discussed in chap.3 and chap.5. At the transition, the renormalized critical exponent, $\frac{\eta}{\eta_{pure}}$, for 1D in the Bogoliubov theory is 1.4.

In chap.4, I calculated the superfluid density (ρ_s) in the same approximation. The results show that the superfluid density vanishes at the same or close to the same critical disorder as that of the order parameter ($0.5 < \Delta_c < 0.6$ in 1D and $0.08 < \Delta_c < 0.1$ in 2D). My result also shows that ρ_s obtained from the linear response theory differs from ρ_s obtained directly from minimizing energy. The physics behind this is not understood at this point.

Since the spin wave theory is accurate for large S, it is of interest to investigate this problem beyond the gaussian approximation (the effect of magnon-magnon interaction). The inclusion of long-ranged Coulomb interaction to our Bogoliubov theory is also of interest to pursue, since one can then directly address to the superconductor-insulator transition.

While I have presented the results in the language of the dirty boson problem,

I have indicated that they will be relevant to quantum spin systems and disordered superconductors also. More generally, the physics obtained here should be relevant to other disordered quantum systems where the disorder couples to the *magnitude* (i.e. quadratically) but not the *phase* (i.e. linearly) of the order parameter.

In chapter 6, I investigated the effect of long-ranged interaction to the dirty charged boson model in the localized phase. I generalized the Efros model for localized charged fermions, so that there was an on-site Hubbard repulsion U between bosons on the same site as well as the long-ranged $1/R$ Coulomb interaction between bosons on different sites. I found that similar to charged fermions, but with modifications, the interplay between disorder and the Coulomb interaction caused a depletion of the DOS at the chemical potential and open a gap in the DOS, known as *Coulomb gap*. In this model, the Coulomb gap width, Δ_{CG}, is of the order of $e^4 g_o$ in 2D for small grains (large U). These features can be probed by a measurement of the tunneling DOS. The hopping conductivity within the temperature $k_B T << \Delta_{CG}$ should have the exponent $\frac{1}{2}$, $\sigma \sim e^{(\frac{const.}{T})^{\frac{1}{2}}}$. Thus, for small grain, (within this model) one expects to observe the 1/2 hopping conductivity due to boson hopping in a wider range of temperature than that of fermion.

In discussing the significance of the Coulomb gap to the hopping conductivity, I have assumed no qualitative difference between phonon-assisted Cooper pair hopping and fermion hopping. This situation is actually rather unclear. For a Cooper pair to hop, phonons not only have to break the Cooper pair in one grain, and recombine it at another, but phase coherence must be reestablished at the end of each hop. This complex problem awaits.